Lecture 6

HDD, Toggle MRAM, STT-MRAM

The spintronics “goose game”

Atom magnetism

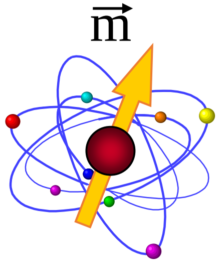

interactions between spins and with the supporting substrate

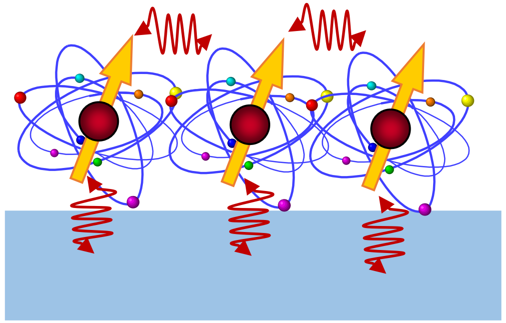

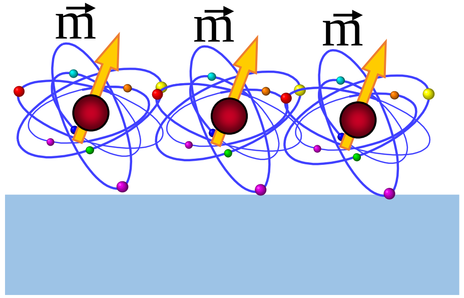

magnetic moment in a cluster and/or on a support

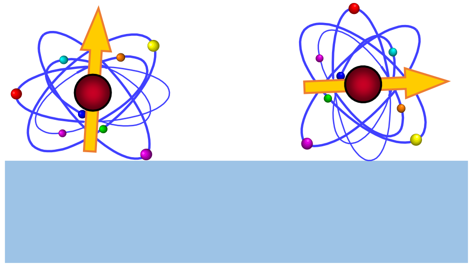

Magnetization easy axis

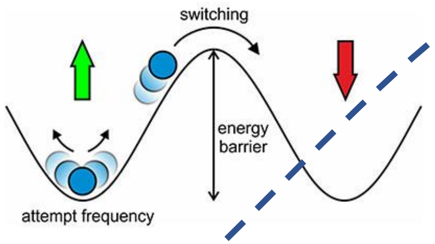

applications

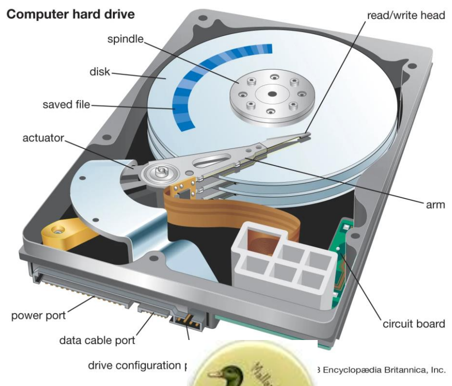

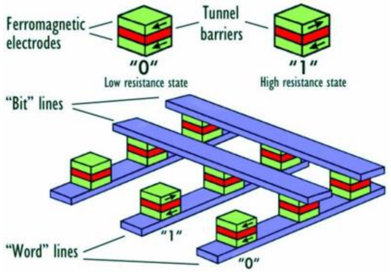

STT - SOT

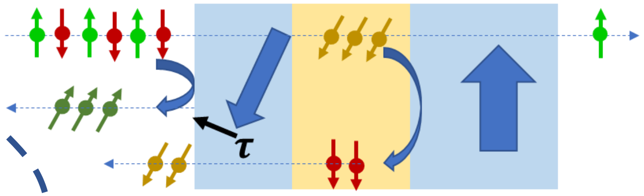

Future

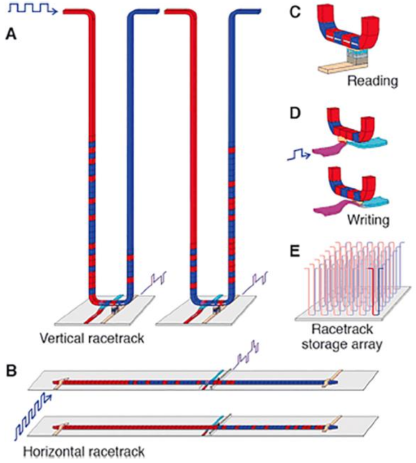

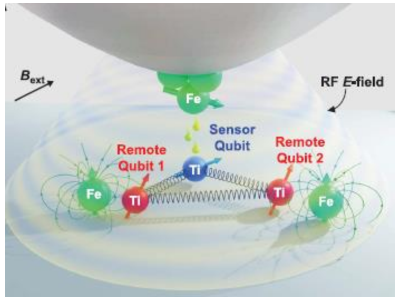

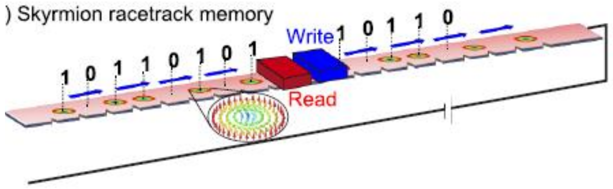

Magnetic memories

Hard Disk Drive (HDD)

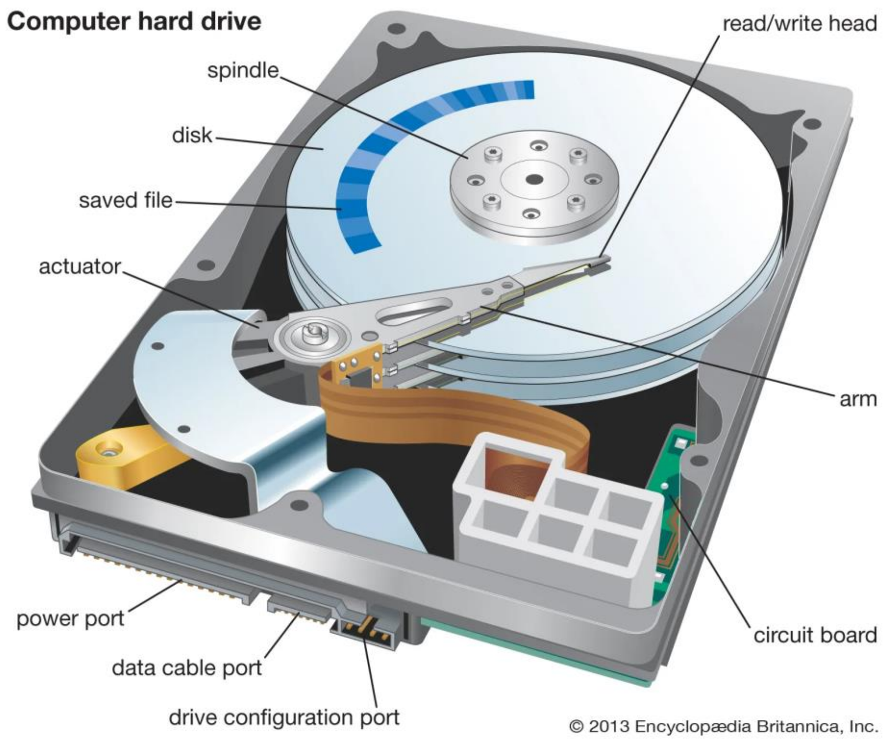

Storage

Magnetic Random Access Memory (MRAM)

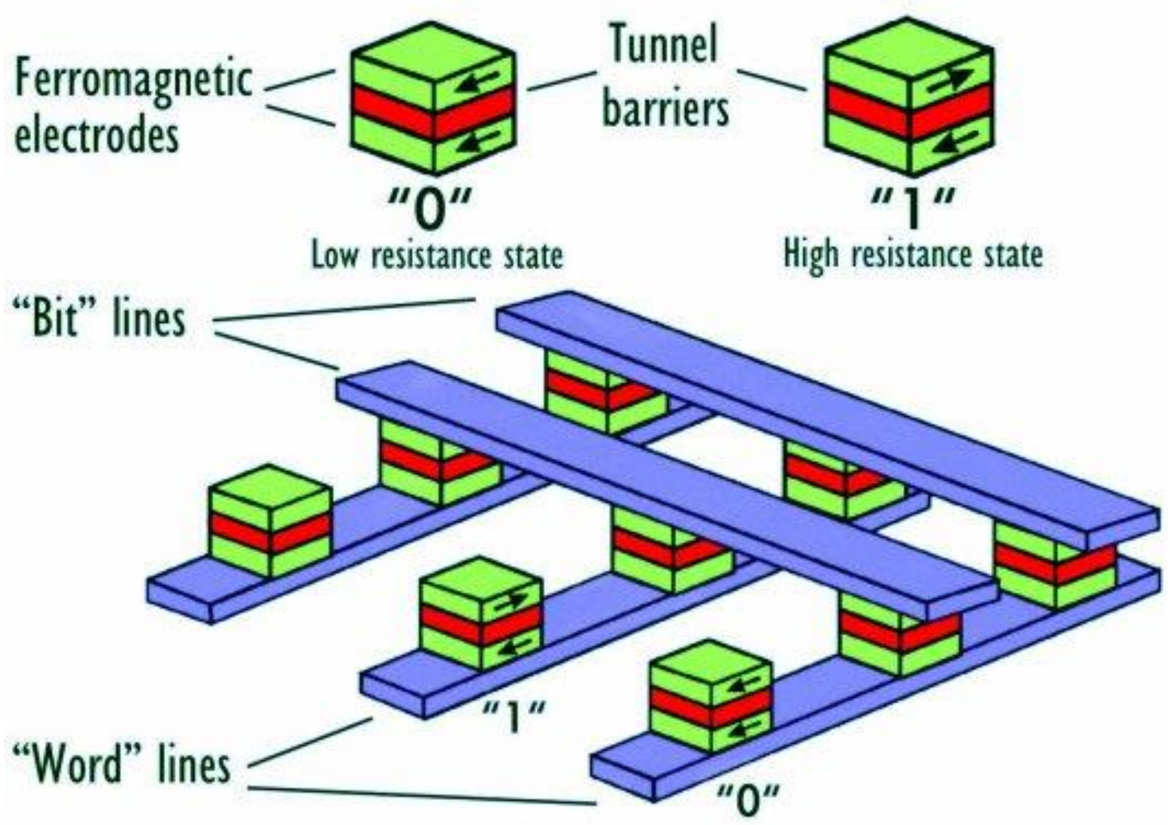

Dynamic memory

Memories performance

DRAM (dynamic random access memory)
SRAM (static random access memory)

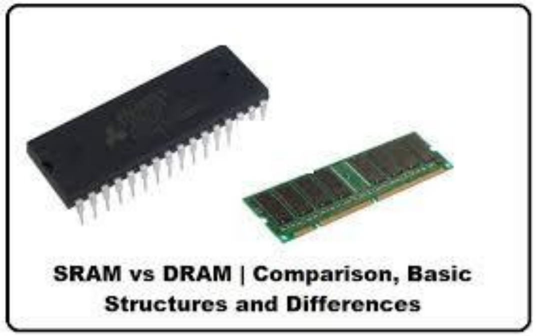

Charge stored in a transistor
Volatile and need frequent refresh (especially DRAM)

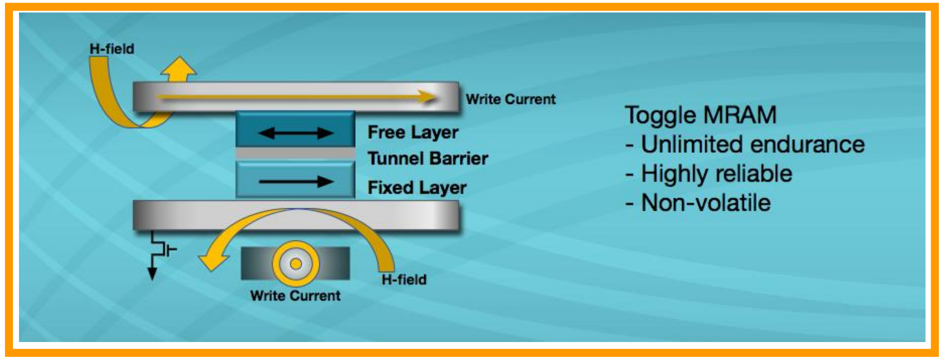

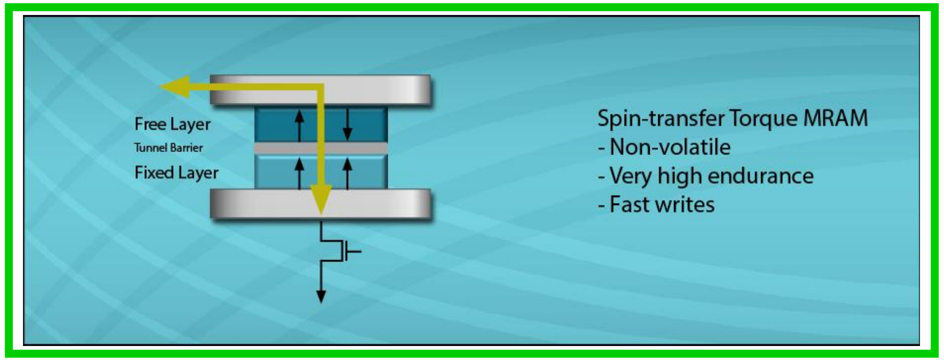

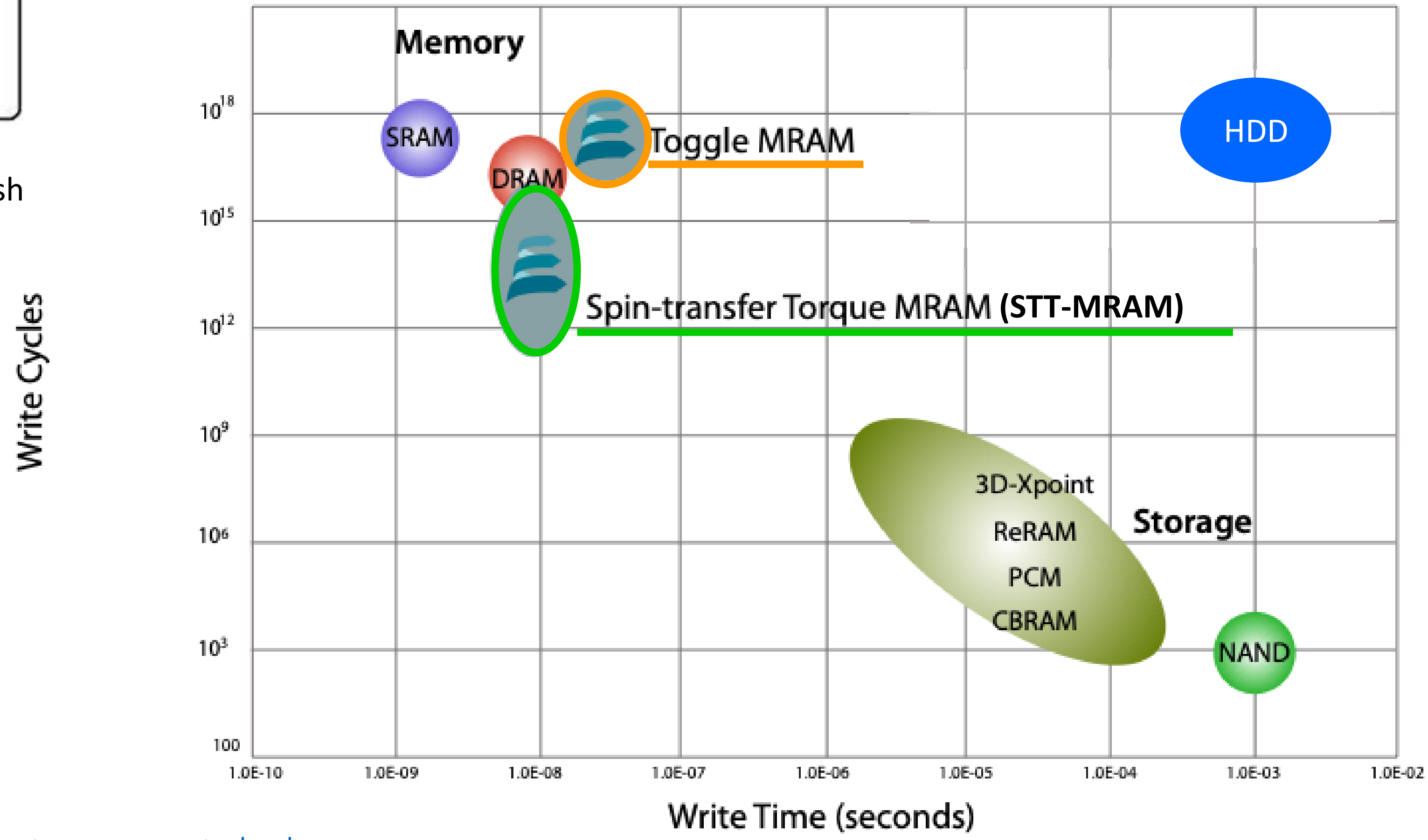

NAND

Charge stored in a transistor
Non volatile

https://www.everspin.com/spin-transfer-torque-mram-technology

Memory hierarchy

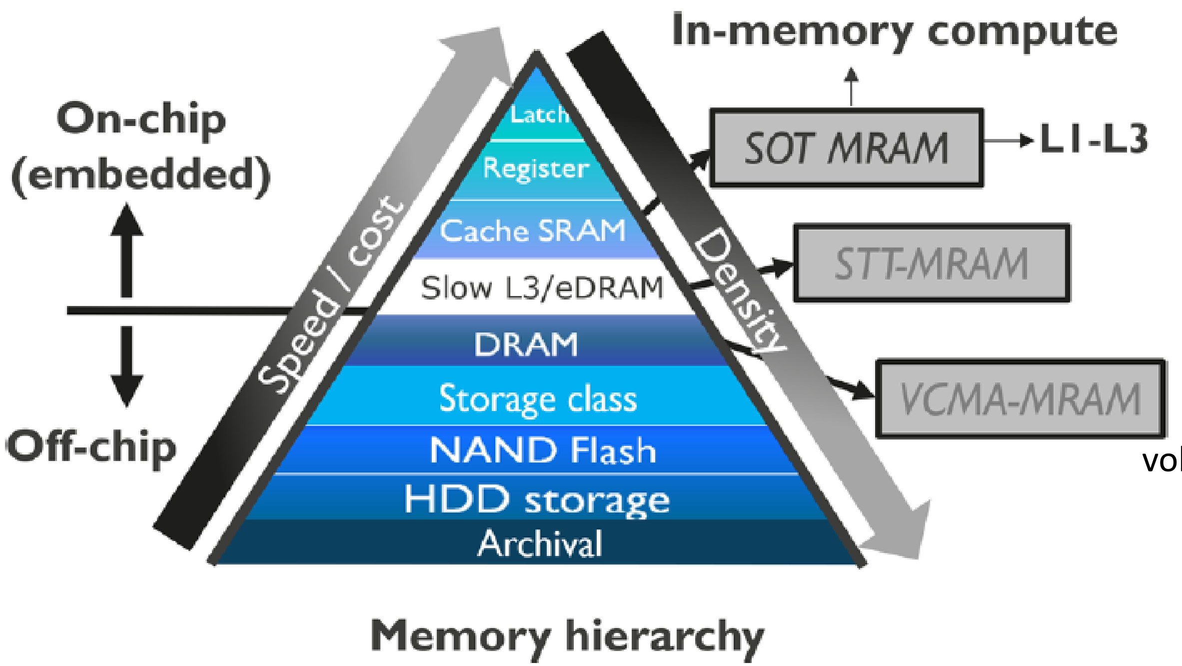

voltage control of magnetic anisotropy (VCMA)

Fig. 1 | Memory hierarchy presents various types of memory. MRAM technologies provide promise to replace charge-based memory devices at different cache levels, ranging from L1 to L4. SRAM and DRAM stand for Static Random-Access Memory and Dynamic Random-Access Memory, respectively, while HDD refers to magnetic hard disk drives. SOT-MRAM is aimed at replacing SRAM due to its fast operation, while STT-MRAM is targeted for high-performance and high-density embedded DRAM applications. Voltage-controlled magnetic anisotropy technology offers potential for low-power operation and is being explored as a replacement for DRAM.

https://doi.org/10.1038/s44306-024-00044-1

The recording mechanism in a HDD: a condensate of concepts

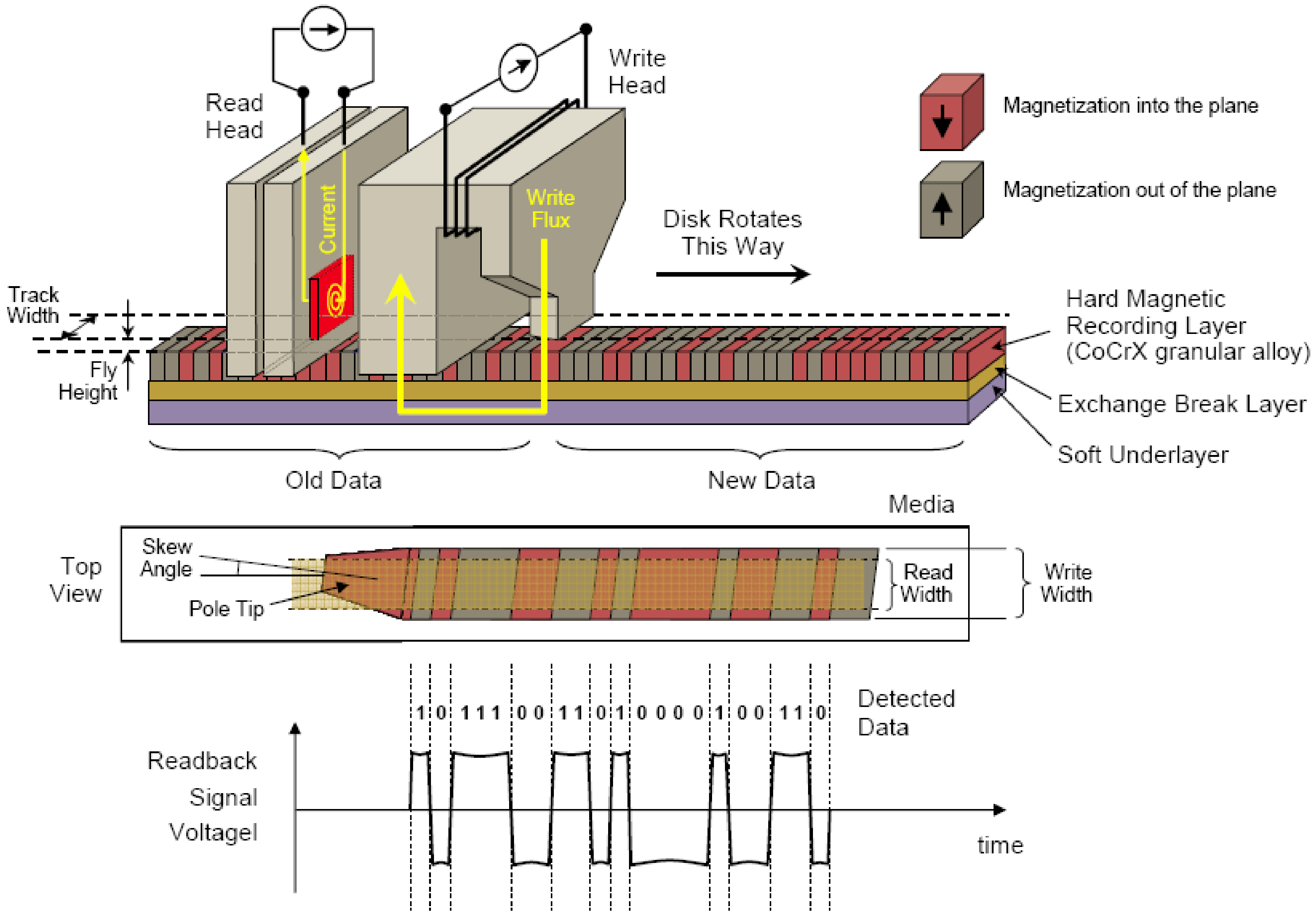

TEM (Transmission electron microscopy) image of CoCrPt recording layer with in-plane magnetization.

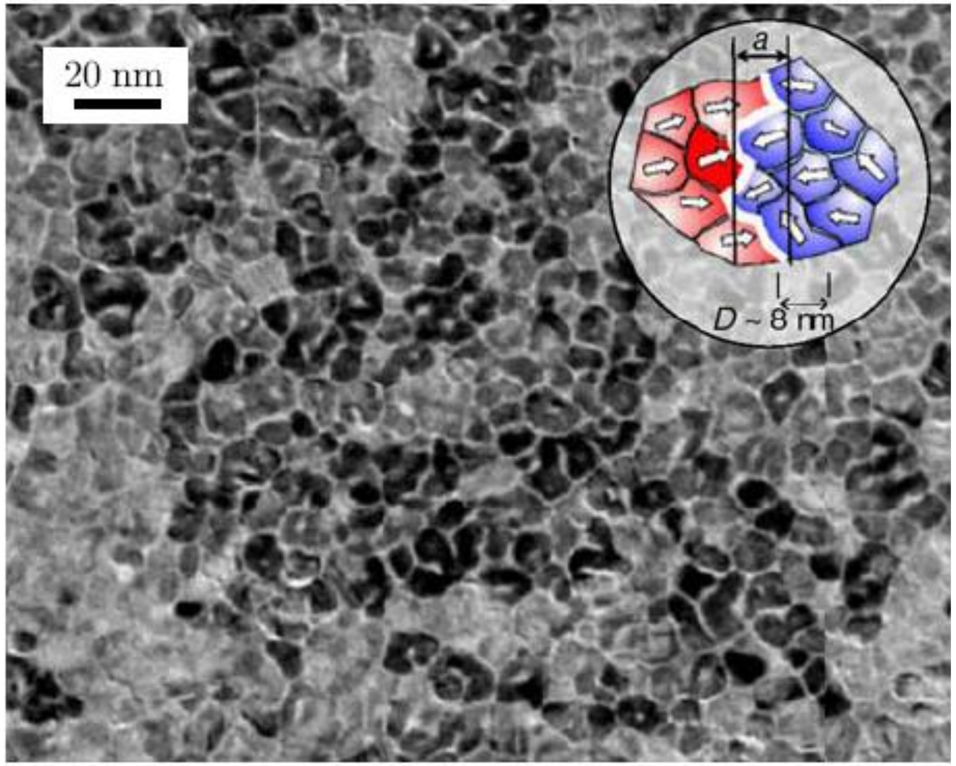

The inset sketch the border between two bits.
Each bit consist of several tens of grains. The bit size and shape is defined during the head writing process

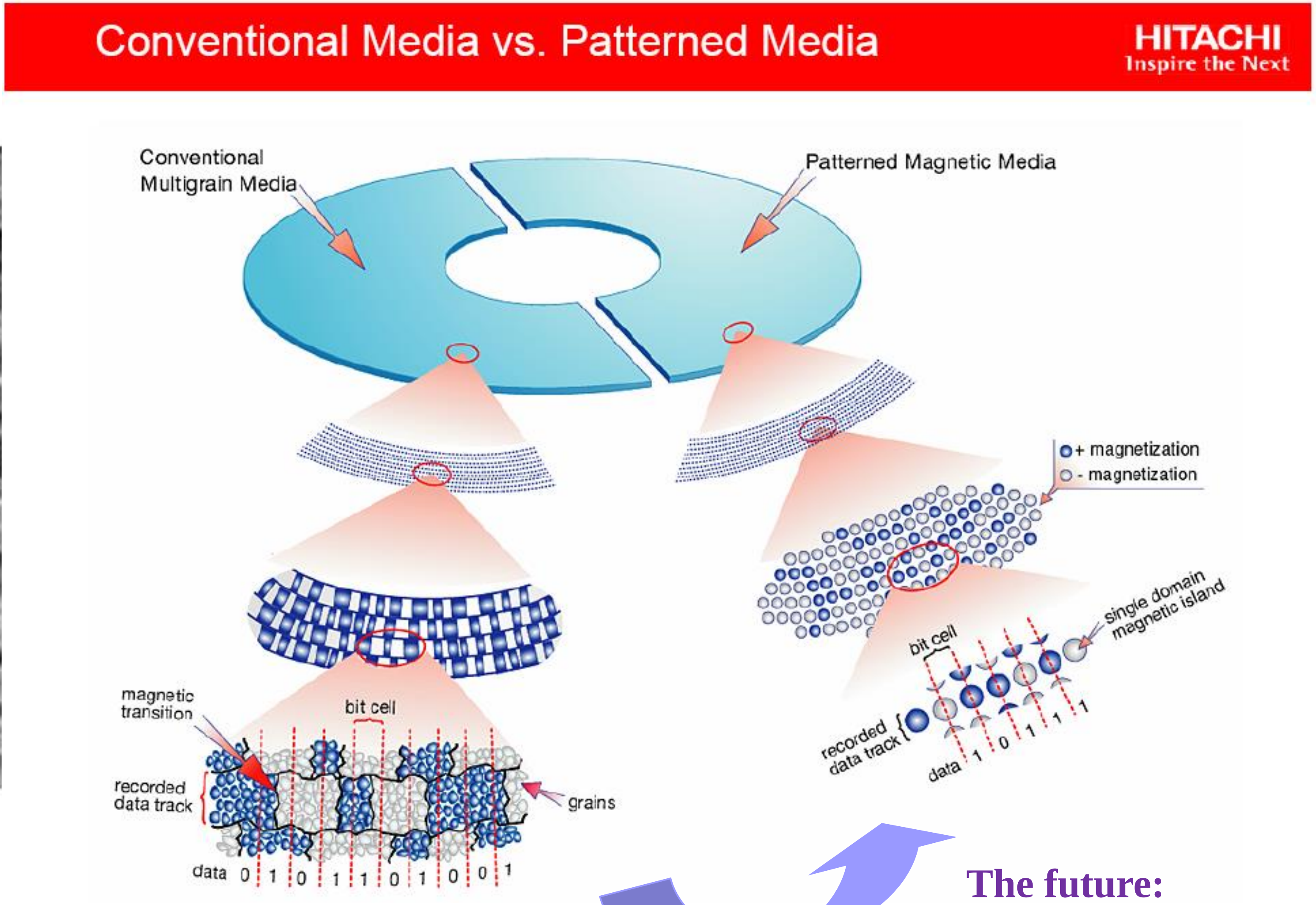

1 bit ≈ 50 grains

The future: single particle per bit

Moser, *et al.* J. Phys. D: Appl. Phys. **35**, R157 (2002). T. R. Albrecht, *et al.* IEEE Trans. Magn. **51**, 0800342 (2015).

Grain as a macrospin

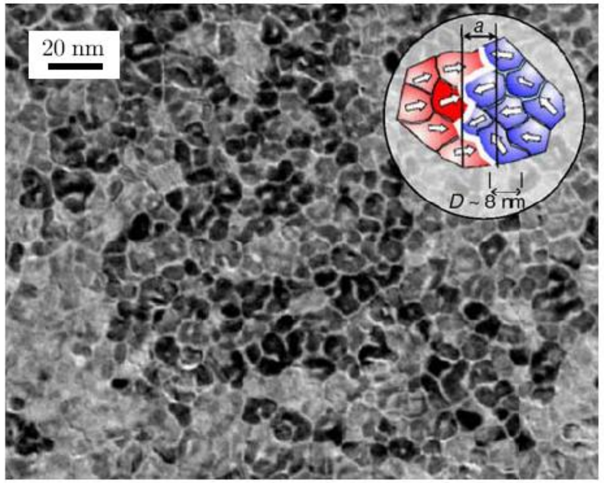

The grain (particle) can be described as a single **macrospin**

$$M = \Sigma_i S_i$$

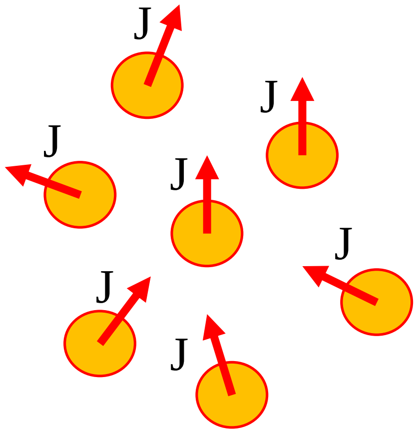

Isolated atoms
with moment J

Grain (particle) formation:
1) Quenching of L
2) $J \approx S$

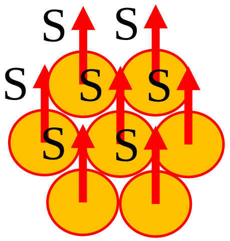

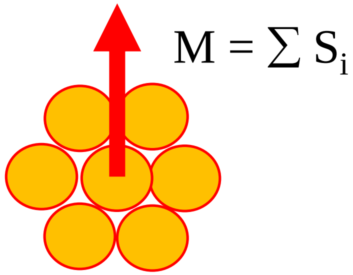

All atomic spins in the grain are ferromagnetically aligned:

Exchange energy:

$-2 J_{ex} S_i S_j$

Exchange breaking layer: oxide phase for grain decoupling

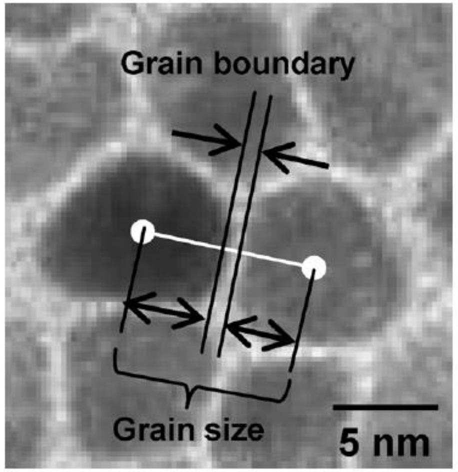

Fig. 1. Plan-view TEM image of CoCrPt-SiO_2 with definition of grain size and grain boundary width. White dots in the image show the centroids of each grain.

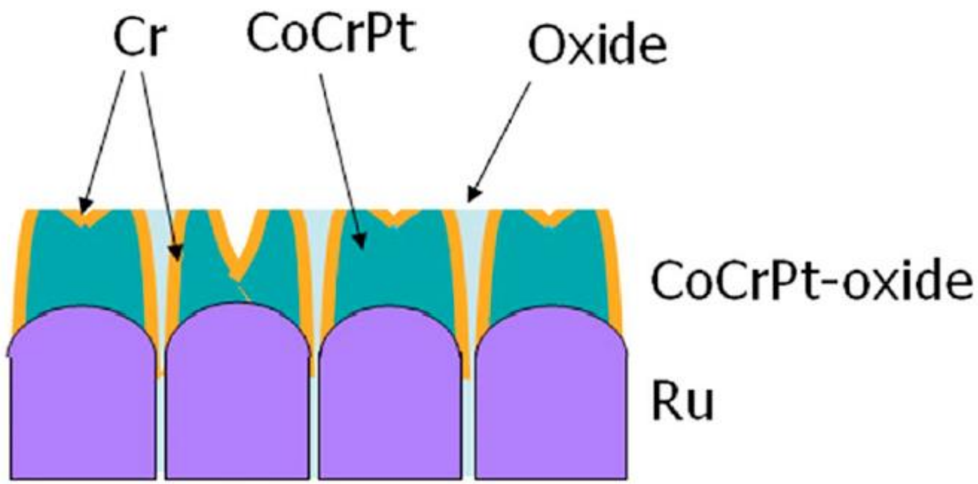

FIG. 3. (Color online) Schematic of a possible mechanism for tooth growth.

SiO_2 is non magnetic (S = 0)

↓

The inter-grain exchange interaction is stopped by the oxide layer: every grain is independent of the others

R. Araki, *et al.* IEEE Trans. Magn. **44**, 3496 (2008).

D. E. Laughlin, *et al.* J. Appl. Phys. **105**, 07B739 (2009).

Exchange breaking layer: Magnetic recording technology

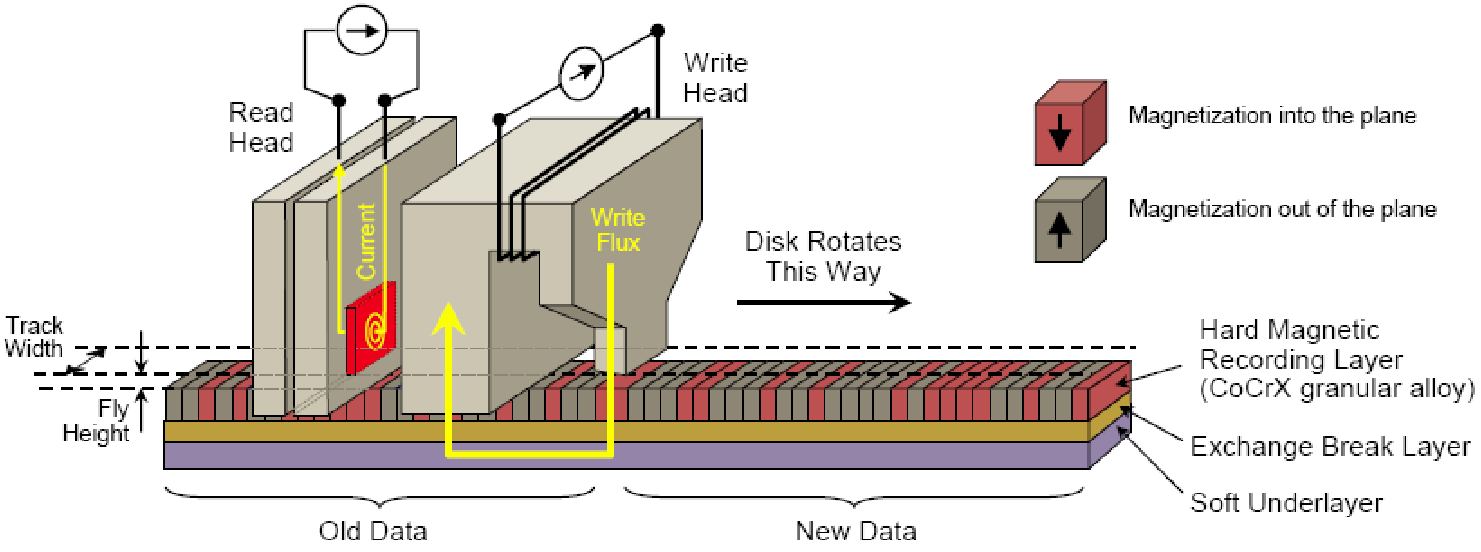

The exchange breaking layer is necessary to decouple the recording layer from the soft underlayer

The soft underlayer helps to close (focalize) the magnetic flux lines reducing the risk of multi-bits writing in PMA media

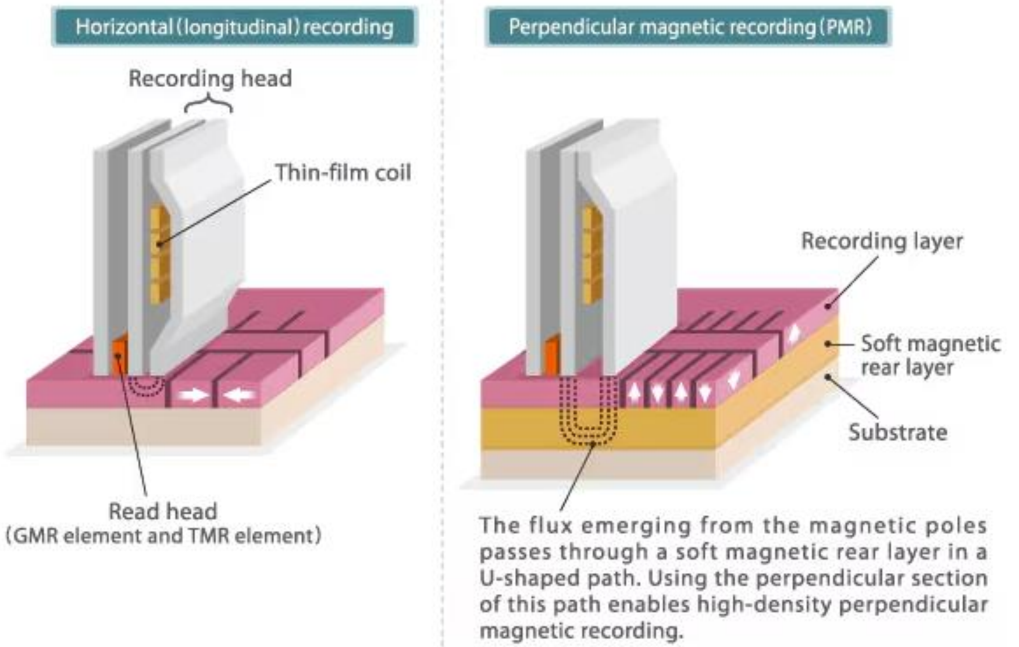

https://www.tdk.com/en/tech-mag/inductive/002

The storage trilemma

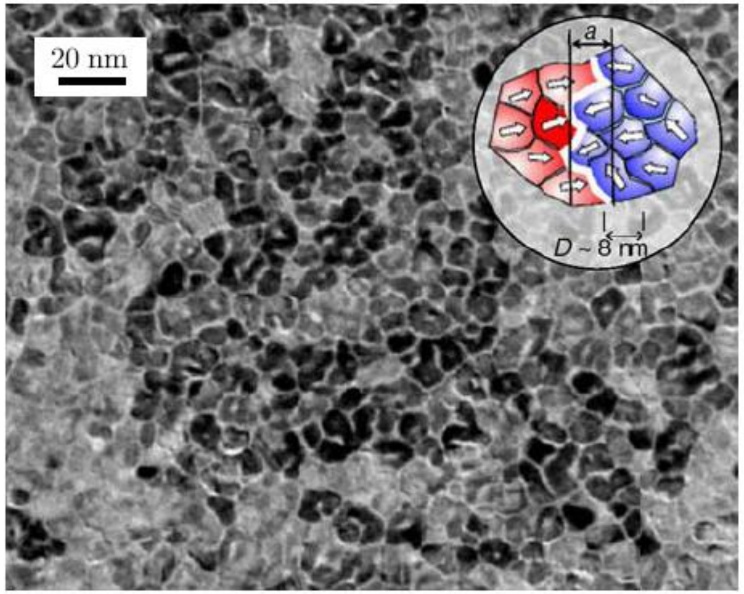

$$\frac{\text{energy barrier}}{\text{thermal energy}} \propto \frac{\text{anisotropy x volume}}{k_B \text{ x temperature}} = \frac{K_u V}{k_B T}$$

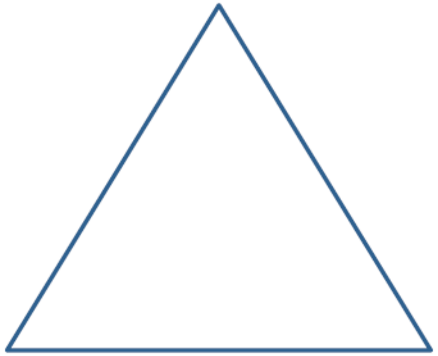

$$SNR \propto \frac{B}{D}\sqrt{\frac{R_W}{D}}$$

B=bit length
D=grain diameter
R_w= reader width

$H_{head} \sim H_{k,}$media $\sim K_u$

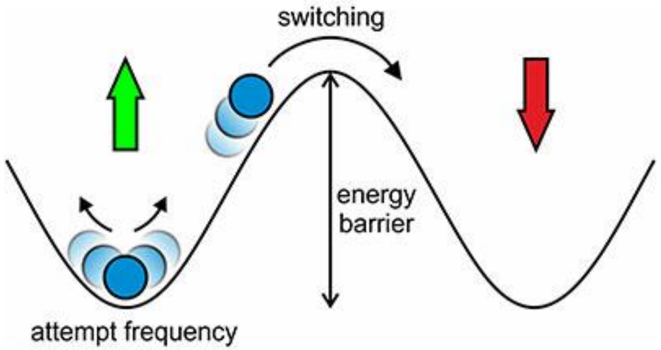

The problem:
To increase SNR, need small grains.
Small grains are thermally unstable.
To avoid thermal instability, increase grain anisotropy Ku.
Increasing Ku increasing media Hc and makes the medium more difficult to write.

Perpendicular recording

HDD media: FePt in the $L1_0$ phase

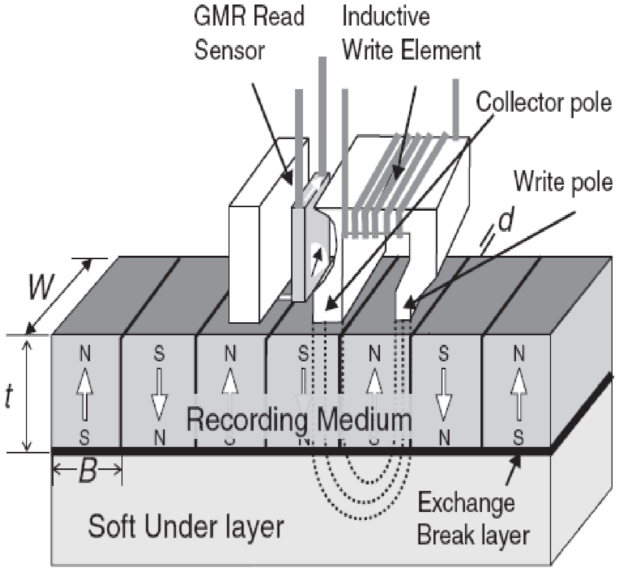

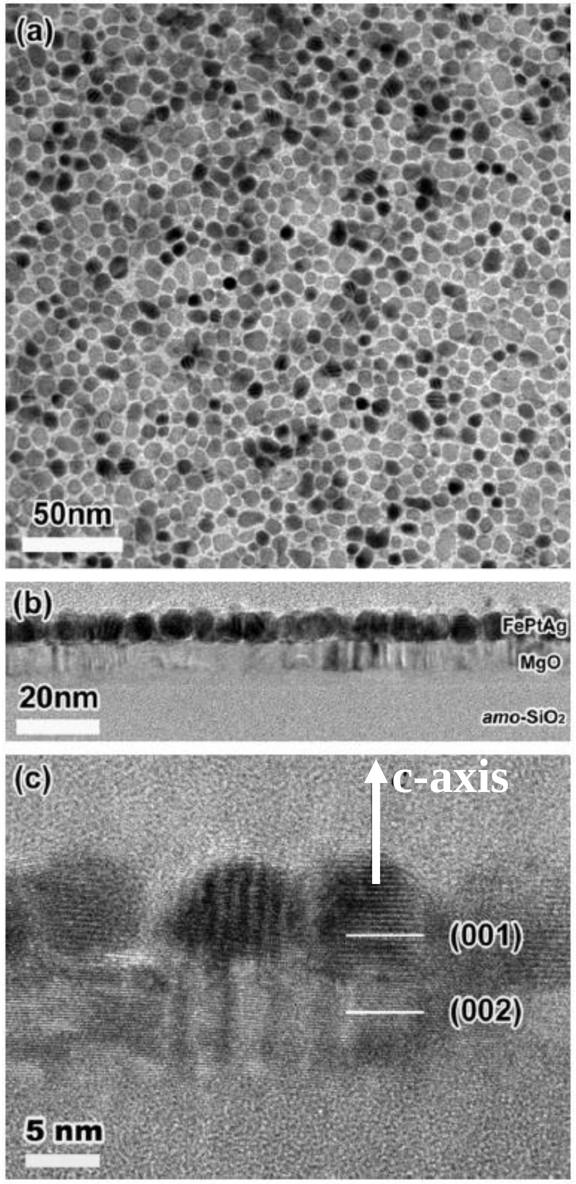

Fig. 8. (a) Bright field plane view image, (b) cross-sectional bright field image, and (c) cross-sectional high-resolution TEM image of the $(FePt)_{0.9}Ag_{0.1}$ −50vol%C film.

L. Zhang *et al.*, JMMM **322**, 2658 (2010)

Effect of crystal structure

Random distribution of Fe and Pt atoms

Ordered distribution of Fe and Pt atoms

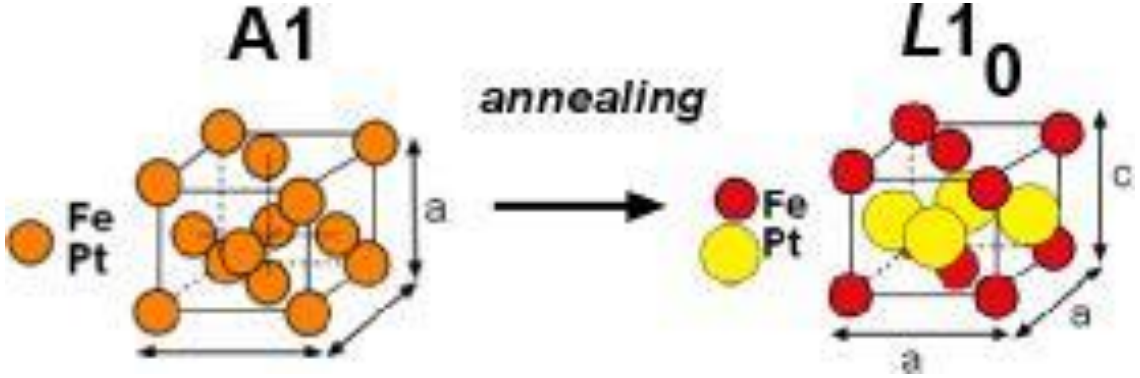

Basically isotropic

Strong easy axis along c-axis

In the alloy, every atom counts the same for the MAE (volume property)

Magnetic media material

	alloy system	material	K_u (10^7 erg/cm^3)	M_S (emu/cm^3)	T = 350 K: H_K (kOe)	T_C (K)	δ=10 nm: D_p (a) (nm)	D_p (b) (nm)	D_p (c) (nm)	δ/<D> =2: D_p (d) (nm)
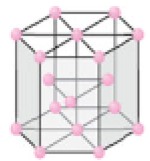	Co-alloys	$CoCr_8Pt_{22}$	0.7	500	28.0	1000[a]	7.3	7.5	8.7	6.4
		Co_3Pt	2	1100	36.4	1200	4.3	5.3	6.1	4.5
		$CoPt_3$	0.5	300	33.3	600	8.6	8.3	9.7	7.2
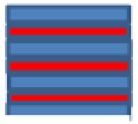	CoX/Pt(Pd) multilayers	Co_3/Pt_{10}	1.2	450	53.3	~700[b]	5.5	6.2	7.2	5.4
		Co_3/Pd_{10}	0.6	360	33.3	~700[b]	7.8	7.8	9.1	6.8
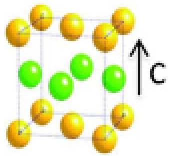	ordered Ll_0/Ll_1 phases	FePd	1.8	1100	32.7	760	4.5	5.4	6.3	4.7
		FePt	7	1140	122.8	750	2.3	3.5	4.0	3.0
		CoPt	4.9	800	122.5	840	2.7	3.9	4.5	3.4
		MnAl	1.7	560	60.7	650	4.7	5.5	6.4	4.8
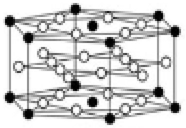 $SmCo_5$	rare-earth transition metals	$Fe_{14}Nd_2B$	4.6	1270	72.4	585	2.8	4.0	4.6	3.4
		$SmCo_5$	20	910	439.6	1000	1.4	2.4	2.8	2.1

D_p is the average thermally stable grain diameter assuming $KV/k_BT = 60$ and $T = 350$ K, $k_B = 1.3807 \times 10^{-16}$ erg K^{-1} and volumes (a) $V = \pi/4 \times D^2 \times 10$ nm (cylinders), (b) $V = D^3$ (cubes), (c) $V = 4/3 \times \pi \times (D/2)^3$ (spheres) and (d) $V = \pi/4 \times D^2 \times \delta$ (cylinders with $\delta/D = 2$). The thickness δ is 10 nm or larger in today's media but will drop for smaller diameters going forward.

[a] T_C in today's alloy media depends on the Cr and Pt content and has increased.

[b] T_C in multilayers strongly depends on the Co thickness.

1 kOe = 0.1T

All these materials require at least a few T to be written

For ex.: fcc with a=0.4 nm (4 atoms in the cube) ➡ 1 erg/cm^3 ≅ 1.2 10^{-8} meV/atom

https://doi.org/10.1002/pssa.201329106

Next-generation: Thermal assisted magnetic recording (TAMR)

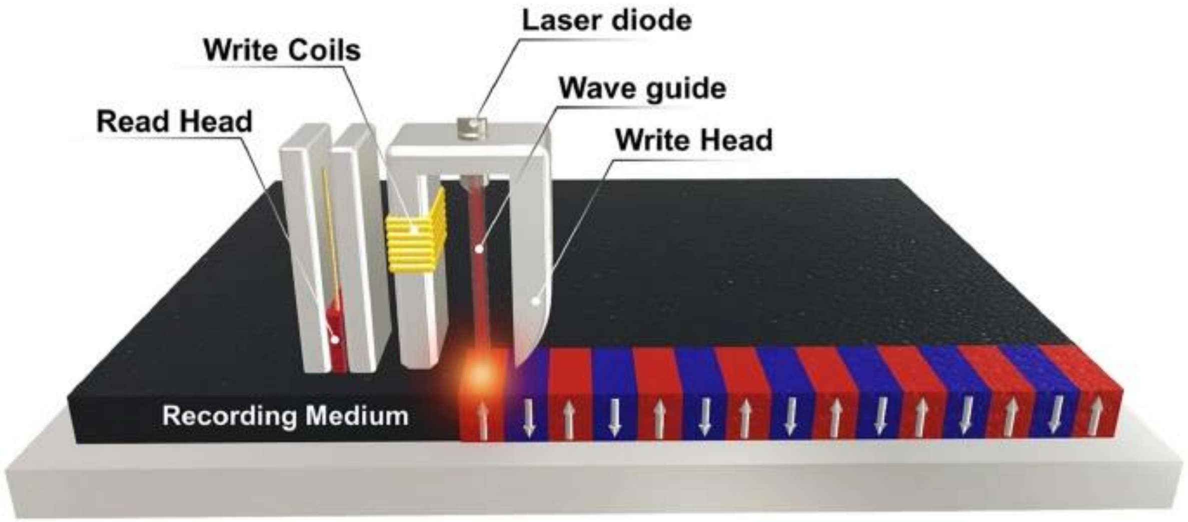

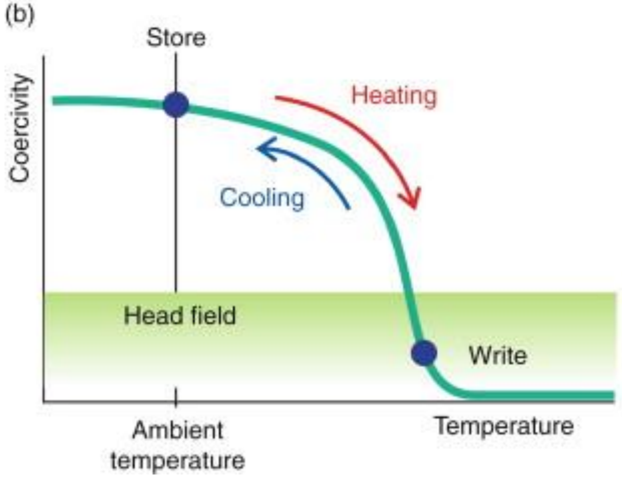

Thermal assisted magnetic recording technology for next-generation HDDs

When the aperture for the laser beam is made smaller than its wavelength, the beam will no longer pass through it, and a near-field beam will be created in a region at or very close to the aperture.

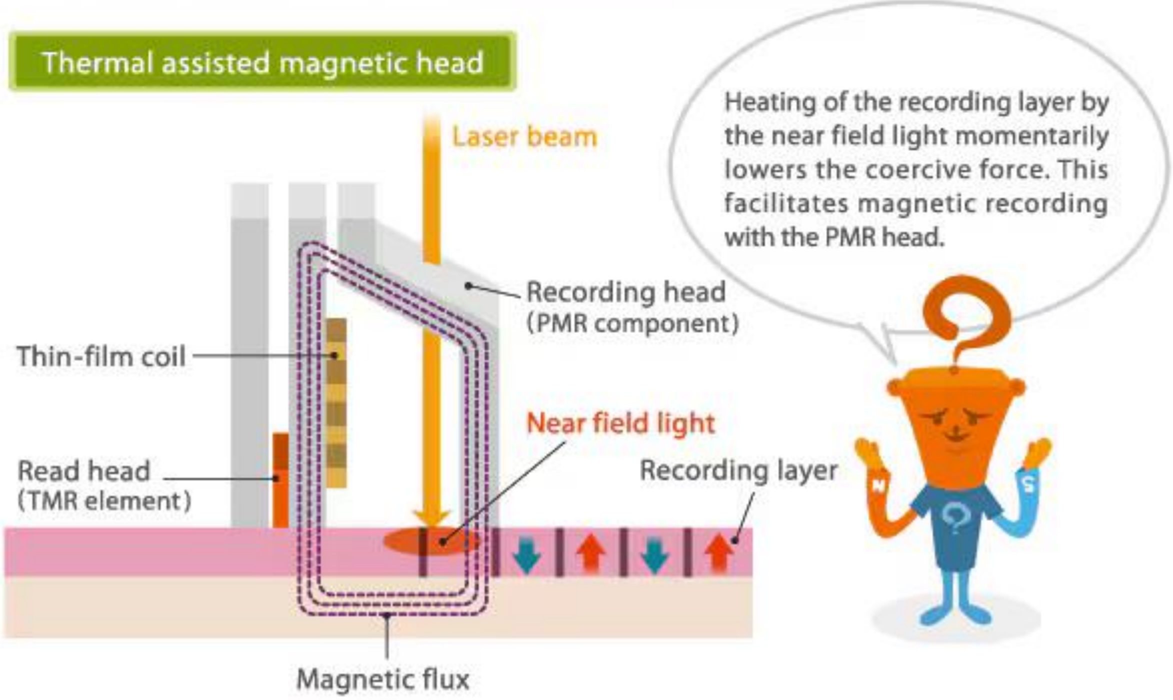

Sci Rep **15**, 2776 (2025). https://doi.org/10.1038/s41598-025-87044-1

https://www.tdk.com/en/tech-mag/inductive/002

Next generation: Multi-level heat-assisted magnetic recording

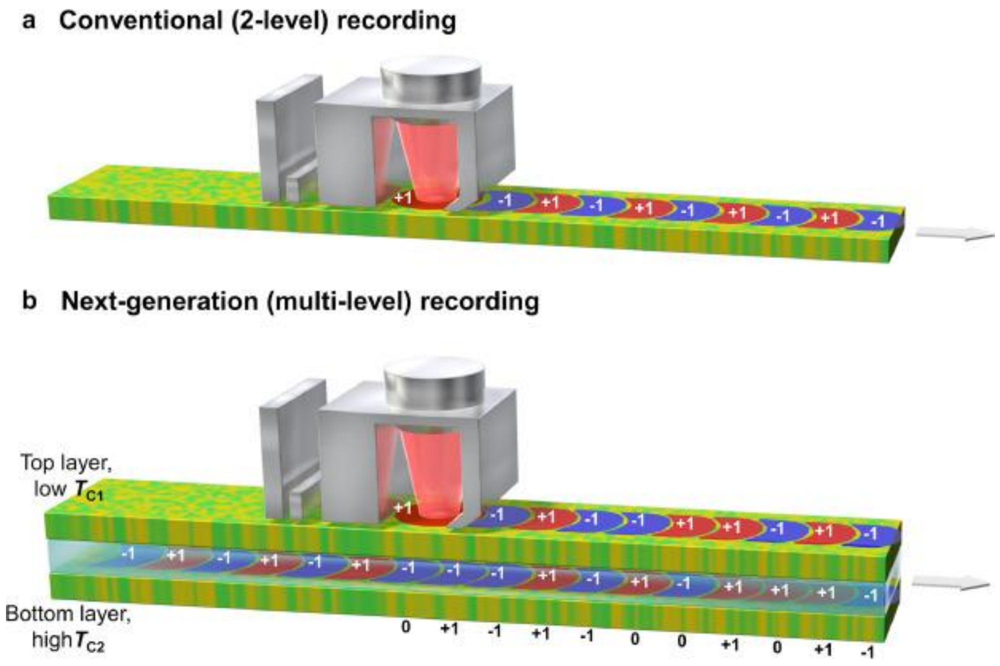

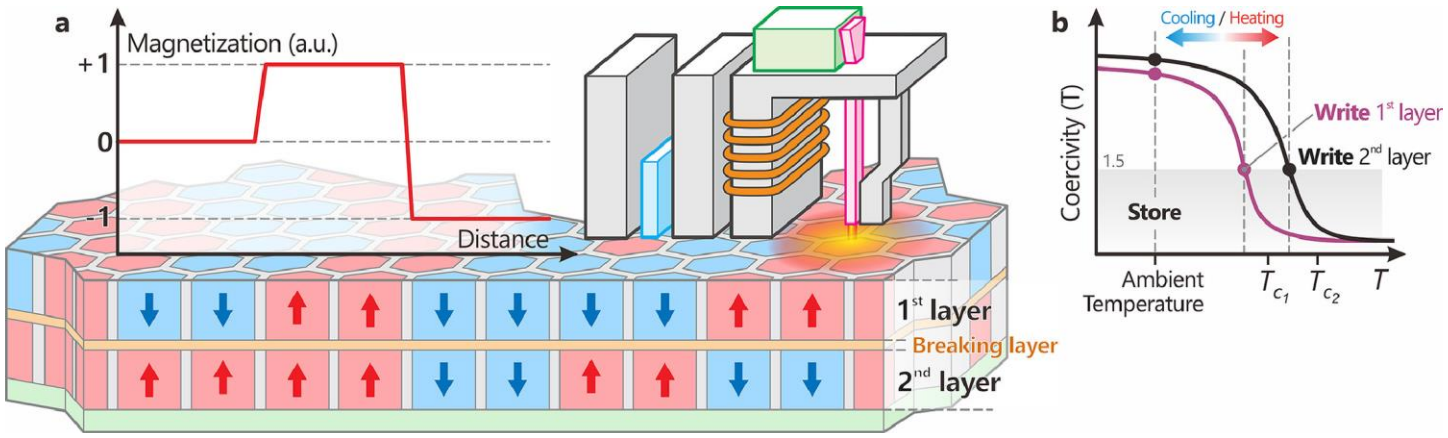

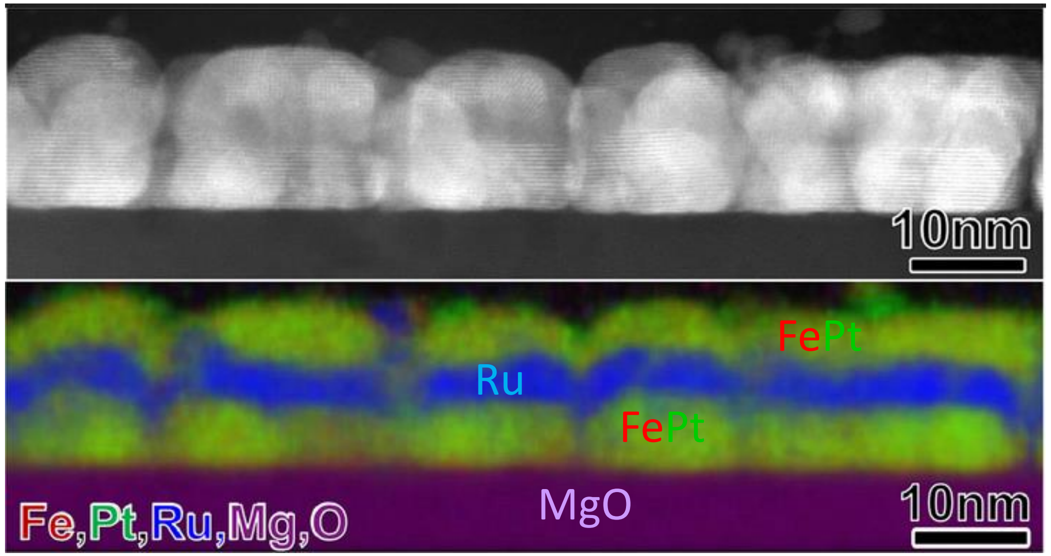

For multi-level recording, the laser power is tuned along with the polarity of the write field to manipulate the magnetization switching of each layer.

During the first write operation, a high laser power is set to heat a small area above T_{c2} of the bottom layer ($T>T_{c2}$) and thus write both layers.

During the second write, the laser power is lowered below T_{c2} ($T>T_{c1}$) to write only the top layer.

This delivers four different magnetic states (↑↑ ("1"), ↓↓ ("−1"), ↑↓ ("0"), and ↓↑ ("0")) which correspond to a 4-level recording. The recording medium is only a few nm thick, while the breaking layer is half that thickness.

https://doi.org/10.1016/j.actamat.2024.119869

Spin valve

Writing:
the head stray field defines the magnetization direction of the recording medium

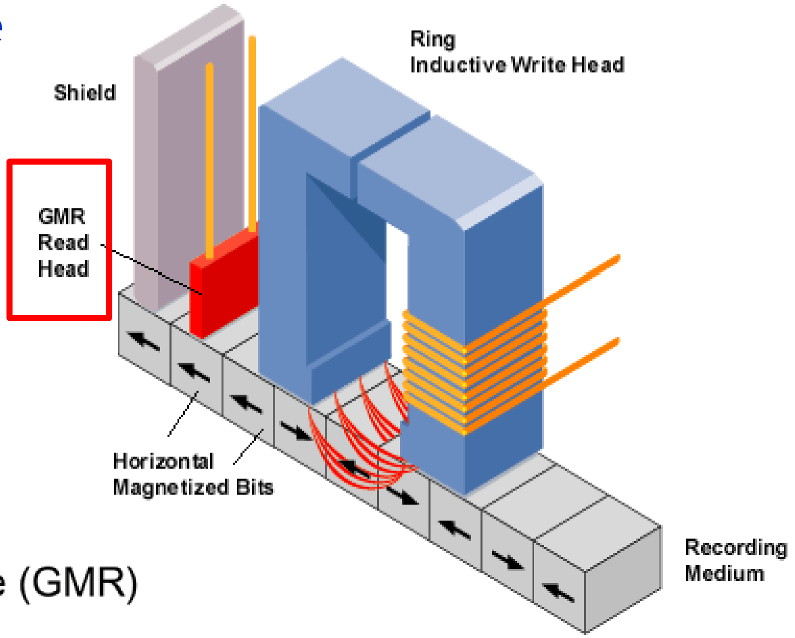

Both reading head in HDD
and
MRAM are spin valves

Reading: spin valve

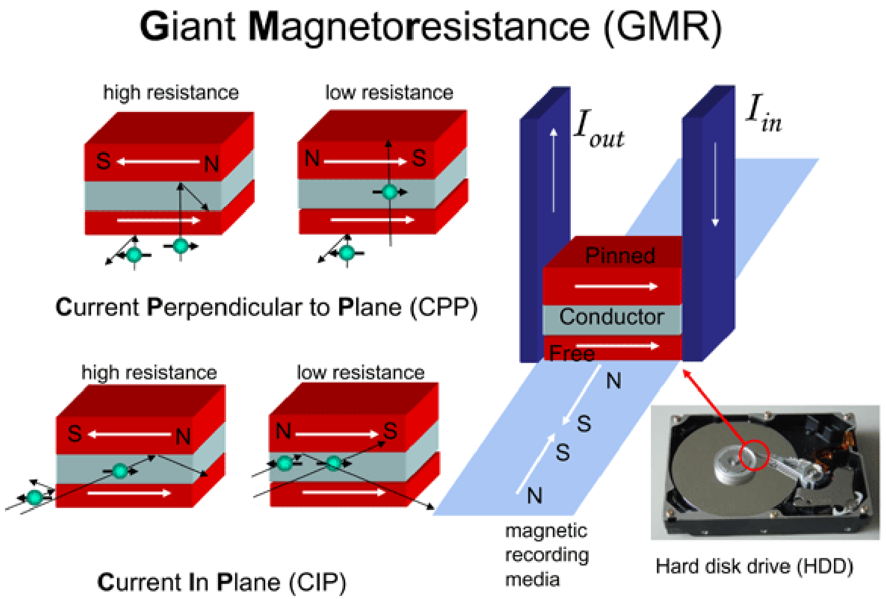

Magnetic random access memory (MRAM)

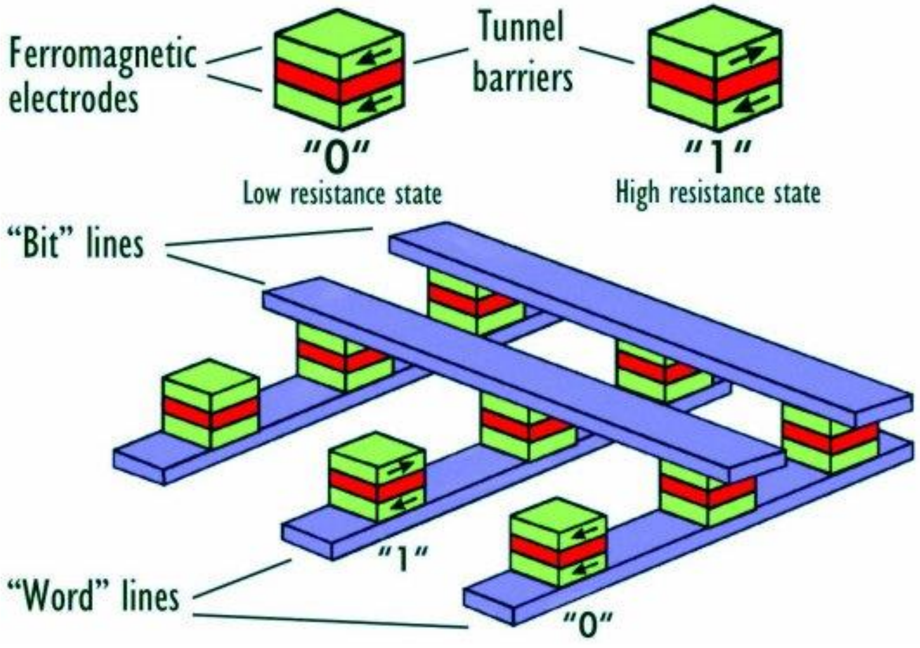

GMR: Giant magneto resistance

1

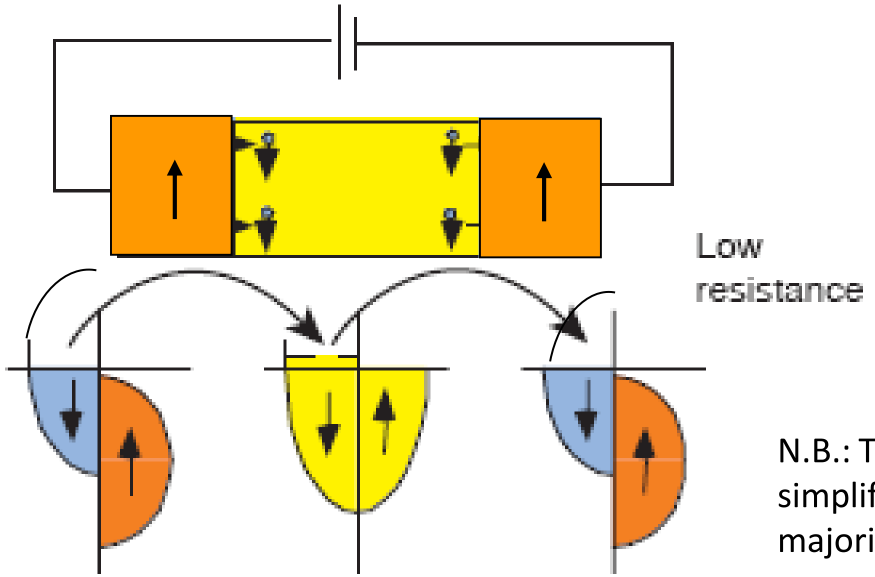

Available free states with the same spin:
Low resistance

N.B.: The DOS correspond to a very simplified sketch with fully occupied majority states

0

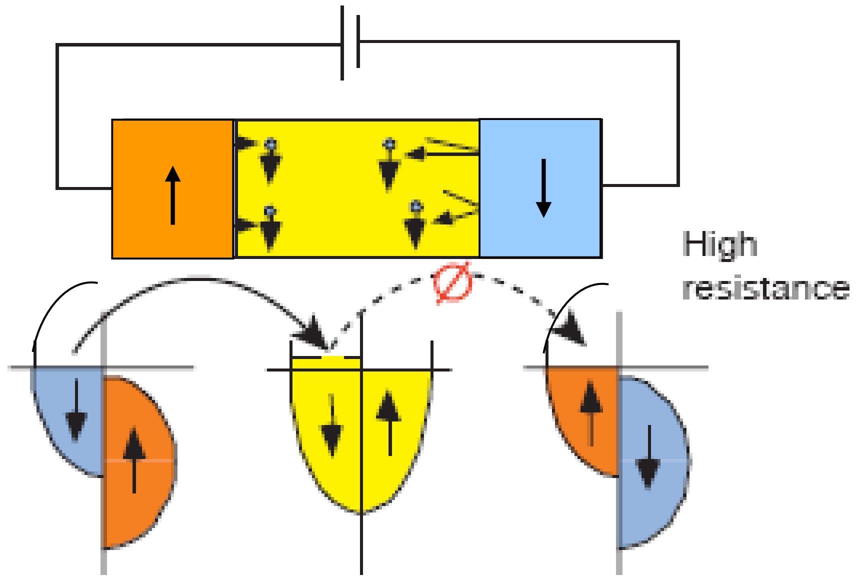

Absence of free states with the same spin:
High resistance

Science **282**, 1660 (1998); Nat. mater. **6**, 813 (2007)

Spin transport in tri-layers with insulating spacer: TMR

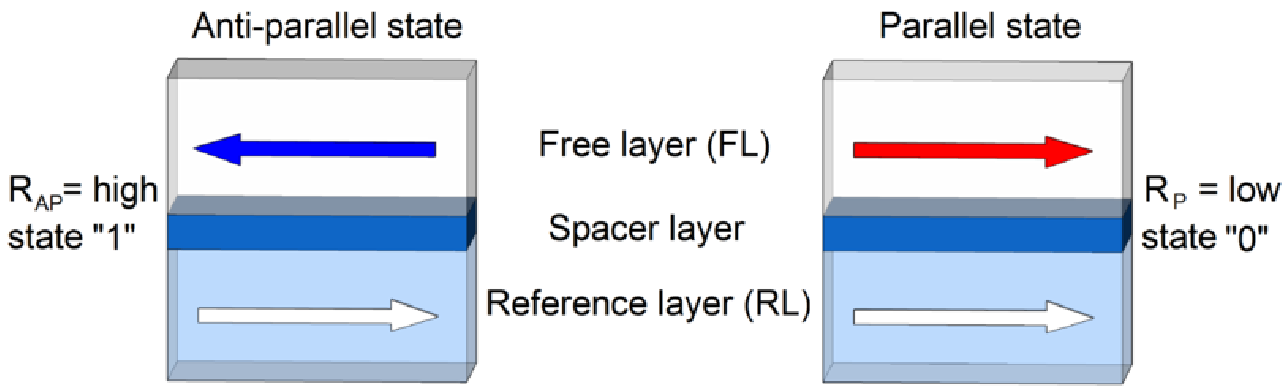

TMR: Tunnel magneto resistance

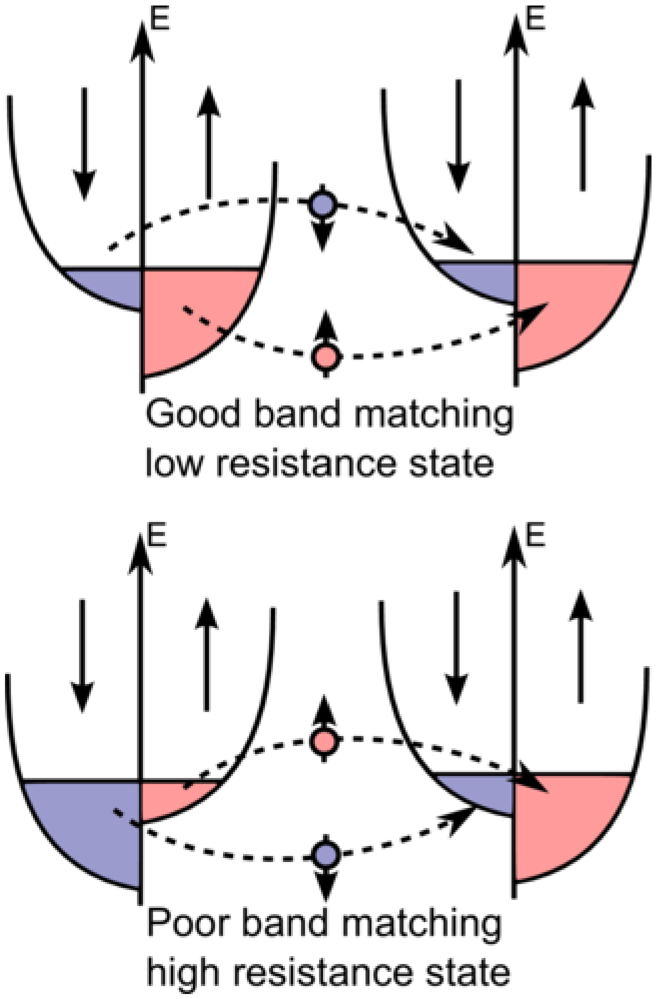

Low resistance

High resistance

In both GMR and TMR the orientation of the magnetization in the free layer is used as a valve to have high or low current: **spin valve**

https://www.iue.tuwien.ac.at/phd/makarov/dissertationch4.html

Spin polarized current

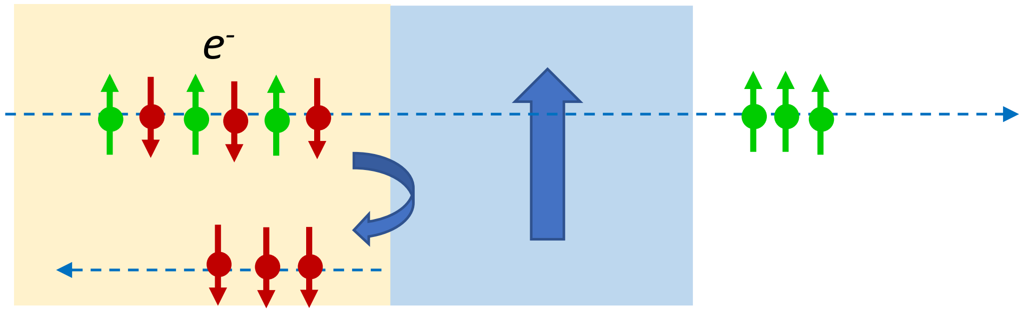

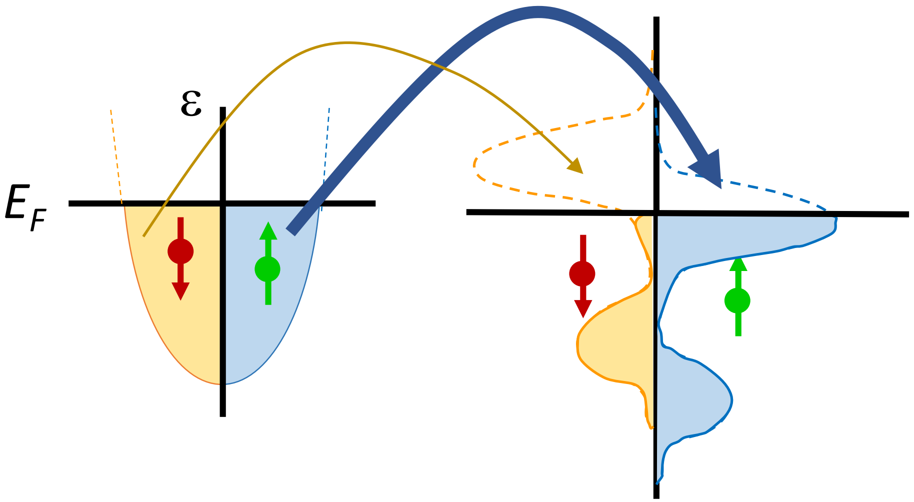

The DOS close to Fermi level determines the current spin polarization

Charge current: $J_c = J^+ + J^-$

Spin current: $J_s = \frac{\hbar}{2e}(J^+ - J^-)$

Spin polarization (at E_F): $P(E_F) = \frac{N_\uparrow(E_F) - N_\downarrow(E_F)}{N_\uparrow(E_F) + N_\downarrow(E_F)}$

Spin polarization at E_F

Material studied	Point	Base	N	P_T (%)	P_C (%)
NiFe	Nb	$Ni_{0.8}Fe_{0.2}$ film	14	25 ± 2	37 ± 5
Co	Nb	Co foil	7	35 ± 3	42 ± 2
Fe	Ta	Fe film	12	40 ± 2	45 ± 2
	Fe	Ta foil	14		46 ± 2
	Nb	Fe film	4		42 ± 2
	Fe	V crystal	10		45 ± 2
Ni	Nb	Ni foil	4	23 ± 3	46.5 ± 1
	Nb	Ni film	5		43 ± 2
	Ta	Ni film	8		44 ± 4
NiMnSb	Nb	NiMnSb film	9	–	58 ± 2.3
LSMO	Nb	$La_{0.7}Sr_{0.3}MnO_3$ film	14	–	78 ± 4.0
CrO_2	Nb	CrO_2 film	9	–	90 ± 3.6

R. J. Soulen Jr. et al., Science **282**, 85 (1998)

Magnetoresistance

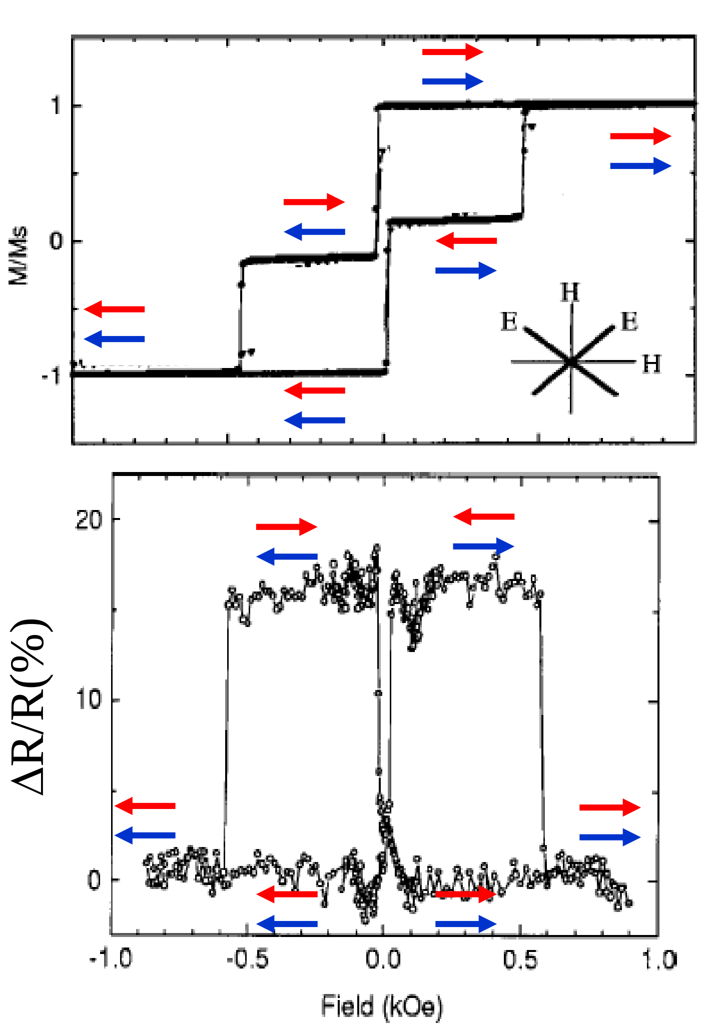

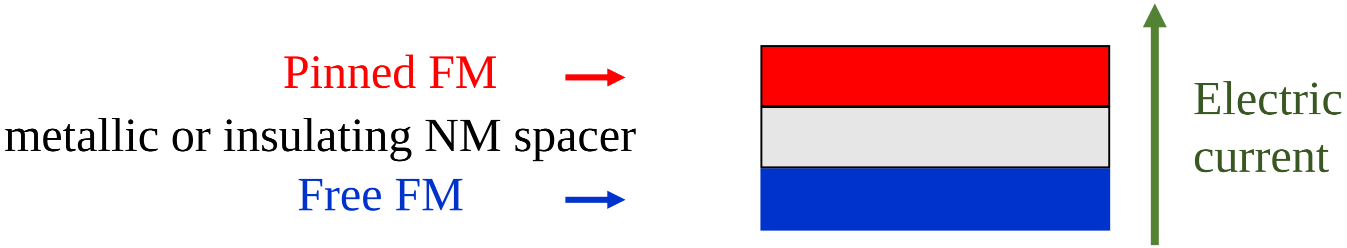

Pinned layer: layer with high reversal field (i.e. high MAE)
Free layer: layer with low reversal field (i.e. low MAE)

Magnetoresistance: $$\Delta R/R = \frac{R_{AP} - R_P}{R_{AP} + R_P}$$

Frequently the optimistic value is used: $\Delta R/R = \frac{R_{AP} - R_P}{R_P}$

High (low) resistance for anti-parallel (parallel) alignment of the magnetization in the two ferromagnetic layers

The atom spins are coupled together by
inter-atomic exchange

Inter-atomic exchange:

MAGNETIC ORDER

$$H_{exc} = -\sum_{i \neq j} J_{ij} \mathbf{S}_i \cdot \mathbf{S}_j$$

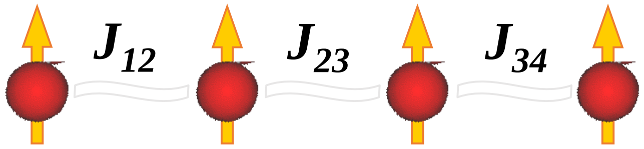

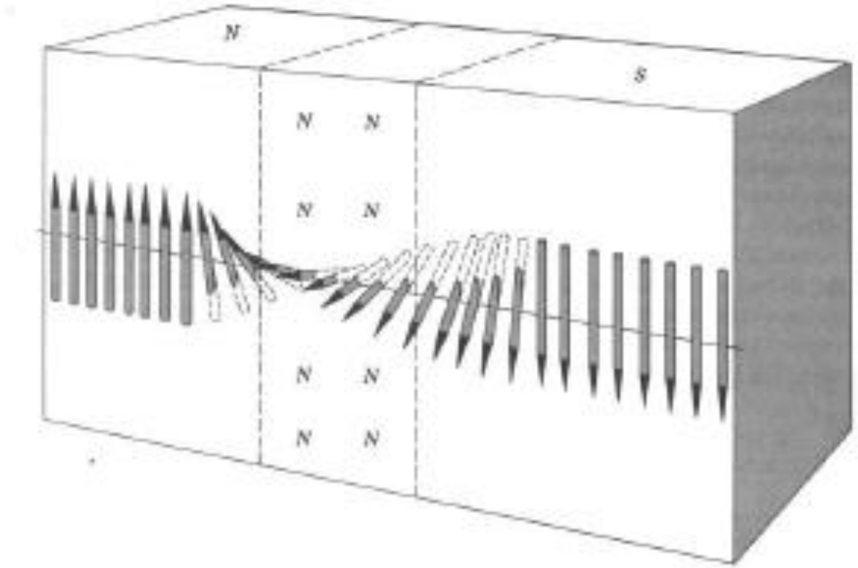

In non magnetic materials $S = 0$ thus $H_{exc} = 0$ $\Rightarrow$ decoupling of free and pinned layer

Pinned layer: Exchange bias or MAE

https://doi.org/10.1016/j.mattod.2017.07.007

Pinned layer:
must not switch

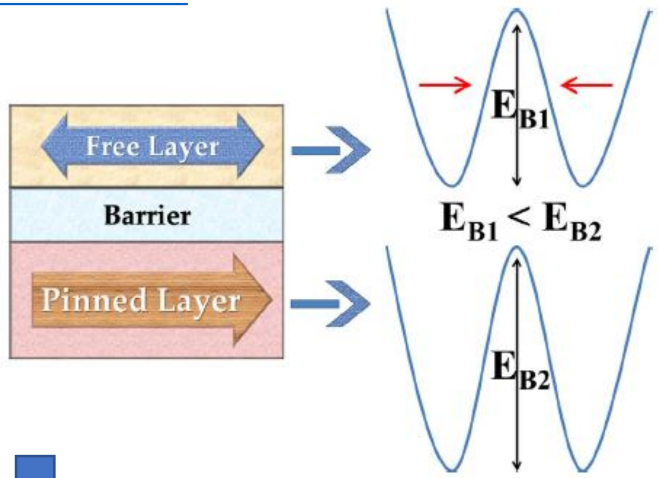

Large MAE

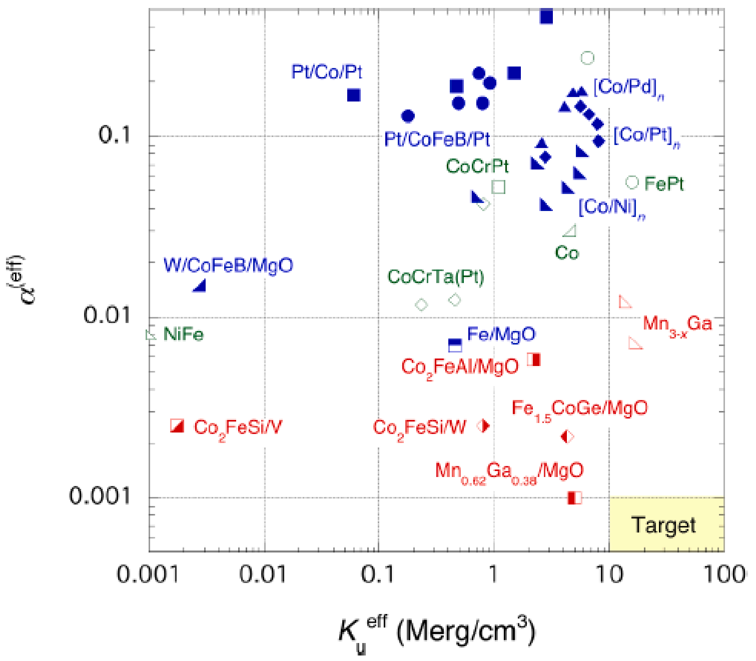

The magnetic field required to reverse the pinned layer is:

$$H_{rev} = H_c + H_E$$

Exchange bias

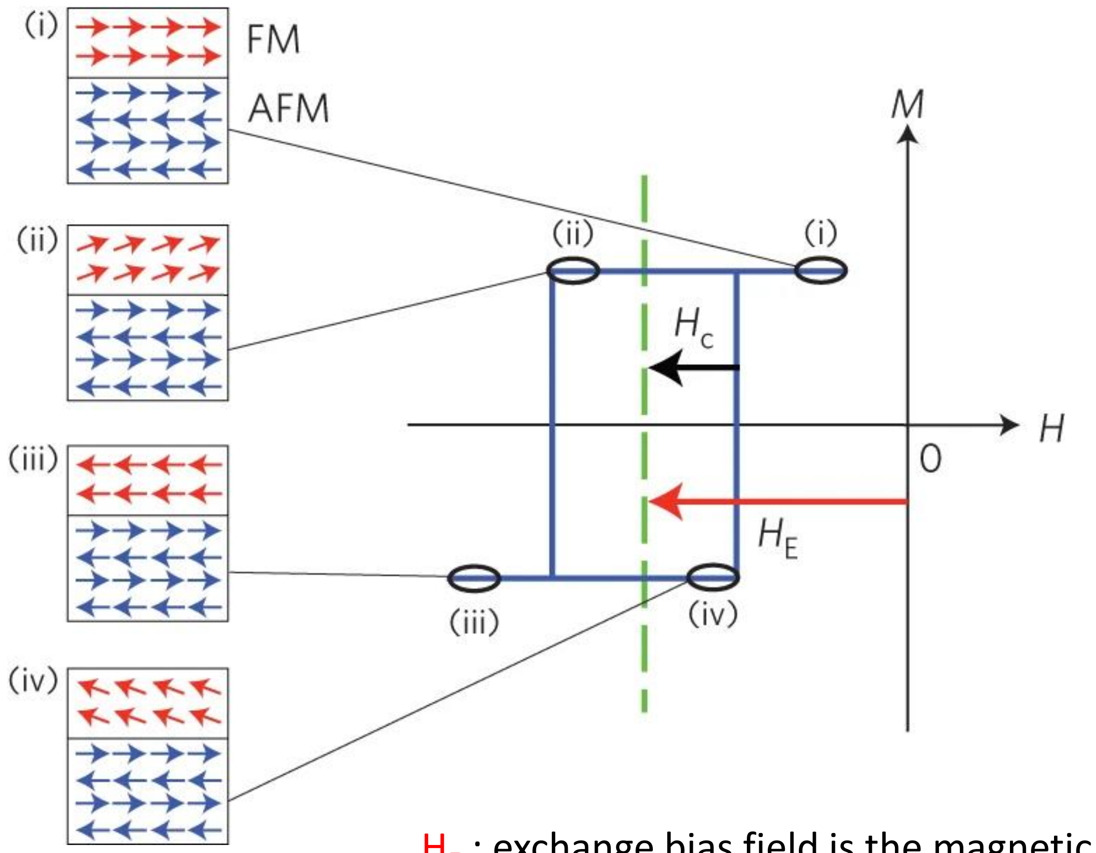

H_E : exchange bias field is the magnetic field shift of the hysteresis curve

https://doi.org/10.1016/j.jmmm.2020.166711

J. Magn. Magn. Mater. **192**, 203 (1999)

GMR (Giant magneto resistance)

The spacer is a metal

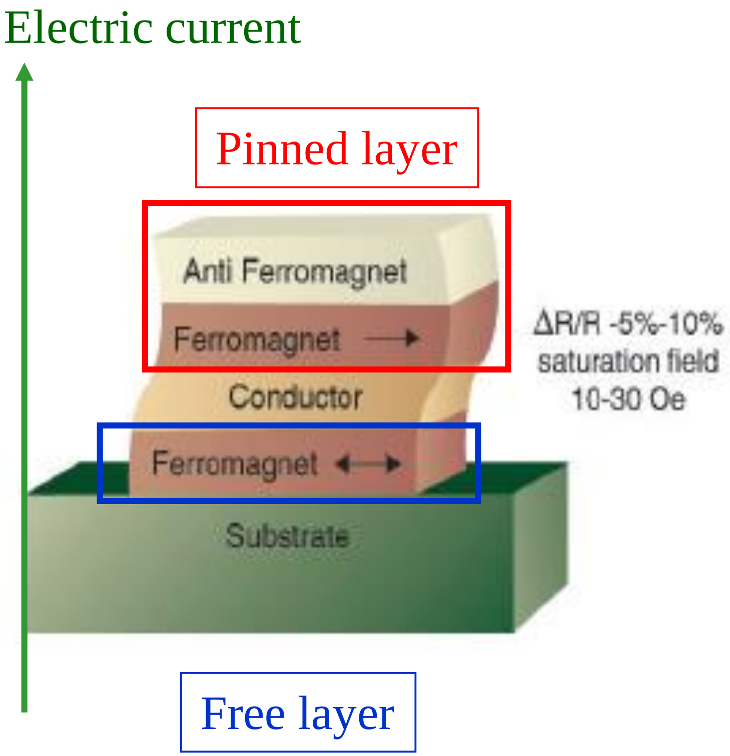

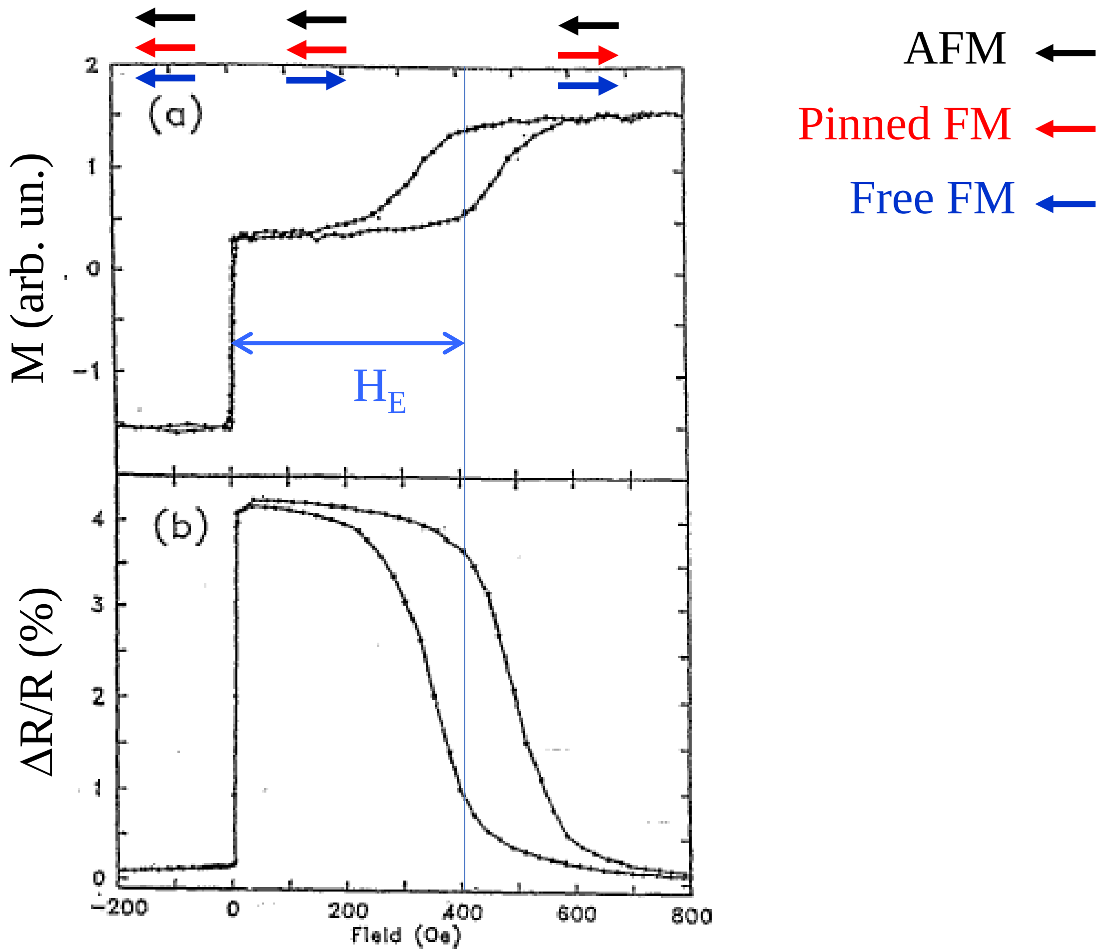

The electric resistance depends on the respective spin orientation of the two FM layers:

Low -> parallel alignment

High -> anti-parallel alignment

J. Appl. Phys. **69**, 4774 (1991); https://doi.org/10.1016/0304-8853(94)00356-4

Spin transport: Mott's "two current model"

- The resistivity arises mainly from electron scattering with energies close to E_F
- Mainly scattering of itinerant *s*-electrons on unoccupied *d*-states ($N_s(E_F)$ is small). Thus, more *d*-states are available, stronger is the scattering and larger is the resistivity
- The spin is conserved (no spin-flip events): $\sigma = \frac{1}{R} = \sigma_\uparrow + \sigma_\downarrow$ (spin-up and spin-down independent channels)

$$\sigma_{\uparrow,\downarrow} = \frac{e^2 n_{\uparrow,\downarrow}\, \tau_{\uparrow,\downarrow}}{m_e}$$

$n_{\uparrow,\downarrow}$= number of free electrons with spin up (down) per unit volume

$$\Gamma_{\uparrow,\downarrow} = \frac{1}{\tau_{\uparrow,\downarrow}} = \frac{2\pi}{\hbar}|\langle d|V_{sd}|s\rangle|^2 N_{\uparrow,\downarrow}(E_F)$$

Fermi's golden rule

Courtesy P. Gambardella

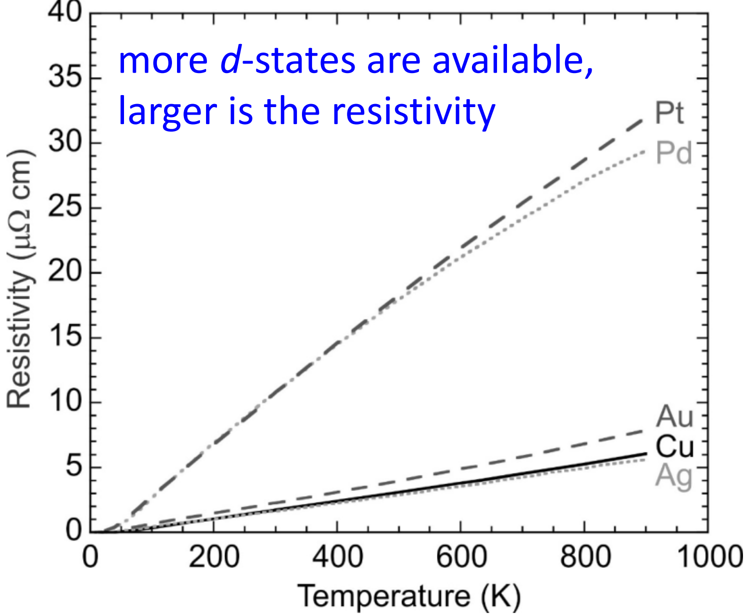

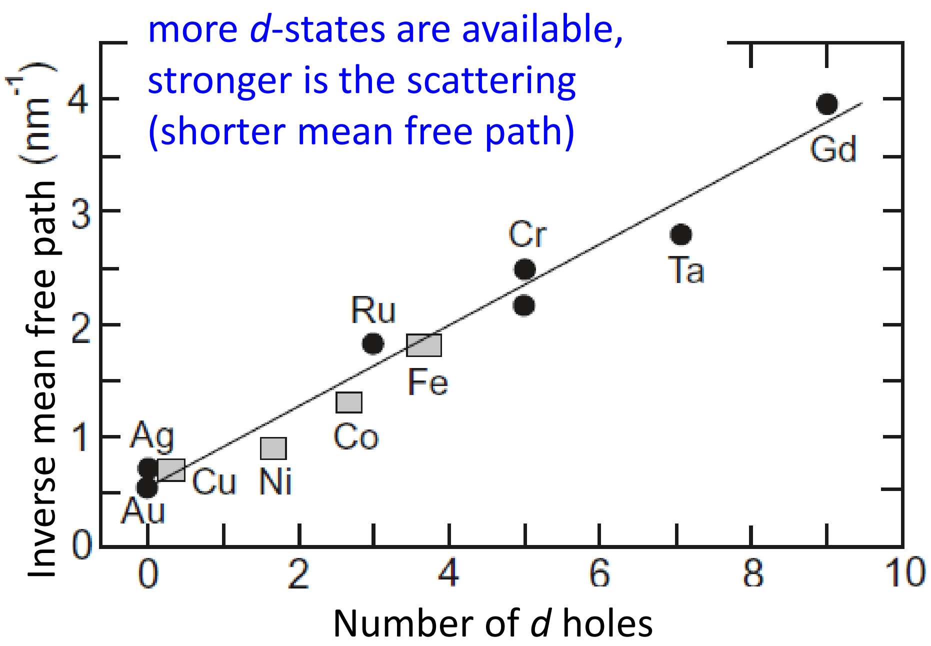

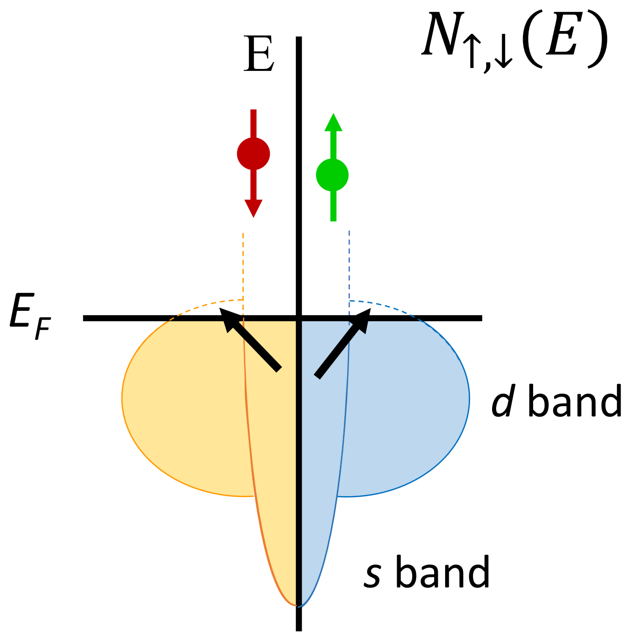

[St&Sie06]

See exercises: 6.1

In a ferromagnet, resistivity for spin-up is different than for spin-down since the scattering probabilities are different due to different density of states at E_F.
These different scattering probabilities and thus resistivities for spin-up and spin-down originates the GMR

Paramagnet: $N_{\uparrow}(E) = N_{\downarrow}(E)$ Ferromagnet: $N_{\uparrow}(E) \neq N_{\downarrow}(E)$

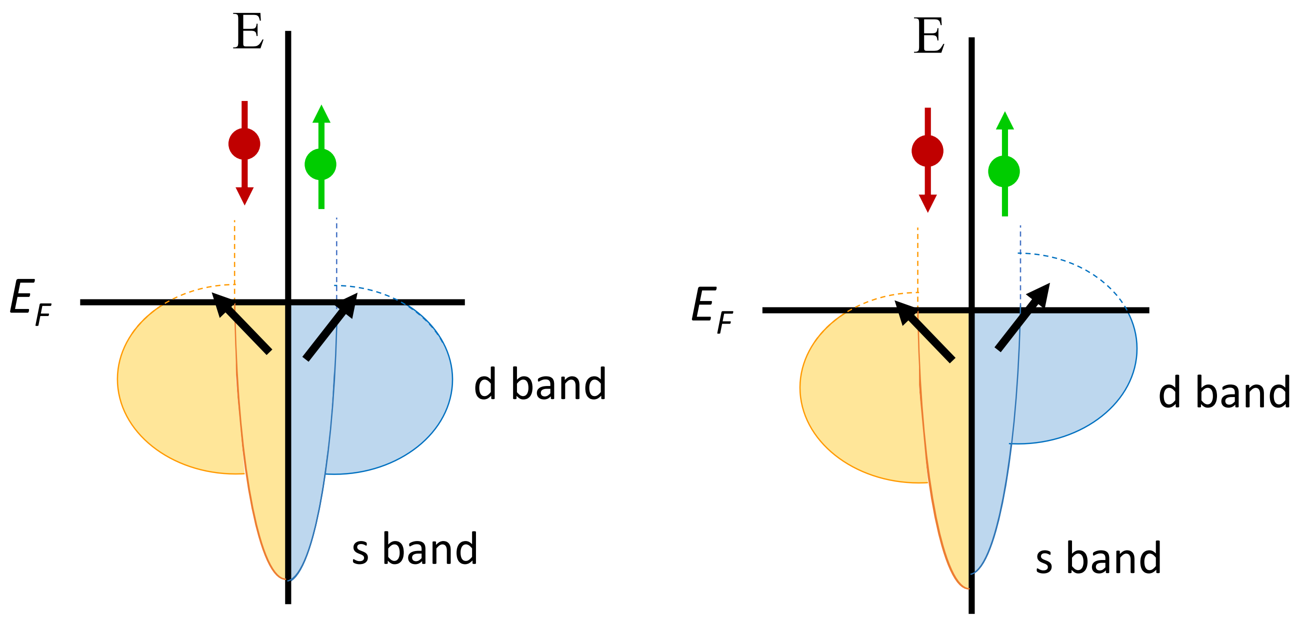

$$\alpha = \frac{\sigma_{\uparrow}}{\sigma_{\downarrow}} = \frac{\rho_{\downarrow}}{\rho_{\uparrow}}$$

$$GMR = \frac{R_{AP} - R_P}{R_P} = \frac{(1-\alpha)^2}{4\alpha}$$

Metal	v_F (10^7 cm/s)	l (Å)	τ (10^{-15} s)	ρ ($\mu\Omega$ cm)
Fe majority	3.3	15	4.5	49
Fe minority	4.1	21	5.1	65
Co majority	7.9	55	7.0	32
Co minority	2.7	6	2.2	141
Cu	10.7	300	28	4.6

$\alpha_{Fe} \approx 1.3$

$\alpha_{Co} \approx 4.7$

Spin transport in tri-layers with insulating spacer: TMR

See exercises: 6.2-6.3

TMR: Tunnel magneto resistance

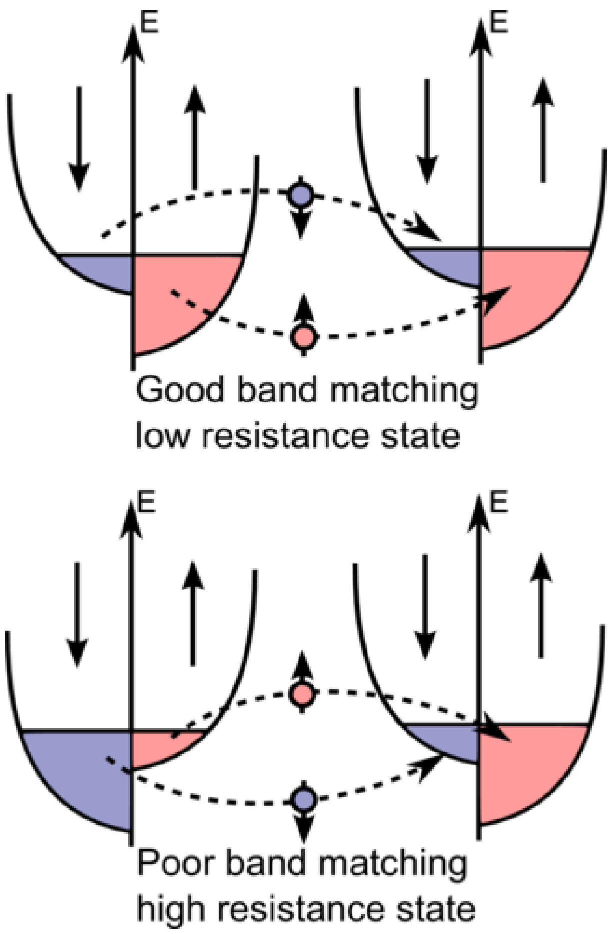

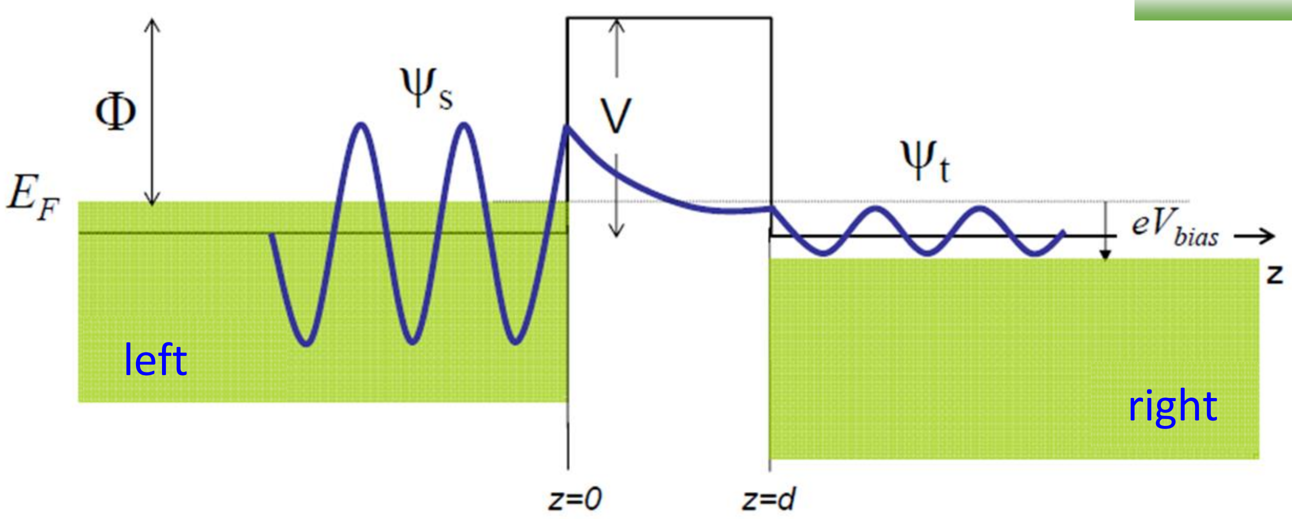

$$\Psi(\mathrm{d}) = \Psi(0)e^{-kd}$$

$$\mathrm{P(d)} = |\Psi(\mathrm{d})|^2 = |\Psi(0)|^2\, e^{-2kd}$$

$$k = \frac{\sqrt{2m\Phi}}{\hbar} \approx 0.51\,\sqrt{\Phi}\ [(\mathrm{eV})^{-0.5}\ \text{Å}^{-1}]$$

$$I \propto V_{bias} N_S(E_F) N_T(E_F) e^{-1.025\sqrt{\Phi}d}$$

$$\mathrm{TMR} = \frac{I_P - I_{AP}}{I_{AP} + I_P} = P_L P_R$$

$P_{L,R}$ is the L, R polarization

Frequently the optimistic value is used: $TMR = \frac{I_P - I_{AP}}{I_{AP}} = \frac{2P_L P_R}{1 - P_L P_R}$

https://www.iue.tuwien.ac.at/phd/makarov/dissertationch4.html

TMR spin valve

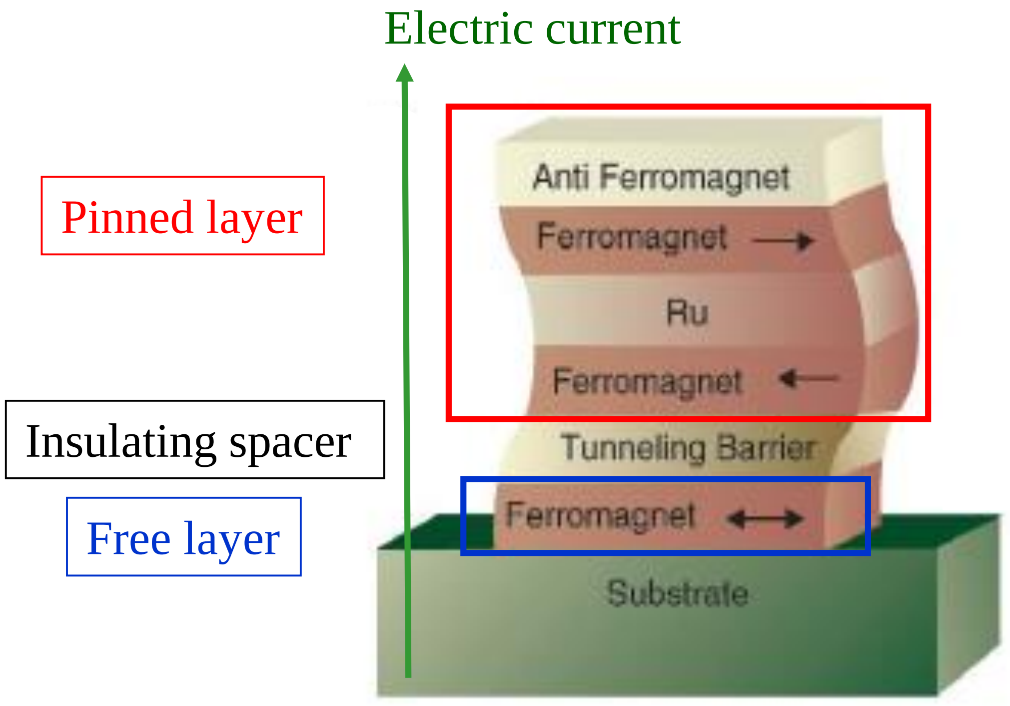

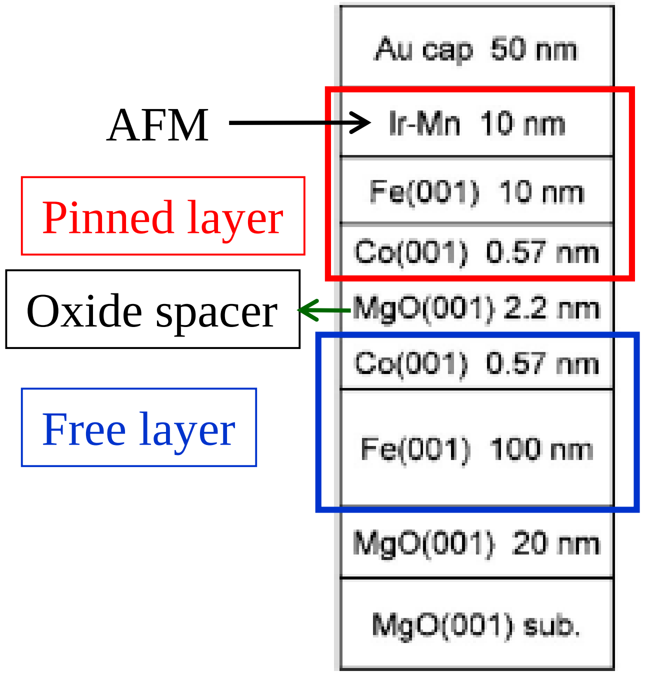

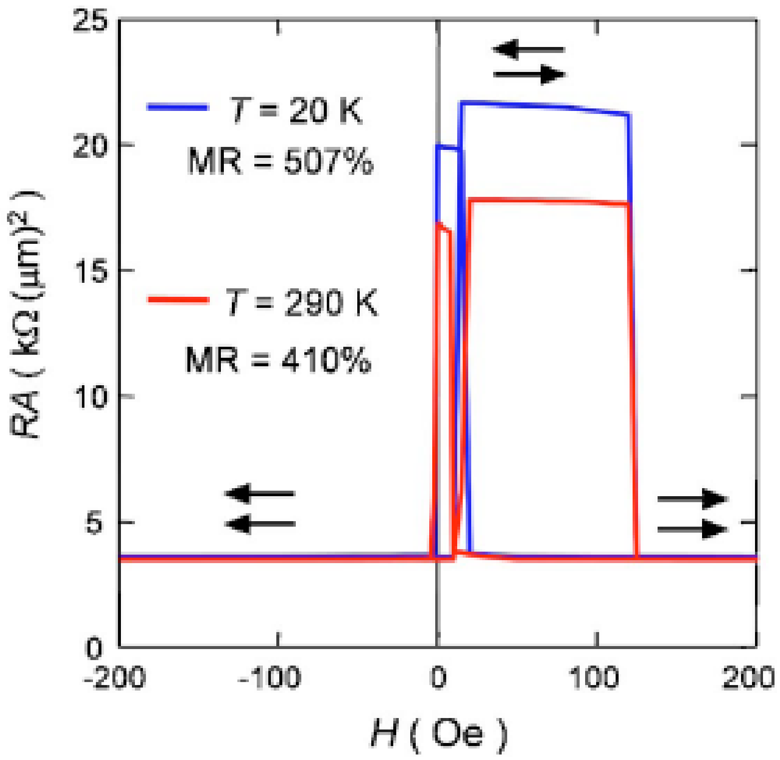

Improved performance with respect to GMR due to:

1) precise control of layer thickness
2) high control of crystallographic structure
3) optimum choice of the materials

Appl. Phys. Lett. **89**, 042505 (2006)

Role of the spacer thickness

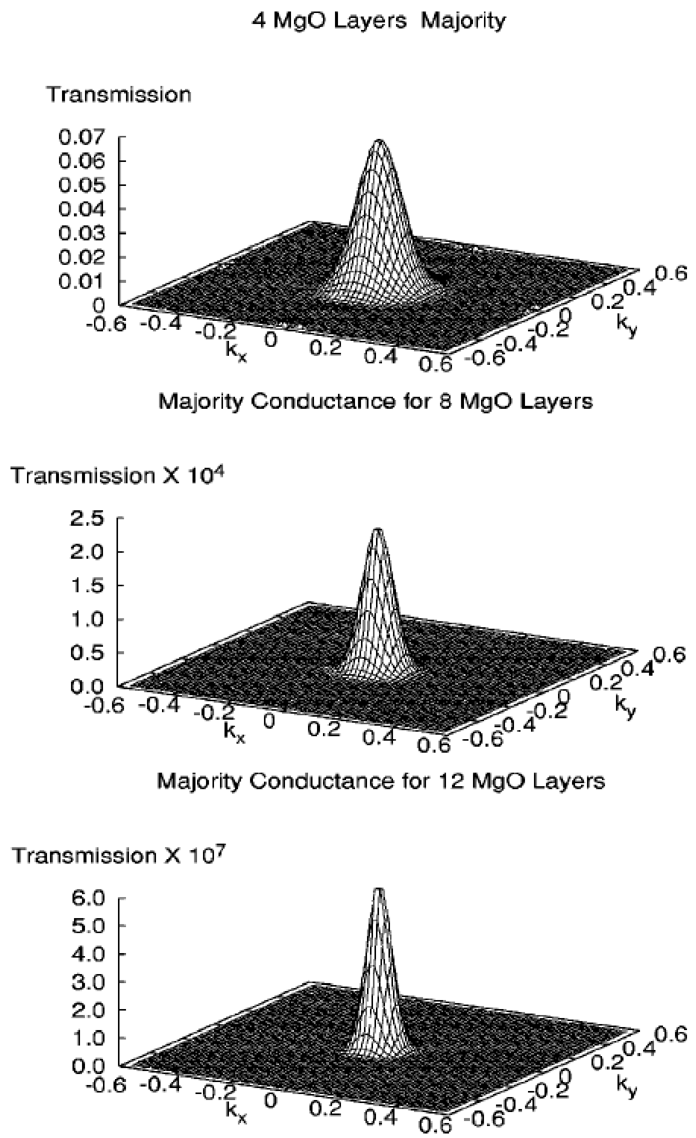

FIG. 6. Majority conductance for 4, 8, and 12 layers of MgO. Units for k_x and k_y are inverse bohr radii.

T = transmission trough the tunnel barrier

$$T \propto e^{-2d\sqrt{\frac{2m(\Phi - E_F)}{\hbar^2} + k_{//}^2}}$$

Transmission strongly dependent on MgO thickness *d* -> Need of high control on MgO roughness to have flat interfaces and thus uniform reading currents

10.1103/PhysRevB.63.054416

Role of composition and crystal structure

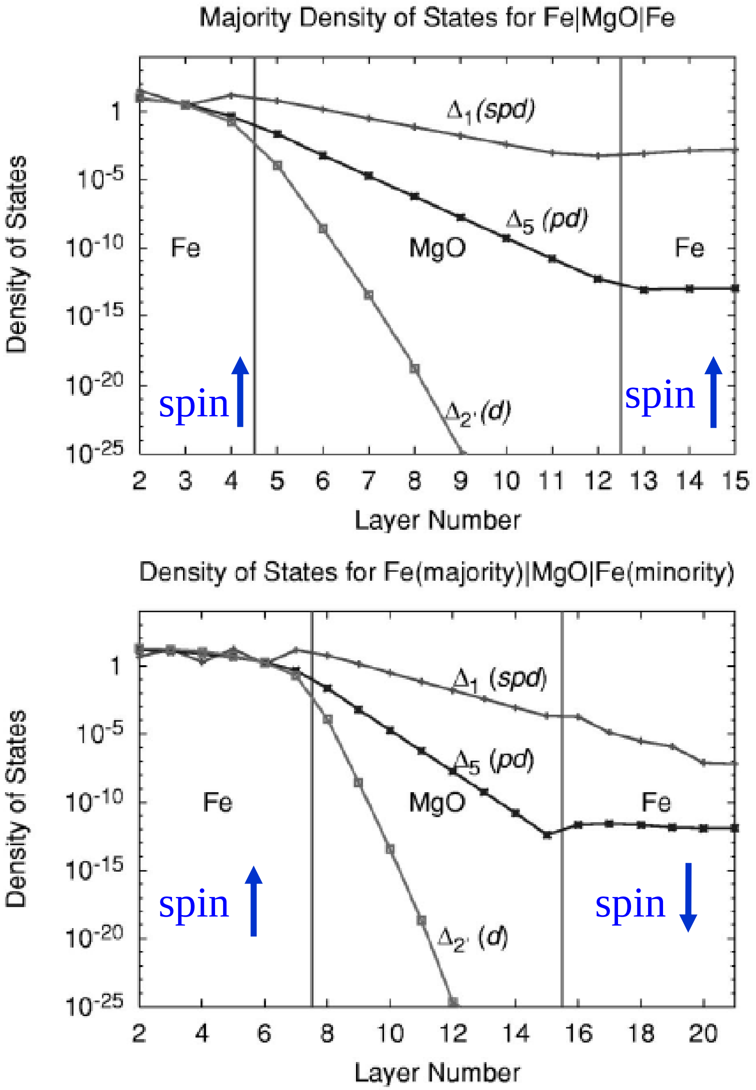

Electron wave function symmetries

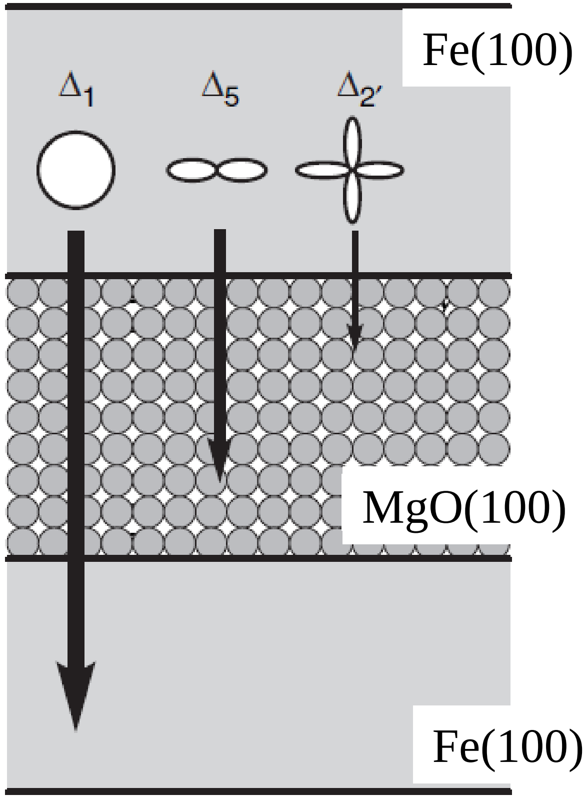

Δ_1 -> totally symmetric wave function with respect to the normal to the tunnel barrier: s, p_z, d_{z^2}.

Δ_1 is a slowly decreasing evanescent state for majority spins.
This is true for tunneling through (100) crystal plane.

Transmission depends on the electronic state symmetry, materials and crystal structure
-> optimization of material crystal structure to optimize the spin junction performance

Phys. Rev. B **63**, 054416 (2001); Phys. Rev. B **70**, 172407 (2004); Encyclopedia of Materials: Science and Technology ISBN: 978-0-0804-3152-9

Role of composition and crystal structure

See exercise: 6.3

Fe/MgO/Fe (100)

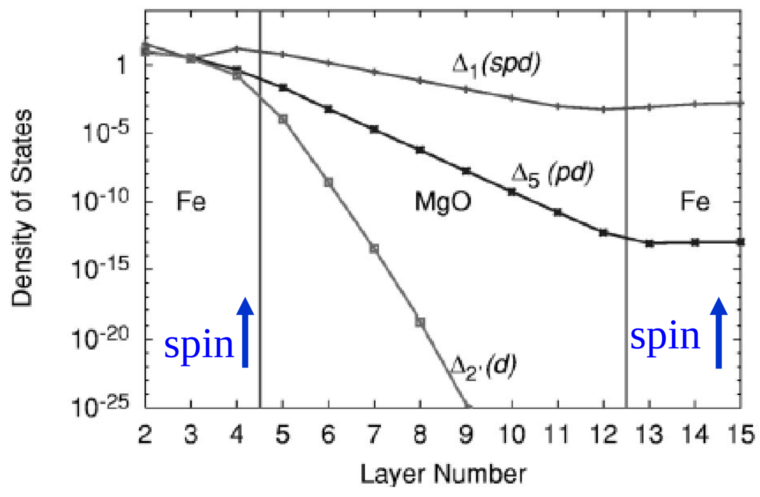

Density of States for Fe(majority)|MgO|Fe(minority)

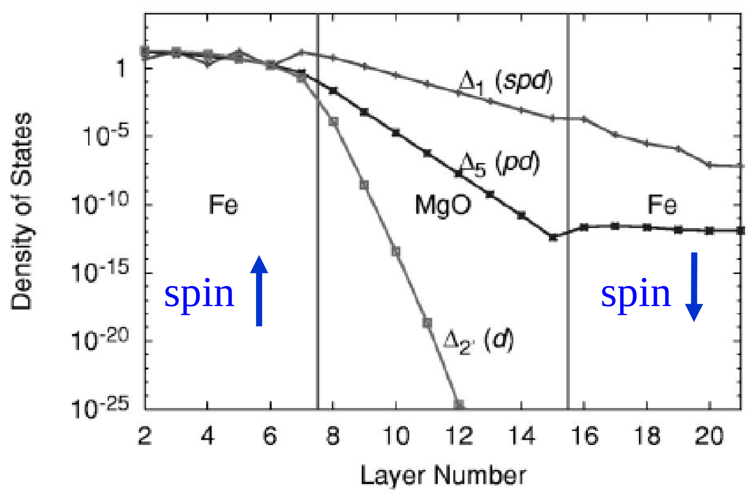

Co/MgO/Co (100)

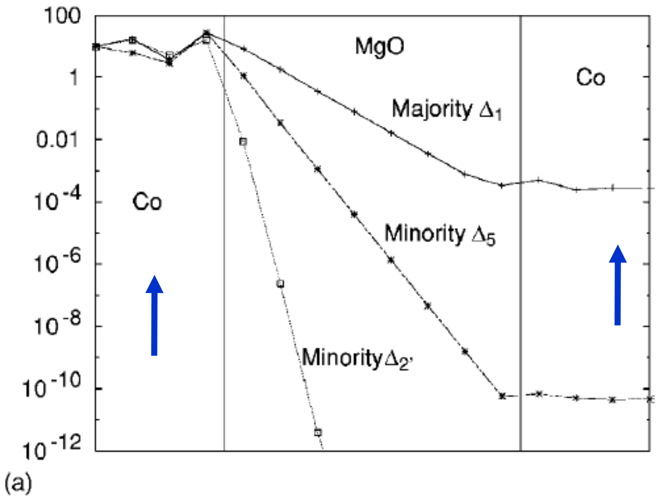

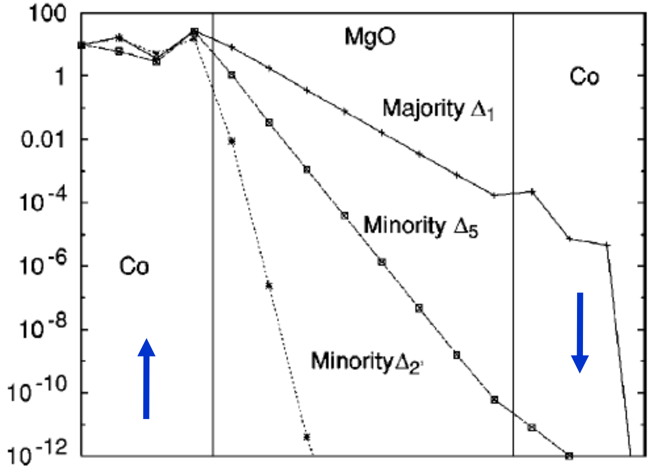

FeCo/MgO/FeCo (100)

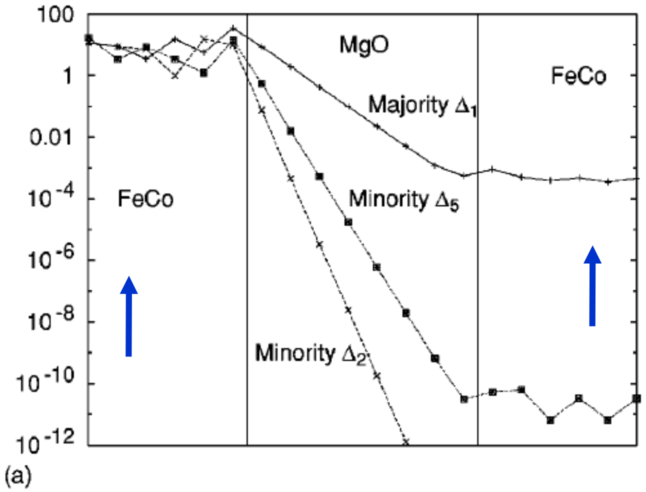

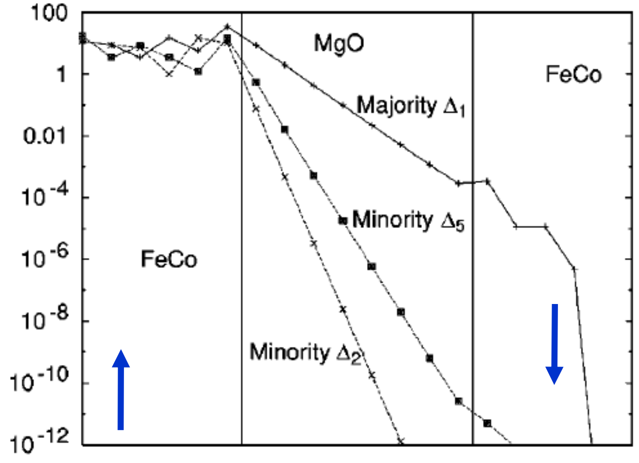

Higher transmission in Fe/MgO/Fe for majority states

Total reflection of tunneling electrons for antiparallel spin alignment in Co/MgO/Co and FeCo/MgO/FeCo junctions -> Fe/MgO/Fe junction has smaller TMR

Phys. Rev. B **63**, 054416 (2001)
Phys. Rev. B **70**, 172407 (2004)

Reading head in HDD

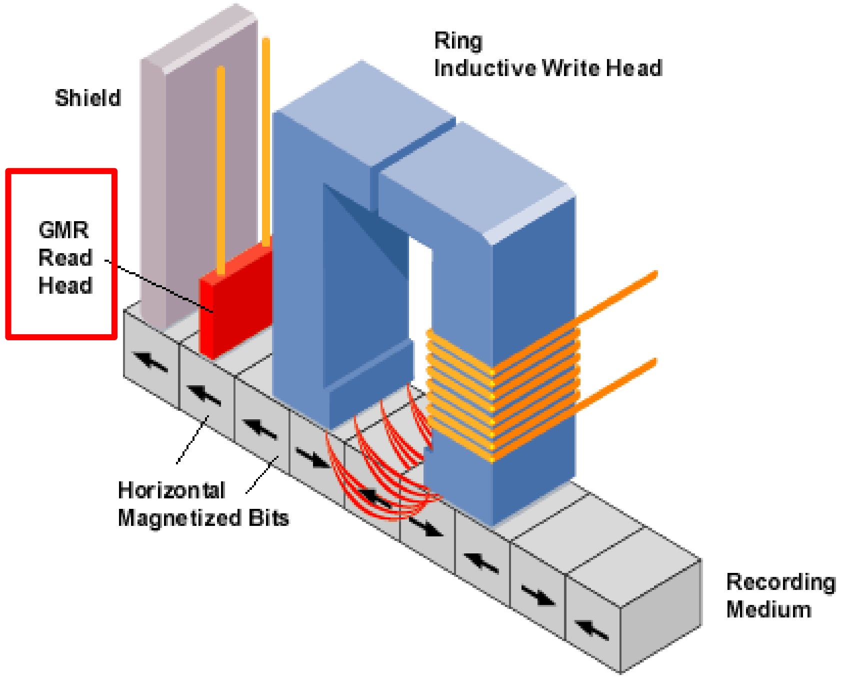

Writing:
the head stray field defines the magnetization direction of the recording medium

Reading:
the bit stray field defines the magnetization direction of the free layer

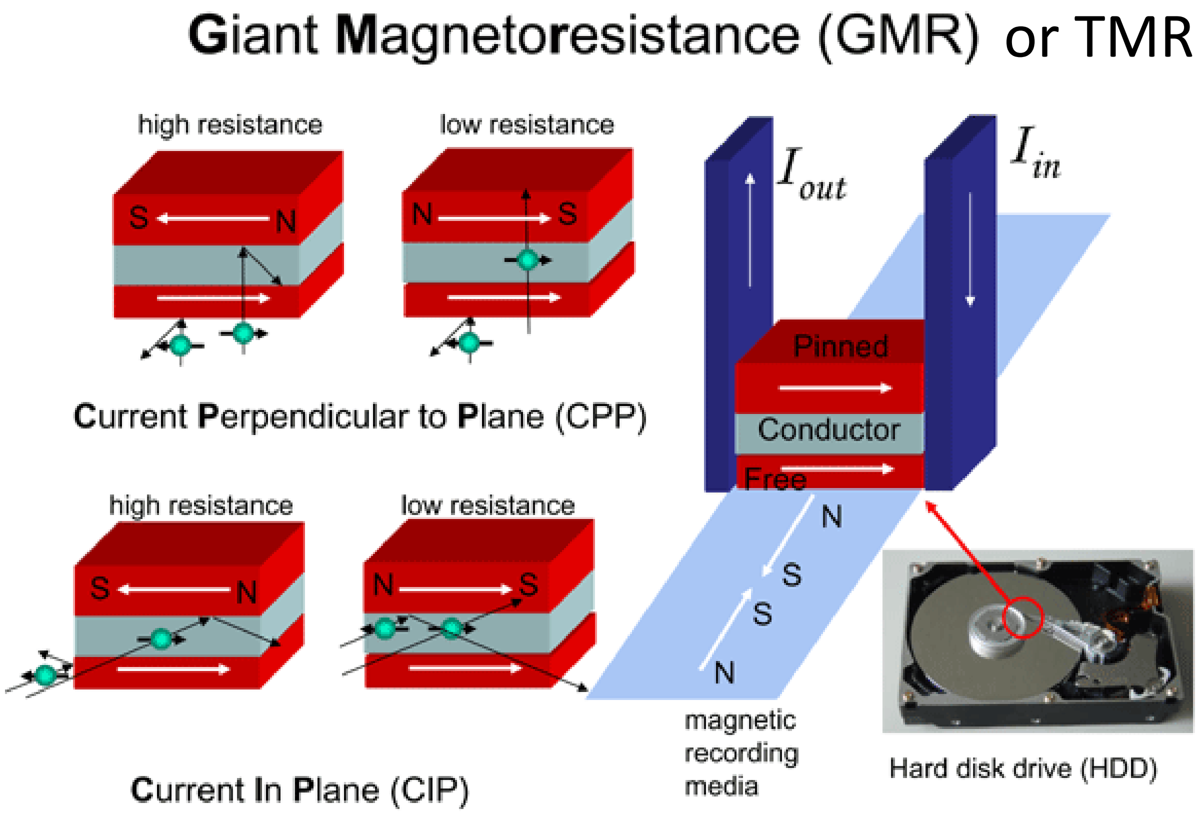

MRAM

EPFL

Magnetic random access memory (MRAM) never requires a refresh.
The memory will keep the information also with the power turned off

→ lower power consumption (up to 99% less) compared to DRAM

With storage density and capacity orders of magnitude smaller than HDD, MRAM is useful in applications where moderate amounts of storage with a need for very frequent updates are required

Items	Everspin 2nd Gen. MRAM (DDR3)	Everspin 3rd Gen. MRAM (DDR3)	Everspin 4th Gen. MRAM (DDR4)
Product Example	EMD3D064M DDR3 ST-MRAM	EMD3D256M DDR3 ST-MRAM	EMD4E001G DDR4 ST-MRAM
Die Size	65.3 mm^2 (11.15 mm x 5.86 mm)	100.1 mm^2 (12.12 mm x 8.26 mm)	105.1 mm^2 (12.29 mm x 8.55 mm)
Technology Node	90 nm	40 nm	28 nm
Memory / Die	64 Mb	256 Mb	1,024 Mb (1 Gb)
Bit Density	0.98 Mb/mm^2	2.56 Mb/mm^2	9.75 Mb/mm^2
Cell Size	0.387 μm^2	0.156 μm^2	0.0396 μm^2
Pitch (WL/BL)	530 nm / 730 nm	150 nm / 520 nm	110 nm / 180 nm
MTJ	In-plane MTJ	pMTJ	pMTJ
MRAM Integration	Between M3 and M4	Between M3 and M4	Between M3 and M4
# Metals	5	5	7
			Speed 700 MHz

Table 1: A comparison of STT-MRAM devices from Everspin Technologies, including in-plane MTJ and pMTJ

https://www.everspin.com/

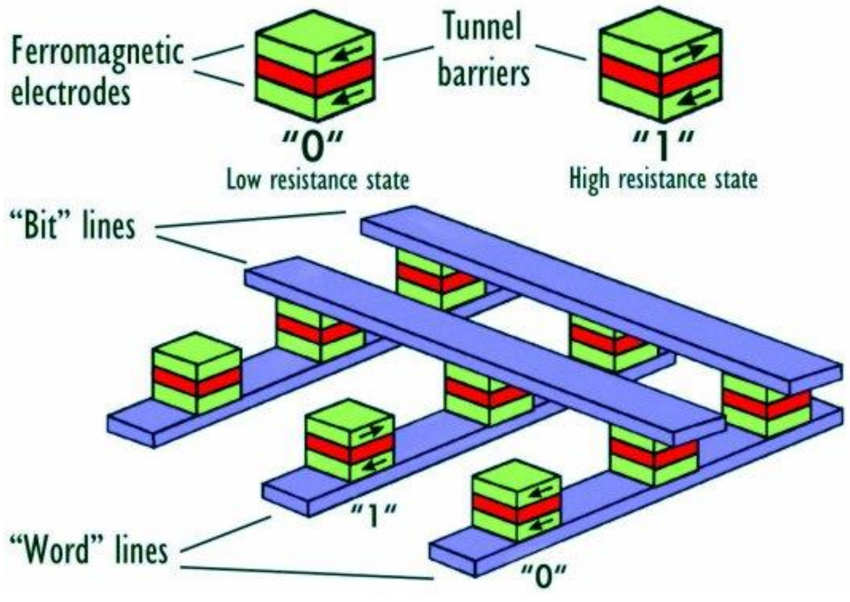

Science **282**, 1660 (1998); Nat. mater. **6**, 813 (2007); doi.org/10.1016/j.mattod.2017.07.007

MRAM

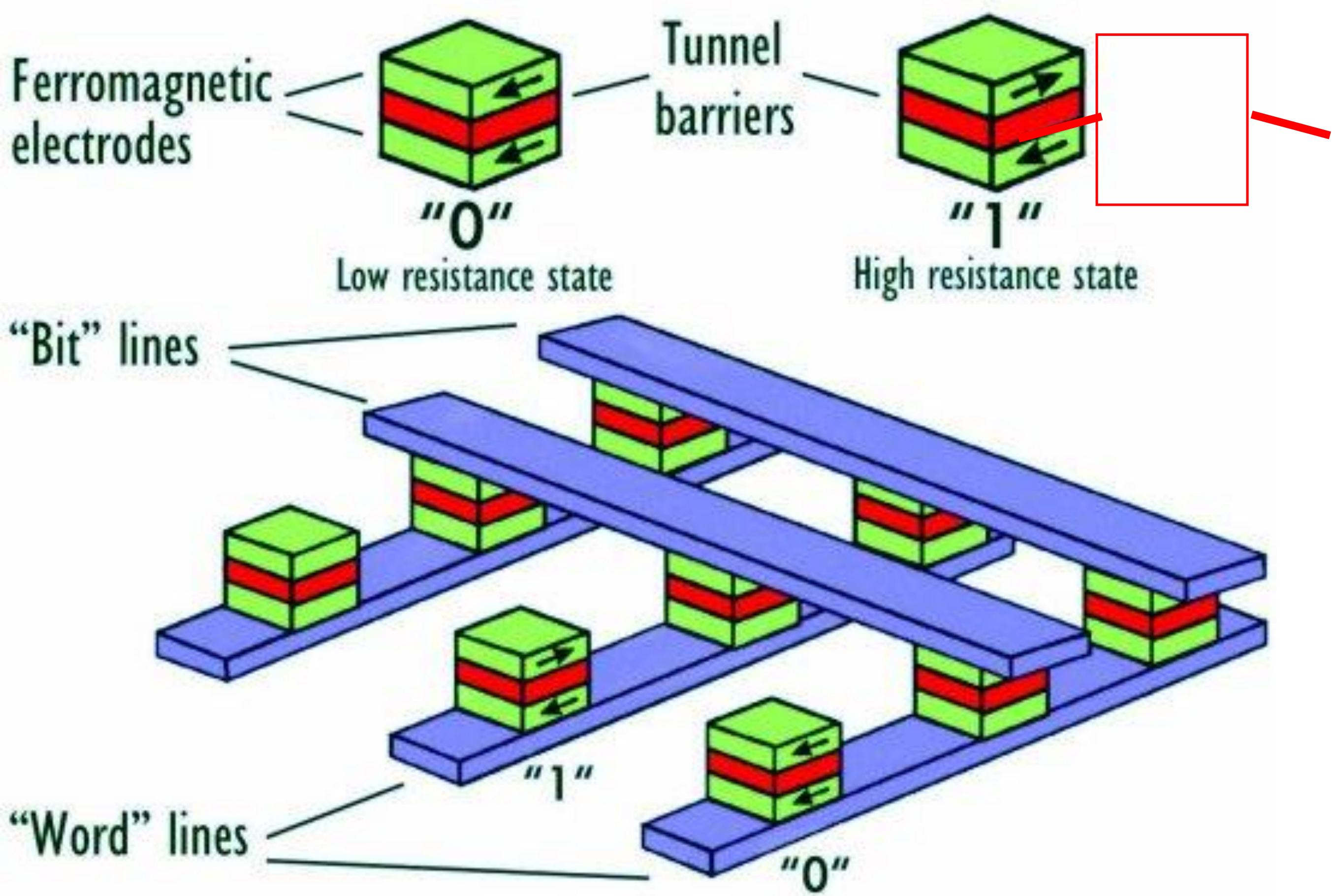

Reading: by measuring the point contact resistance between a bit and a word line

Writing: by magnetic fields (toggle-MRAM) or by injecting spin polarized current i.e. spin transfer torque (STT-MRAM) through the point contact

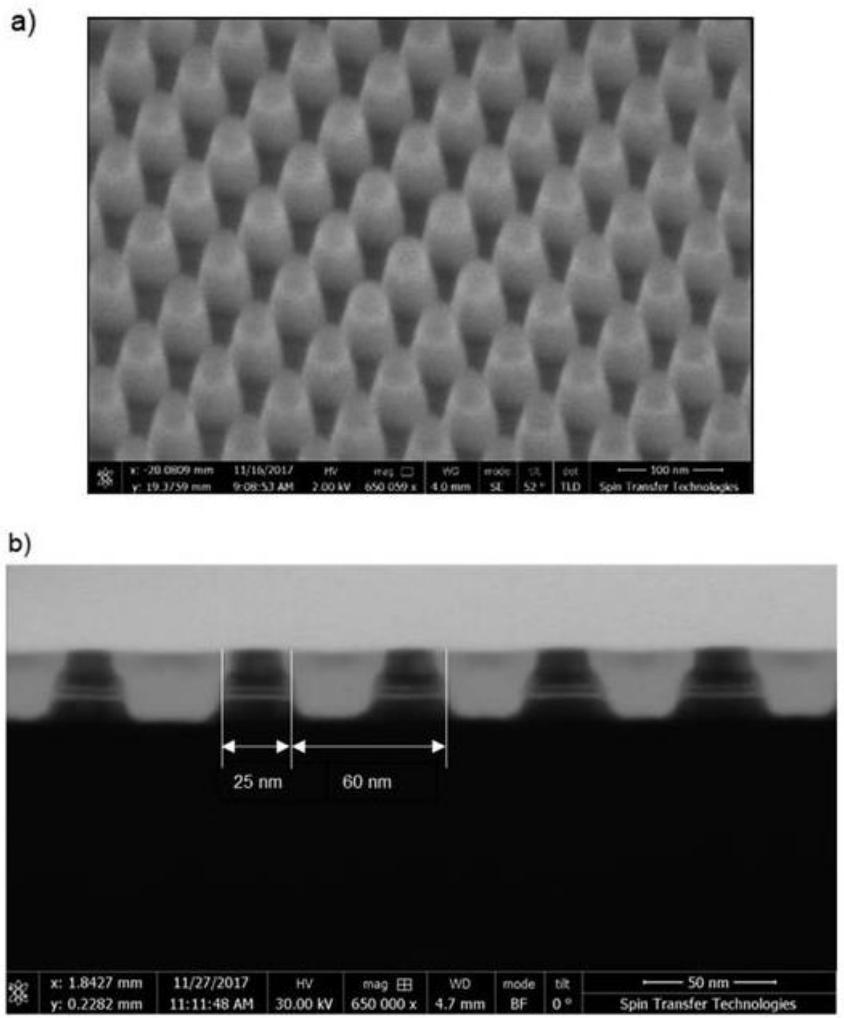

VIEW LARGE DOWNLOAD SLIDE

(a) SEM picture shows the wafer surface for high density processing at an intermediate processing step. The pillar structures are shown after photoresist and reactive ion etching of the hard mask layer. The hard mask layer protects the pMTJ structure during the ion beam etching. (b) The cross section of the high density pillars after they are formed. The pillar diameters are ~25 nm with ~60 nm pitch, demonstrating capabilities to make high density chips.

Science **282**, 1660 (1998); Nat. mater. **6**, 813 (2007)

https://doi.org/10.1063/5.0075945

Toggle MRAM: writing by using a magnetic field

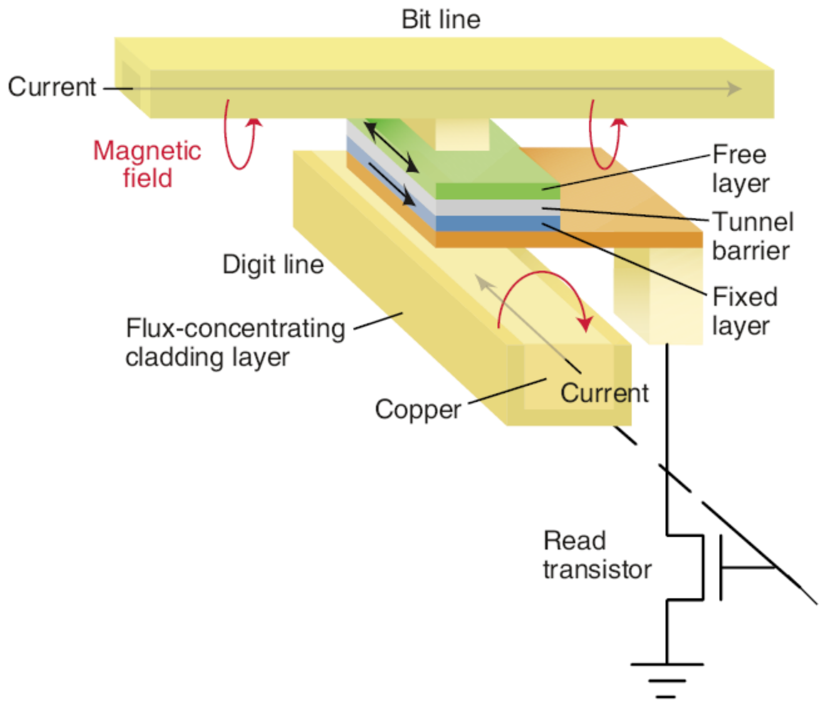

The MRAM is engineered in such a way that the bit easy axis points at 45° to the bit and digit lines

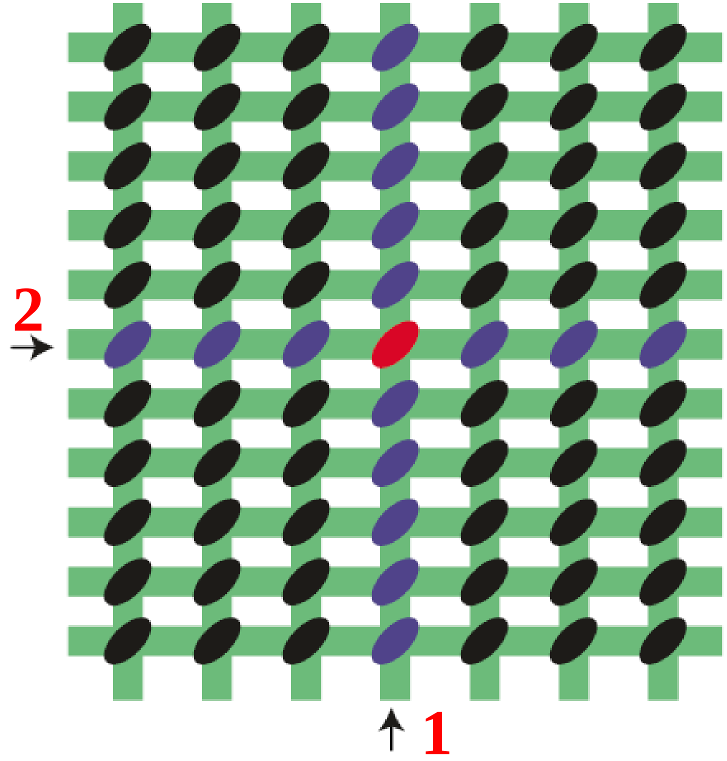

Word line = digit line

Line 1 produces the magnetic field necessary to turn by 45° the bit magnetization

Line 2 produces the magnetic field necessary to complete the reversal of the magnetization of the selected (red) bit

Switching off the magnetic fields generated by bit and digit lines, the magnetization of the non-selected bits relaxes back to the original direction

J. Akerman, Science **308**, 508 (2005)

In-plane magnetized pillar

Switching by applying a magnetic field

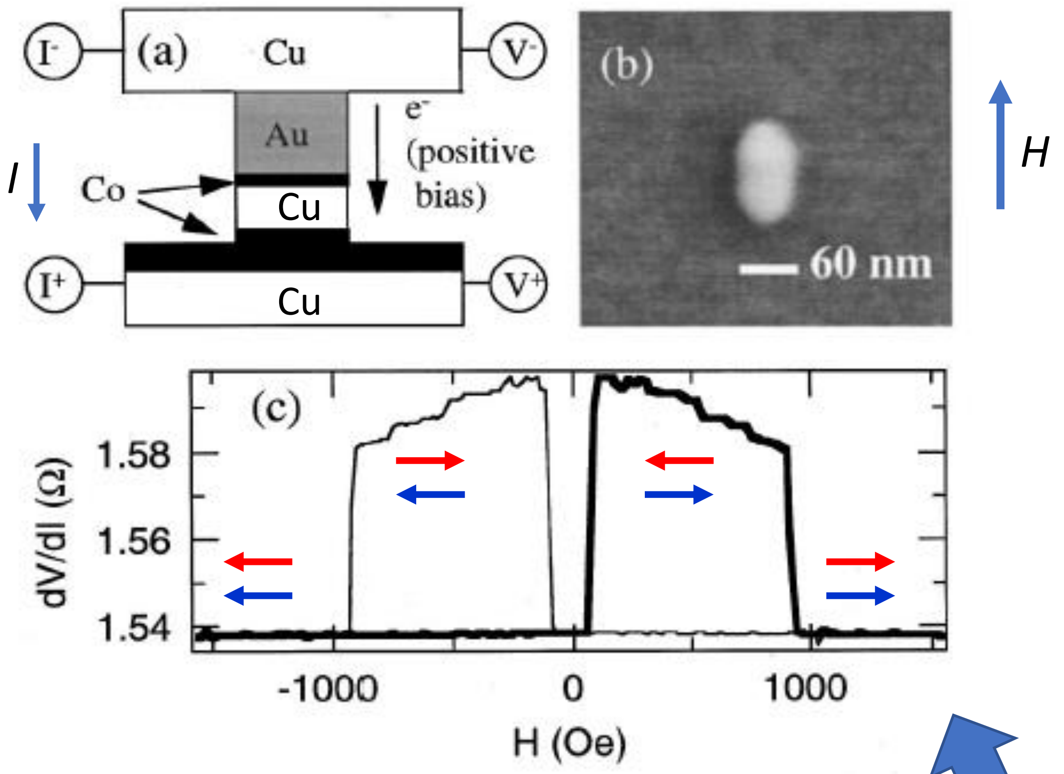

Switching by using a spin polarized current

$$J_c = \frac{I}{A} = \frac{5\ mA}{60\ \times 130\ nm^2} \approx 60\ MA\ cm^{-2}$$

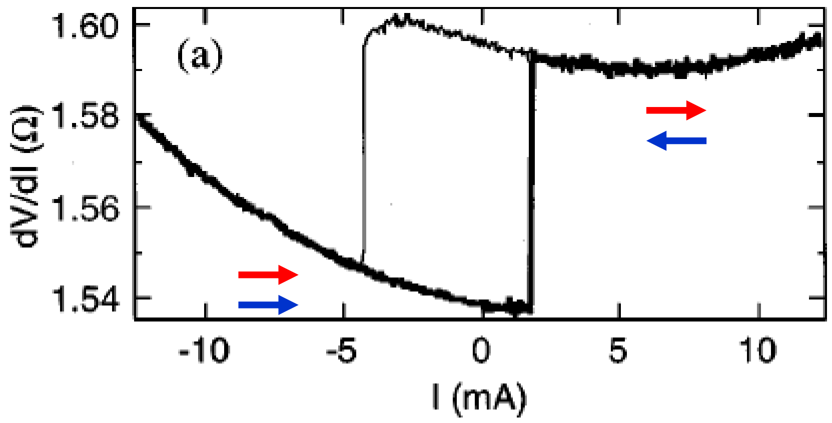

The current is defined as positive when the spin-polarized electrons are flowing from the nanomagnet to the thick Co film

The same high-low conductance level can be reached by applying an external magnetic field or by injecting a spin polarized current

F. J. Albert et al. Appl. Phys. Lett. **77**, 3809, *(2000)*

Spin transfer torque (STT) switching

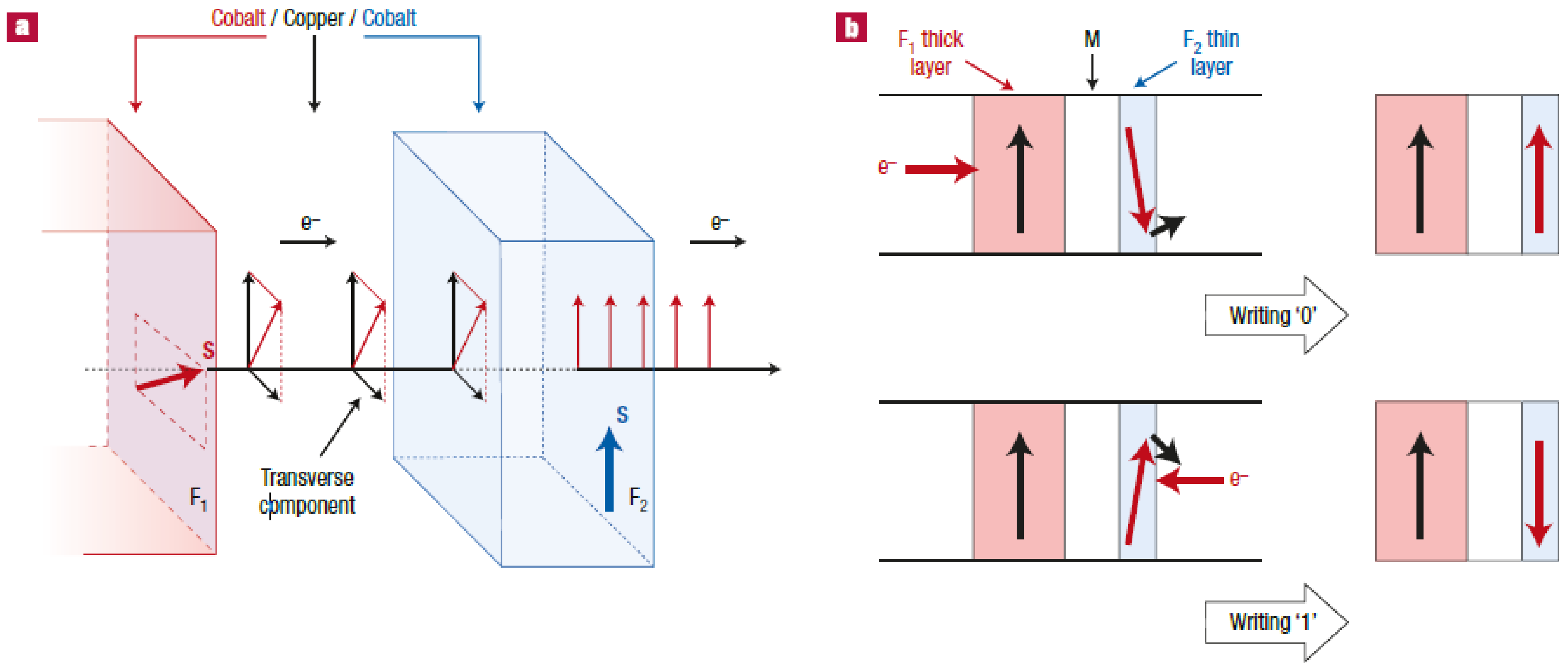

Figure 6 Spin-transfer switching. **a**, Principle of the STT effect, for a typical case of a Co(F1)/Cu/Co(F2) trilayer pillar. A current of *s* electrons flowing from left to right will acquire through F1 (assumed to be thick and acting as a spin polarizer) an average spin moment along the magnetization of F1. When the electrons reach F2, the *s–d* exchange interaction quickly aligns the average spin moment along the magnetization of F2. To conserve the total angular momentum, the transverse spin angular momentum lost by the electrons is transferred to the magnetization of F2, which senses a resulting torque tending to align its magnetization towards F1. **b**, Principle of STT writing of a MRAM cell: reversing the current flowing through the cell will induce either parallel or antiparallel orientation of the two ferromagnetic layers F1 and F2.

doi:10.1038/nmat2024

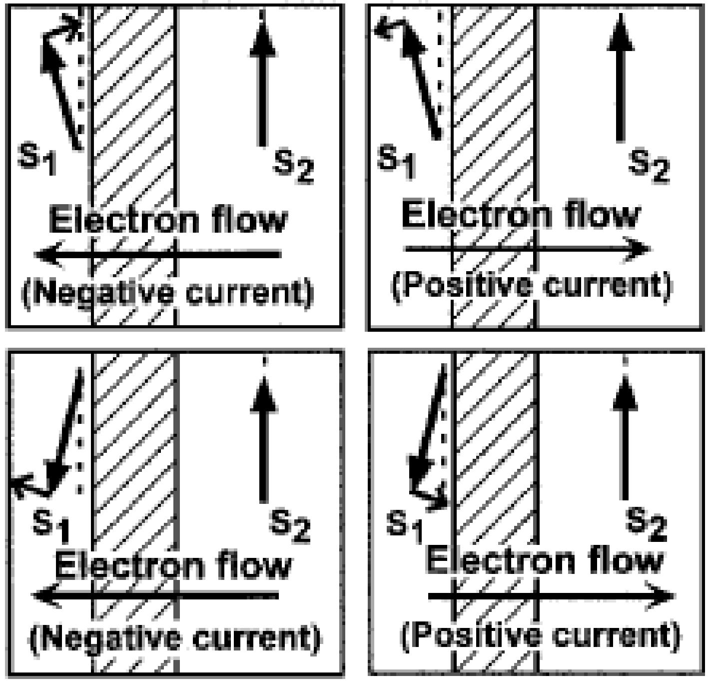

The current is defined as positive when the spin-polarized electrons are flowing from the free to the pinned layer

Energy + angular momentum conservation (s-d exchange)

- The current flowing through the pinned layer gets spin polarized
- The free layer exerts a torque on the spin of electrons flowing through it
- According to the Newton's third law, the electron must exert an equal and opposite torque on the magnet, which causes the magnetization reversal

$$\boldsymbol{\tau} = \frac{d\boldsymbol{s}_{1,2}}{dt} = \boldsymbol{I}\, g(P)\ \boldsymbol{s}_{1,2} \wedge (\boldsymbol{s}_1 \wedge \boldsymbol{s}_2)$$

Torque depends on:

1) the current direction (parallel or antiparallel alignment of the magnetization of pinned and free layer can be selected)
2) Spin polarization *P* (factor *g(P)*)

Science **285**, 867 (1999)

J. C. Slonczewski, J. Magn. Magn. Mater. **159**, L1 (1996); DOI: 10.1103/PhysRevB.71.024411

Microscopic vs continuum description of the STT

The torque has two components:

1) A field-like τ_{FL} torque responsible for spin precession. The injected spin precess around the field generated by the free layer. An equal and opposite torque applies on the free layer

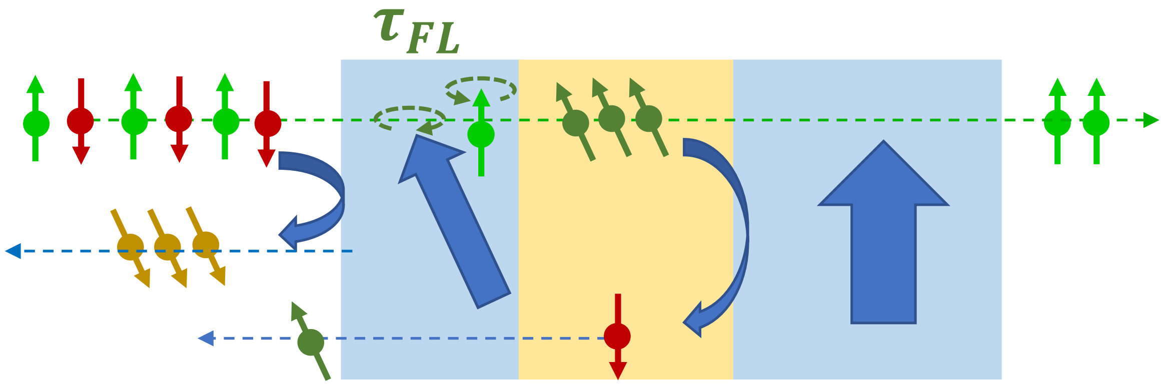

2) A damping-like τ_{FL} torque responsible for spin precession. The current coming out the FM is spin polarized due to reflection of minority spin. The loss of minority spin correspond to a rotation of the current magnetization into the majority spin direction which corresponds to the pinned layer magnetization. An equal and opposite torque applies on the free layer

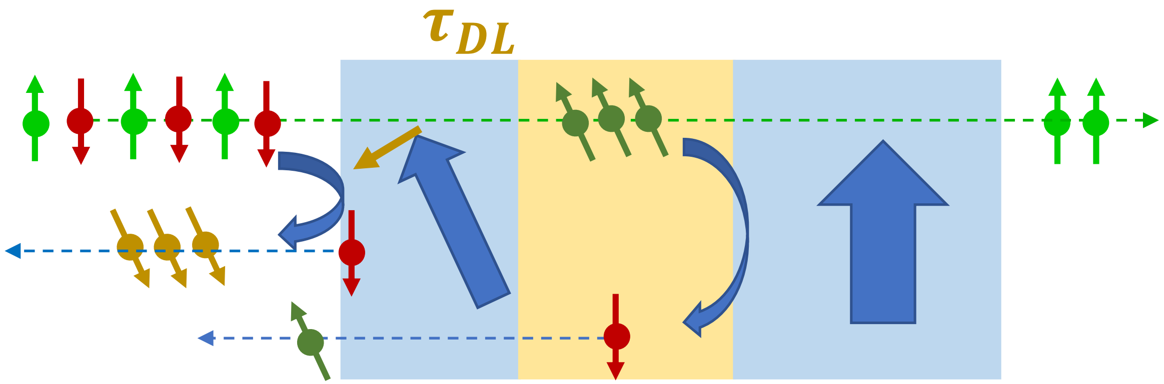

Microscopic view of the STT: spin-flip due to *s-d* exchange

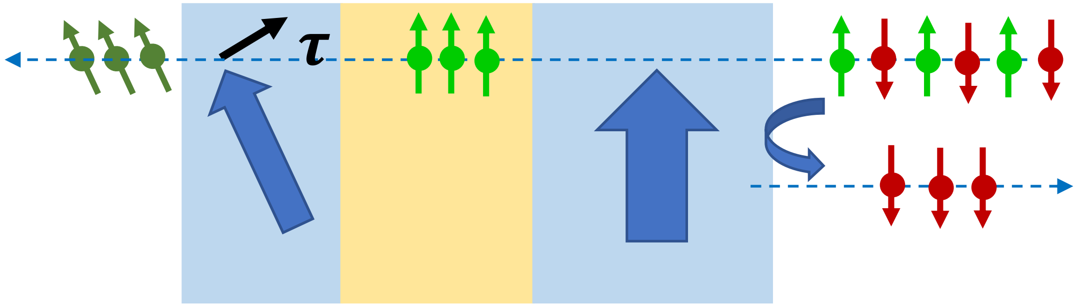

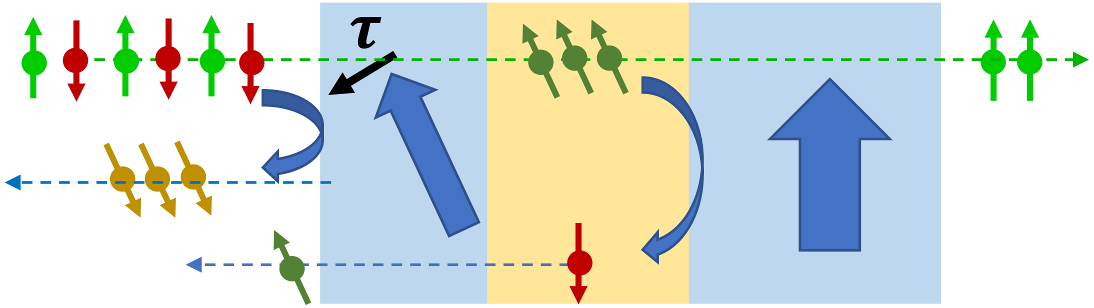

I

Writing “1”

Science **285**, 867 (1999)

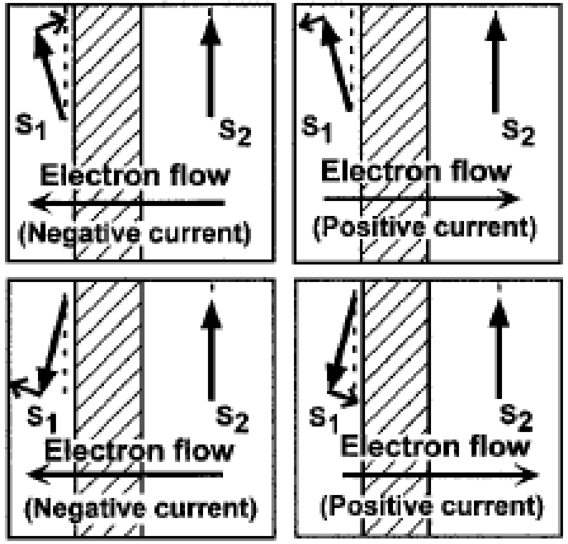

I

Writing “0”

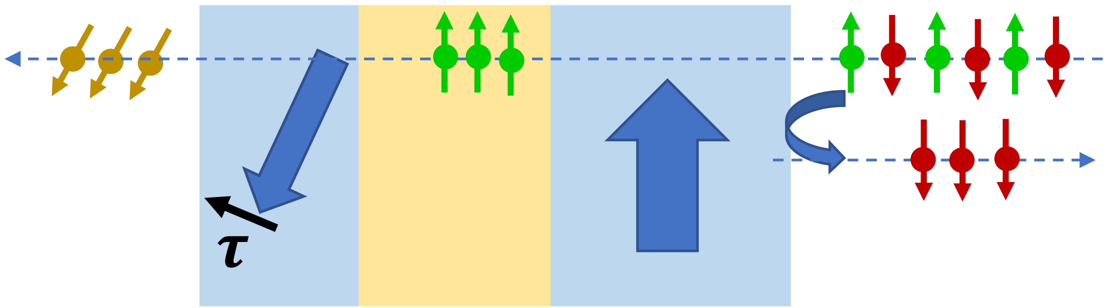

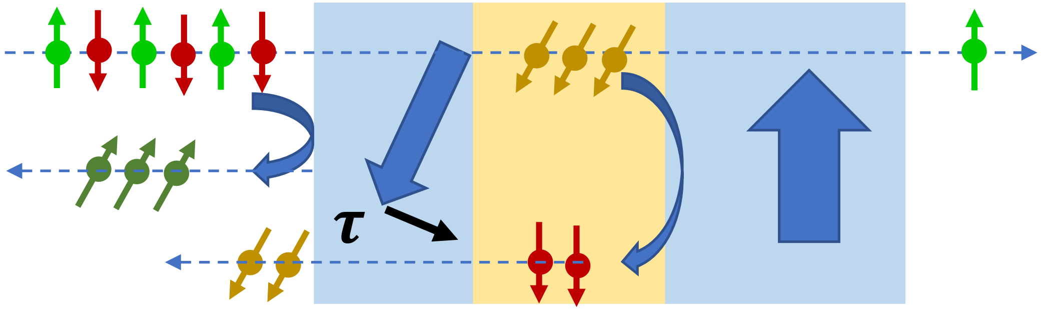

Pinned layer

Torque exists also on the pinned layer: in the situation shown in the sketch, electron spin is pointing down before entering into the pinned layer while is pointing up when it comes out of the layer

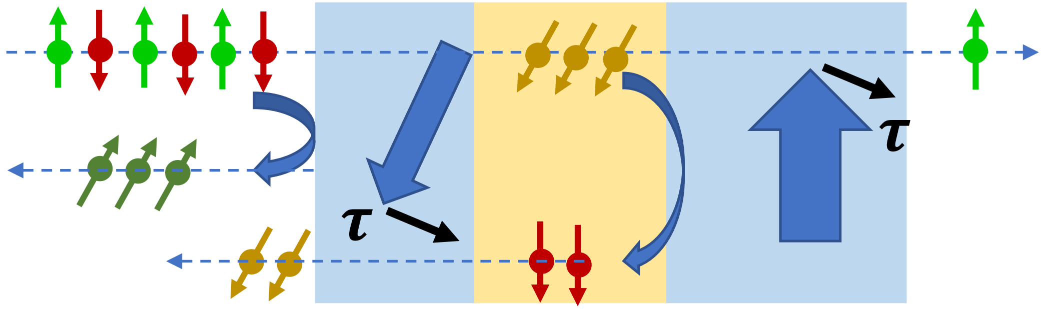

However, the pinned layer is designed to have very large MAE, i.e. it is very difficult to flip the pinned layer magnetization

STT in GMR nanopillars with PMA

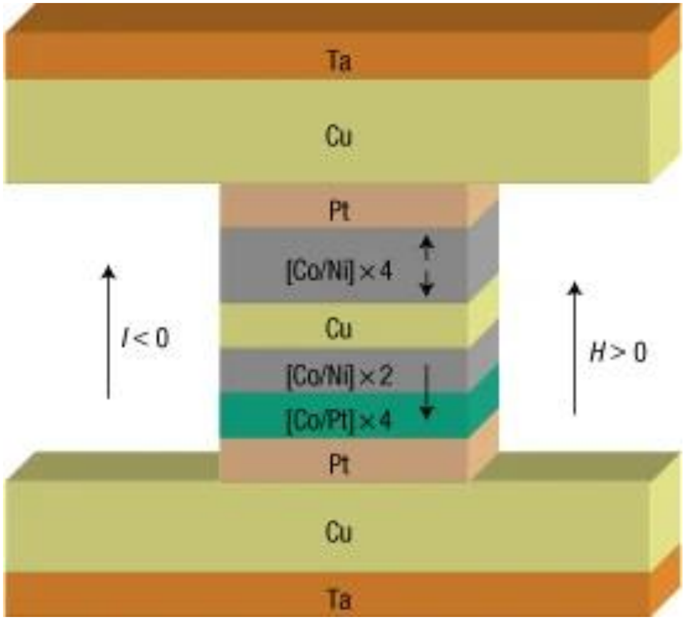

The reference layer is a composite [Co/Pt] × 4/[Co/Ni] × 2 multilayer and the free layer is a [Co/Ni] × 4 multilayer. The magnetization direction of the reference layer, positive field direction and the direction of electron flow for negative current are shown.

Higher MAE with respect to in-plane magnetized pillars

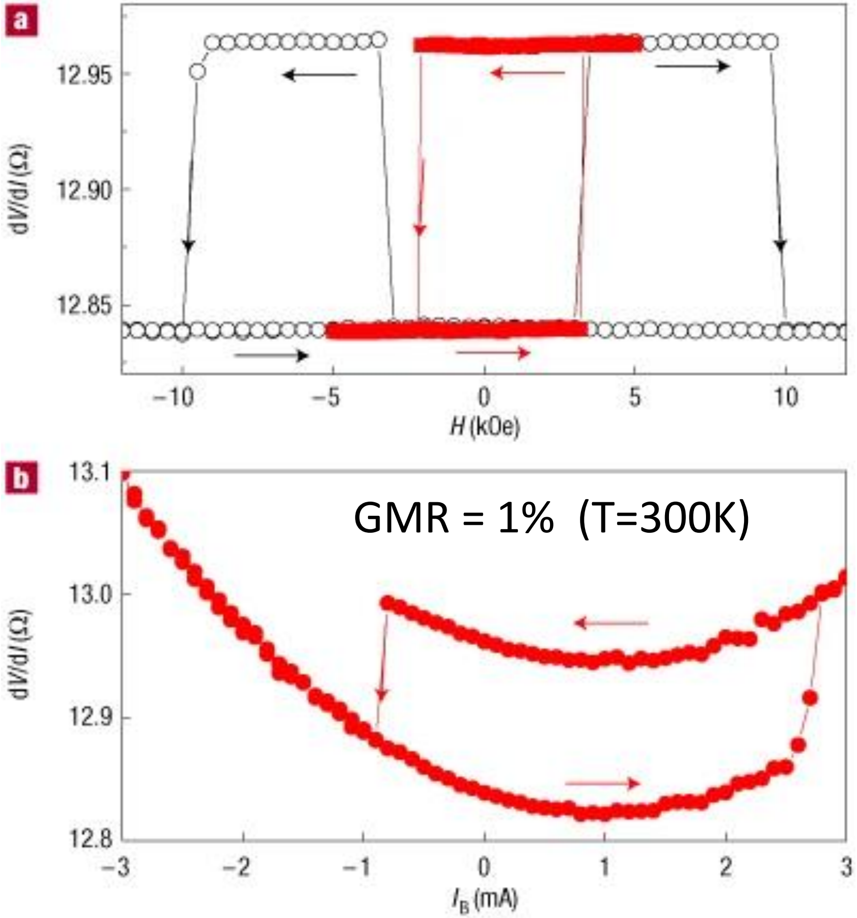

a dV/dI versus H for H perpendicular to the film plane. The open symbols correspond to the major loop showing discrete transitions between the parallel and antiparallel states. The filled symbols are a minor loop where only the free layer reverses (the minor hysteresis loop is offset by 650 Oe from the origin owing to the average dipolar field (H_{dip}) from the pinned layer that favors parallel alignment)
b dV/dI versus I_B for H=0 showing discrete transitions between the antiparallel and parallel states.

I_C^{P-AP}=2.7 mA (J_c =75 MA cm^{-2})
and switches back for
I_C^{AP-P}=−0.85 mA (J_c = −26 MA cm^{-2}).

https://doi.org/10.1038/nmat1595

Magnetoresistance and STT measurements for p-MTJ (r = 90 nm) at room temperature

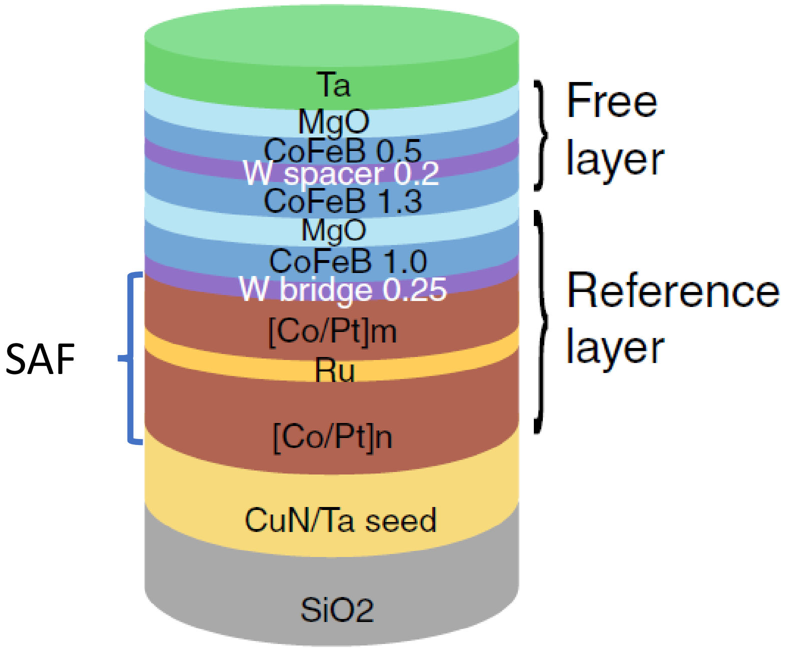

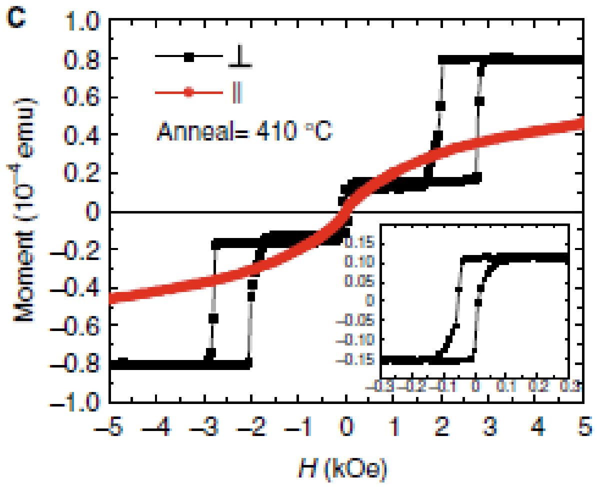

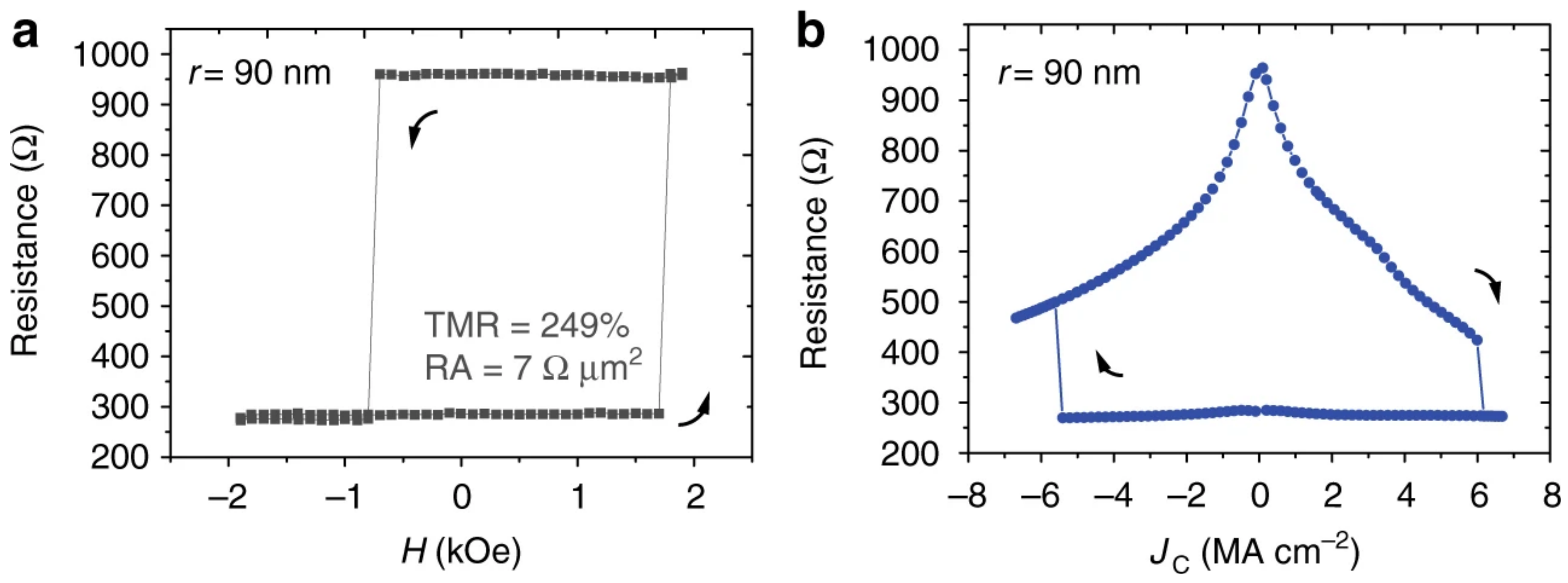

a Magnetoresistance (T=300 K) as a function of out-of-plane magnetic field

b STT switching measured by DC current sweep.

Arrows show the perpendicular magnetization transitions from AP to P states or the opposite situation

https://doi.org/10.1038/s41467-018-03140-z

writing current vs magnetoresistance

Macrospin model: $$I = \frac{4e\alpha_G}{\hbar\eta} E_b$$

$$\eta = \frac{\sqrt{m_r(m_r+2)}}{2(m_r+1)} \qquad m_r = \frac{\Delta R}{R} = \frac{R_{ap} - R_p}{R_p}$$

m_r is a measurement of the spin polarization

E_b is the energy barrier for coherent reversal

Larger is the magnetoresistance m_r, larger is η and thus smaller is the current required for reversal:

GMR: m_r = 1% = 0.01 -> η = 0.07
TMR: m_r = 250% = 2.5 -> η = 0.48

https://doi.org/10.1038/s41467-018-03140-z

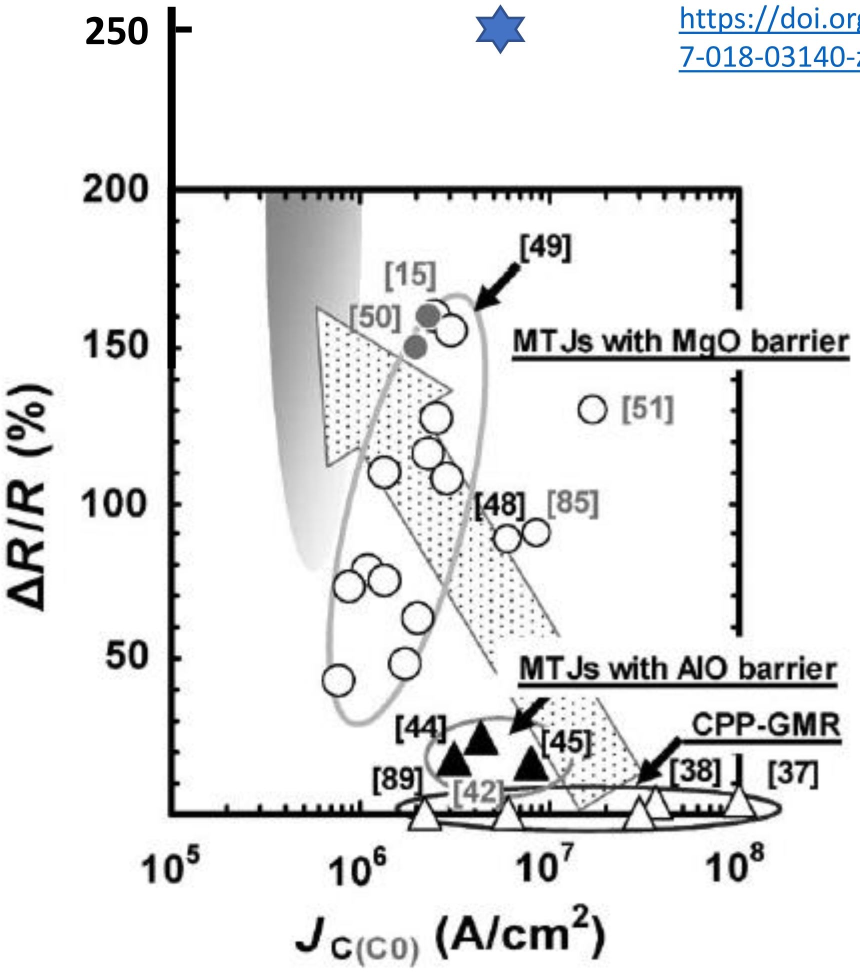

Relationship between $\Delta R/R$ and critical current $J_C(C0)$. The references, shown in black and gray, correspond to J_C (measured at RT at current pulse-width ranging from 100 ms to 1 s) and J_{C0} [J_C at 1 ns (extrapolated)], respectively.

https://doi.org/10.1063/5.0075945

DOI: 10.1109/TED.2007.894617 (2007)

Landau-Lifshitz-Gilbert-Slonczewski (LLGS) equation

Generalization of the LLG eq. describing the magnetization dynamics when a spin-polarized electrons flux transfers spin angular momentum to the local magnetization M: spin transfer torque (STT)

Continuum (classical) approach: ***m*** is a vector of constant length

$$\frac{d\boldsymbol{m}}{dt} = -\gamma(\boldsymbol{m} \wedge \boldsymbol{H}_{eff}) + \frac{\alpha}{m}\left(\boldsymbol{m} \wedge \frac{d\boldsymbol{m}}{dt}\right) + \frac{\gamma}{M_S}\boldsymbol{T}$$

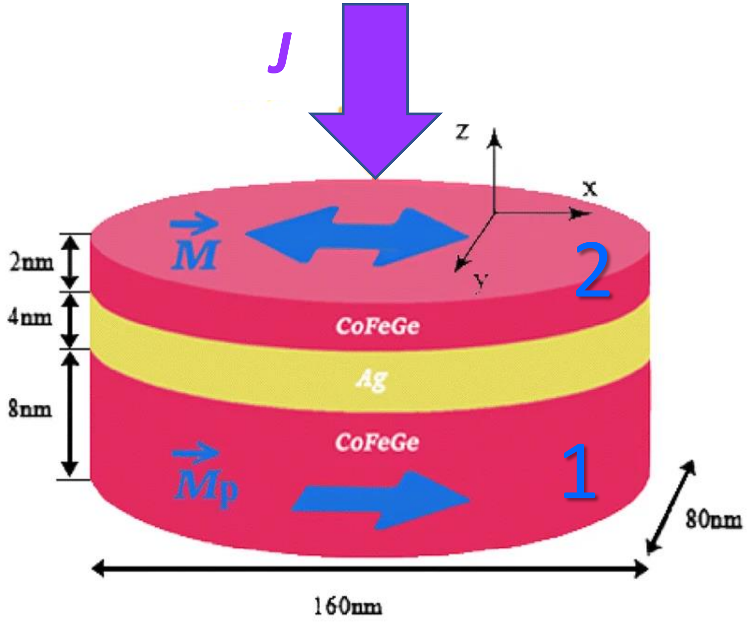

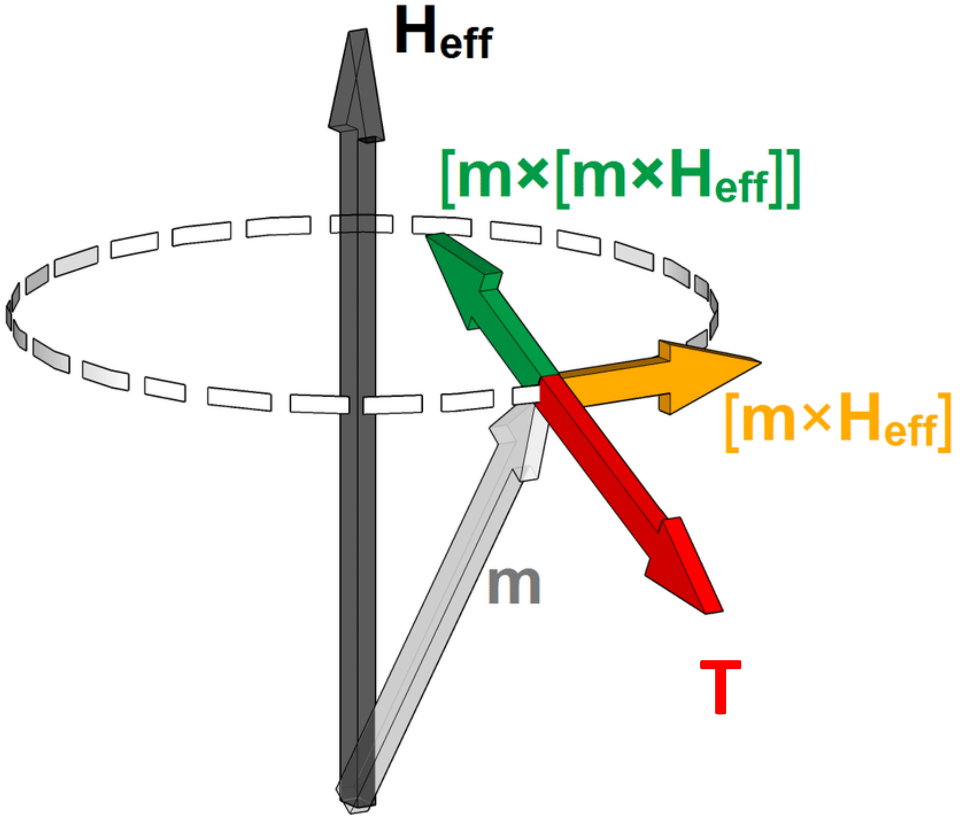

Layer 1: pinned layer ⇒ produces the spin polarized current *J*

Layer 2: free layer

https://www.iue.tuwien.ac.at/phd/makarov/dissertationch5.html

Landau-Lifshitz-Gilbert-Slonczewski (LLGS) equation

spin transfer torque (STT)

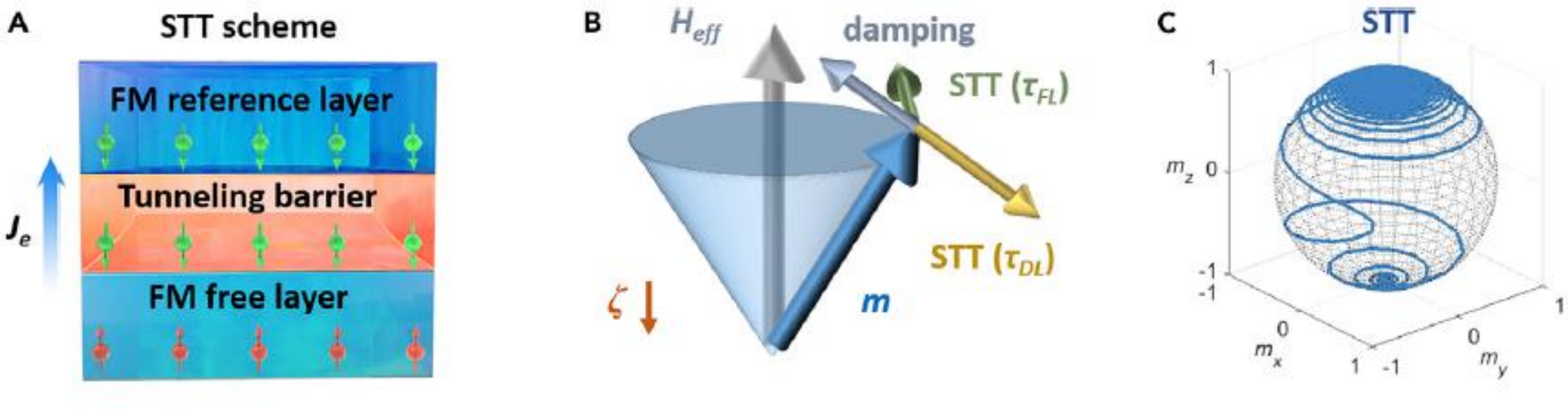

$$\frac{d\boldsymbol{m}}{dt} = -\gamma\left(\boldsymbol{m} \wedge \boldsymbol{H}_{eff}\right) + \frac{\alpha}{m}\left(\boldsymbol{m} \wedge \frac{d\boldsymbol{m}}{dt}\right) + \frac{\gamma}{M_s}\boldsymbol{T}$$

$$\frac{d\boldsymbol{m}}{dt} = -\frac{\gamma}{1+\alpha^2}\left(\boldsymbol{m} \wedge \boldsymbol{H}_{eff}\right) - \frac{\gamma}{1+\alpha^2}\frac{\alpha}{m}\left(\boldsymbol{m} \wedge \left[\boldsymbol{m} \wedge \boldsymbol{H}_{eff}\right]\right)$$

$$\boldsymbol{T} = \tau_{FL}\, \boldsymbol{m} \wedge \boldsymbol{\zeta} + \tau_{DL}\, \boldsymbol{m} \wedge (\boldsymbol{m} \wedge \boldsymbol{\zeta})$$

$\boldsymbol{\zeta}$ is a unit vector determined by the incoming spin polarization $\Rightarrow$ equivalent to an effective magnetic field

T consists of:

- a field-like term $\tau_{FL}\, \boldsymbol{m} \wedge \boldsymbol{\zeta}$ (similar to $\boldsymbol{m} \wedge \boldsymbol{H}_{eff}$) that makes $\boldsymbol{m}$ to precess around $\boldsymbol{H}_{eff}$
- a damping-like term $\tau_{DL}\, \boldsymbol{m} \wedge (\boldsymbol{m} \wedge \boldsymbol{\zeta})$ that tends to align $\boldsymbol{m}$ along $\boldsymbol{z}$

https://doi.org/10.1016/j.isci.2020.101614

J. C. Slonczewski, J. Magn. Magn. Mater. **159**, L1 (1996)

Example of micromagnetic calculations for STT driven switching

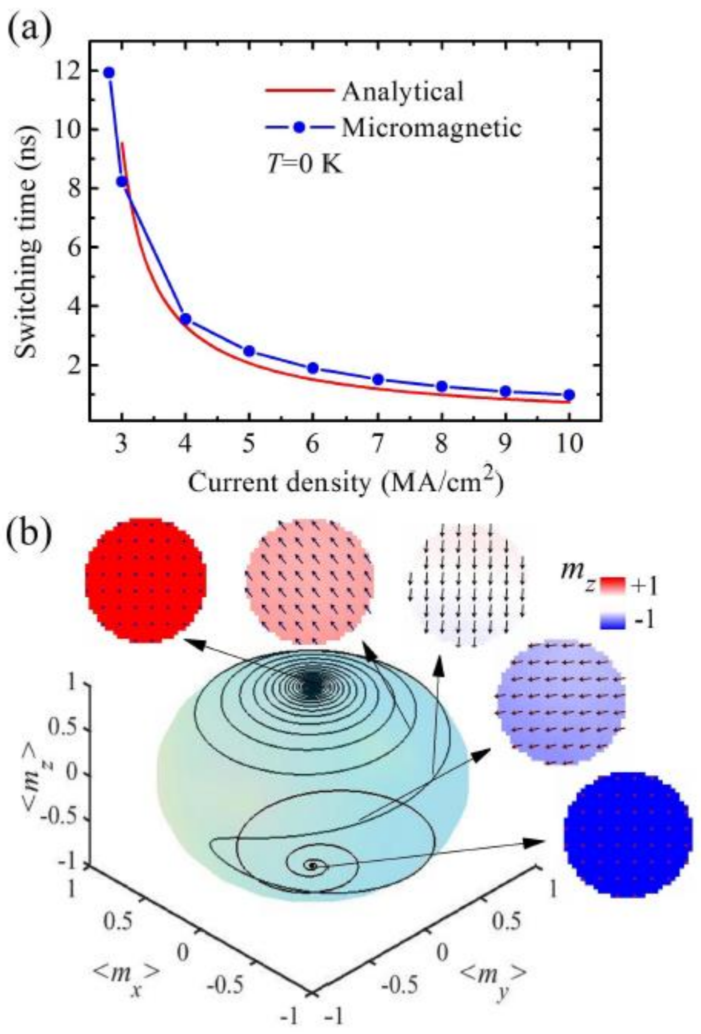

Fig. 1. (a) Switching time as a function of the current density obtained from the analytical (red line) and micromagnetic computations (blue line with circles) at $T = 0$ K. (b) Switching trajectory obtained from micromagnetic simulations at $J_{MTJ} = 5.0$ MA/cm^2 with some representative magnetization snapshots displayed as insets (red positive, blue negative out-of-plane component of the magnetization).

10.1109/TMAG.2018.2799856

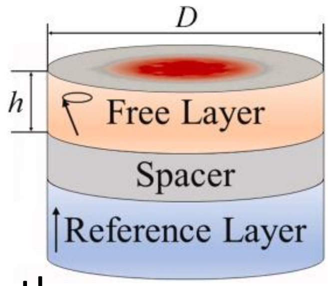

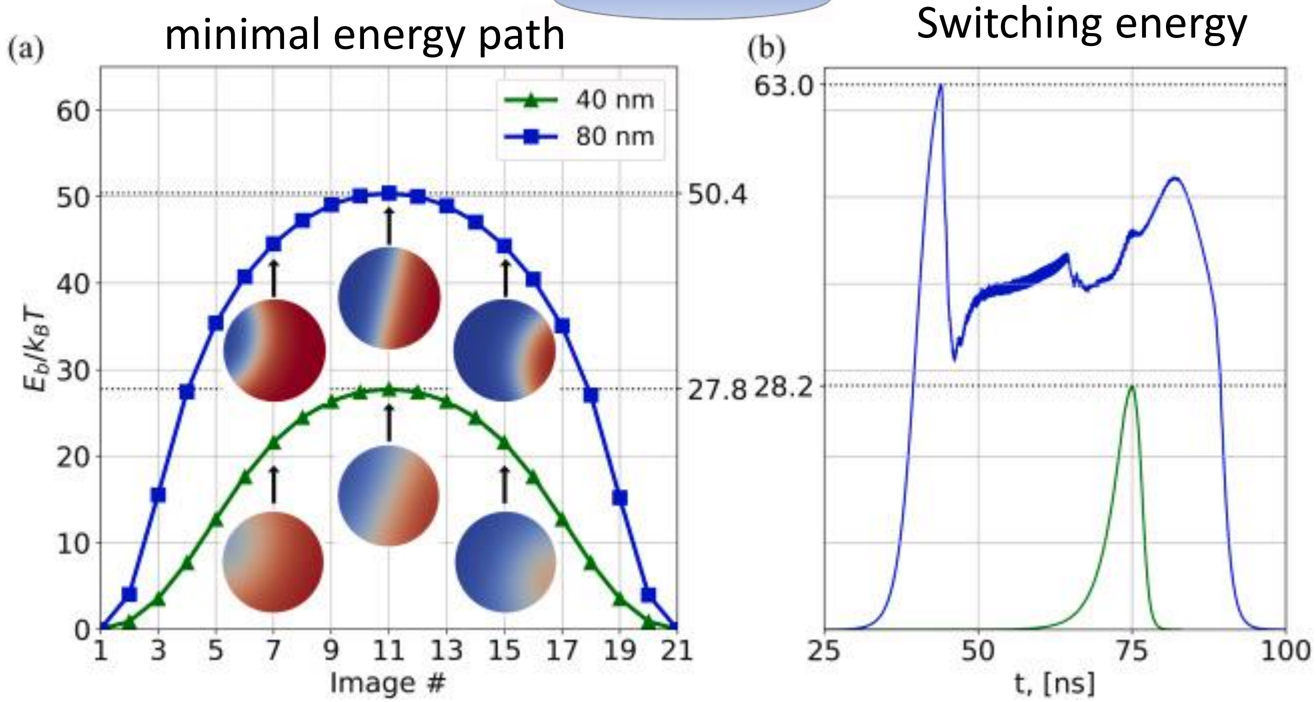

The energy corresponding to switching and the minimal energy path for *D* = 40 nm follow a similar track in terms of max energy. On the other hand, for *D* = 80 nm , the energy corresponding to switching follows a different, more complicated track than the minimal energy path, which is because of more complicated dynamics for larger MTJ sizes.

https://doi.org/10.1016/j.jmmm.2023.170361

Racetrack memory

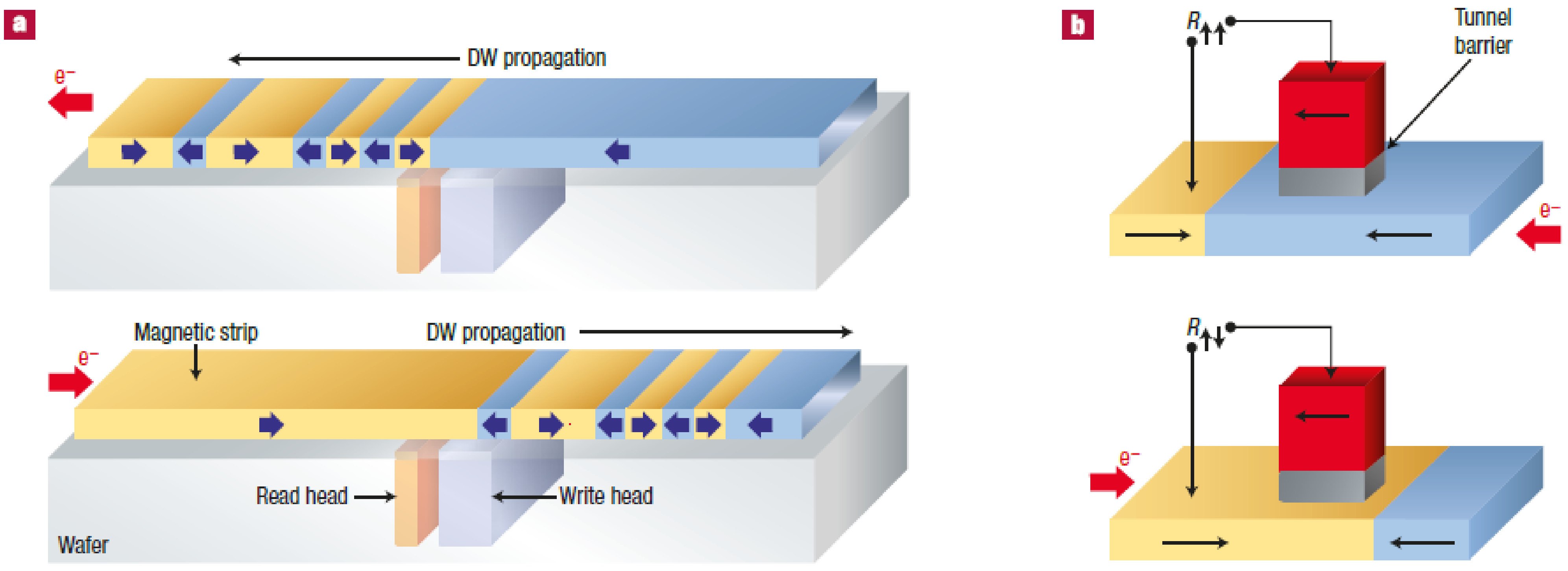

Figure 8 Domain wall storage devices. Examples of storage devices using current-induced domain wall (DW) propagation. **a**, In the concept first proposed by Parkin[94], the binary information is stored by a chain of domain walls in a magnetic stripe. An electrical current in the stripe, by applying the same pressure to all the domain walls, moves them simultaneously at the same speed for a sequential reading (or writing) at fixed read and write heads. A reverse current can move the domain walls in the opposite direction for resetting, or in an alternative solution the domain walls might turn on a loop. This mimics the fast passing of bits in front of the head in HDD recording, but here there is no moving part and addressing a sector would be done by CMOS electronics at microsecond access times. The initial scheme[94] proposes to store data in vertical stripes: this would open the way to very compact high capacity 'storage track memory devices'. Other schemes now propose multilayers of in-plane domain tracks, which would be easier to fabricate. **b**, Scheme of a MRAM cell using domain wall propagation from one stable position to another on either side of a magnetic tunnel junction (ref. 95).

doi:10.1038/nmat2024

Nat. Nanotech. **10**, 195–198 (2015) https://doi.org/10.1038/nnano.2015.41; 10.1109/JPROC.2020.2975719

Racetrack memory: exploiting the 3D

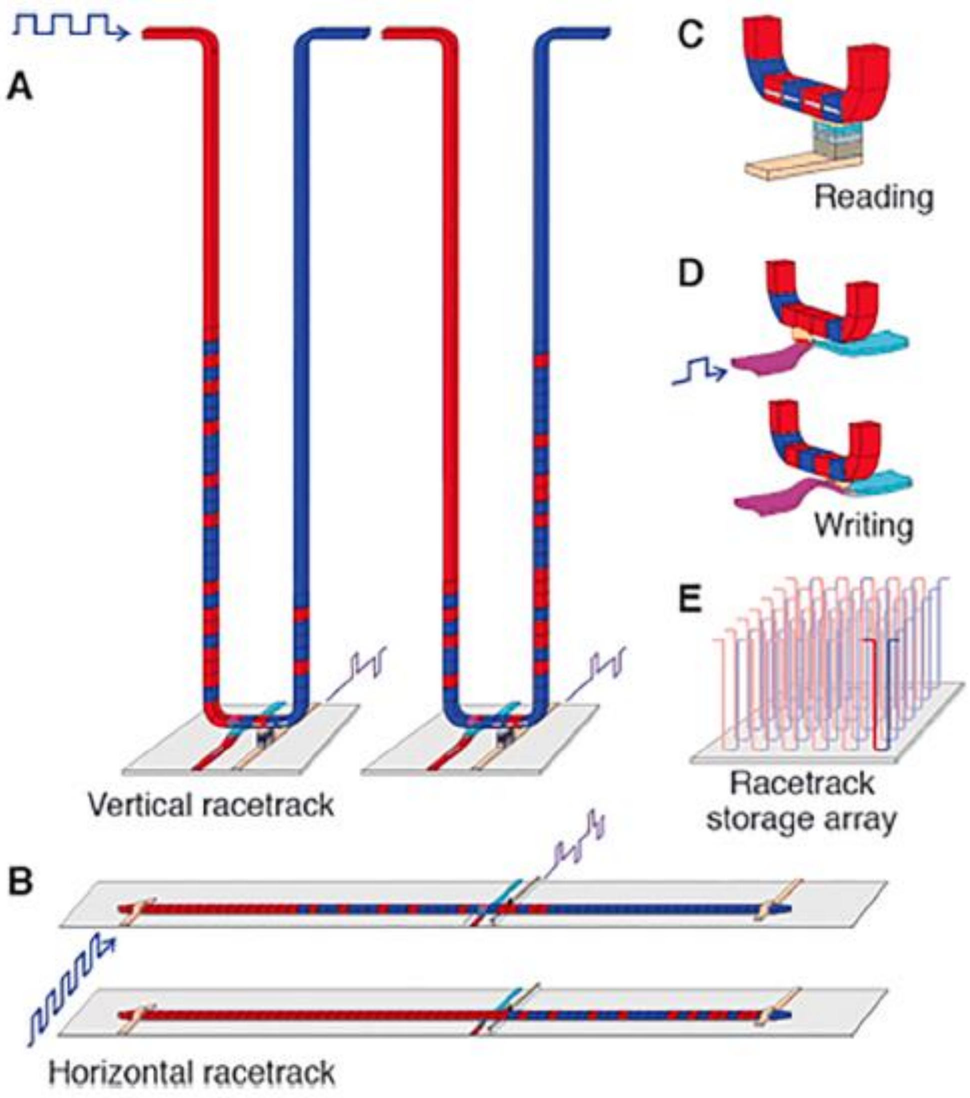

Fig. 17. Schematic diagram of a racetrack memory concept in (A) vertical and (B) horizontal configurations. (C) Reading and (D) writing operation can be carried out electrically. (E) 3D-array concept [368].

exchange interaction between conduction electrons and spins of a domain wall

The current has two effects:
1) momentum transfer (due to the reflection of conduction electrons)
2) spin torque

DOI: 10.1103/PhysRevLett.92.086601; DOI: 10.1103/PhysRevLett.92.207203

Advantages:
1) No mechanical moving parts (the reading/writing head is fixed)
2) 3D memories: use of the third dimension to increase the amount of stored information

Parkin, S. S. P. , Shiftable magnetic shift register and method using the same. US patent 6,834,005B1 (2004).

Observation of DW displacement via STT

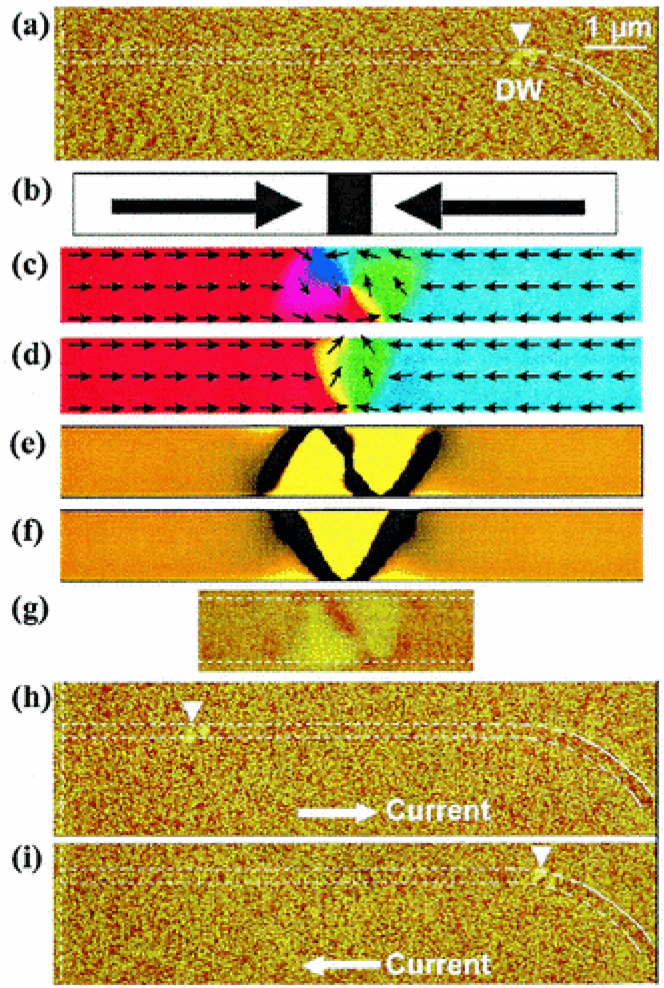

Domain wall in a permalloy ($Ni_{81}F_{19}$) layer

(a) MFM image after the introduction of a DW. DW is imaged as a bright contrast, which corresponds to the stray field from positive magnetic charge.

(b) Schematic illustration of a magnetic domain structure inferred from the MFM image. DW has a head-to-head structure.

(c) Result of micromagnetics simulation (vortex DW).

(d) Result of micromagnetics simulation (transverse DW).

(e) MFM image calculated from the magnetic structure shown in Fig. 2c.

(f) MFM image calculated from the magnetic structure shown in Fig. 2d.

(g) Magnified MFM image of a DW.

(h) MFM image after an application of a pulsed current from left to right. The current density and pulse duration are 120 MA/cm^2 and 5 µs, respectively. DW is displaced from right to left by the pulsed current.

(i) MFM image after an application of a pulsed current from right to left. The current density and pulse duration are 120 MA/cm^2 and 5 µs, respectively. DW is displaced from left to right by the pulsed current.

https://doi.org/10.1103/PhysRevLett.92.077205

Two mechanisms for DW displacement via STT

3d transition metals

STT induced motion

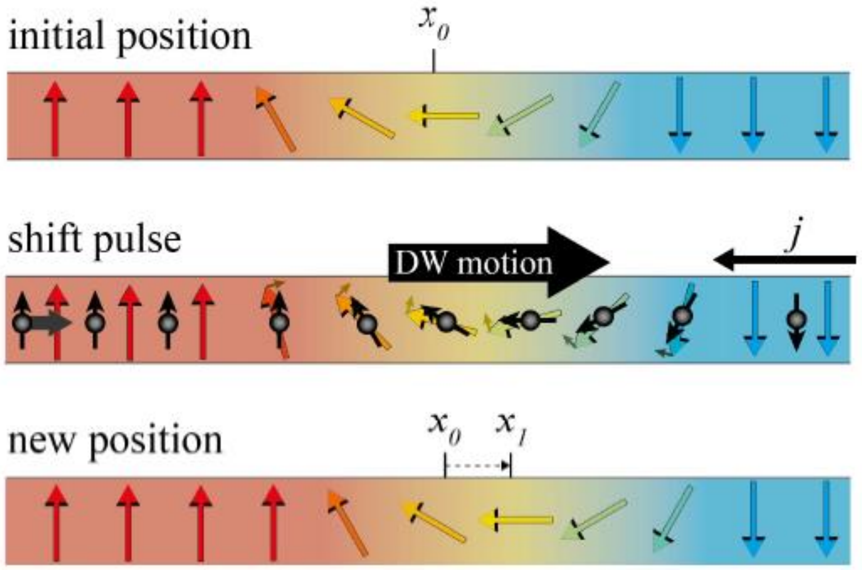

Fig. 6. *Magnetic DWs are shifted by current pulses which rotate the local magnetization (indicated by colored arrows). In the 1.0 and 2.0 RTM versions, motion is governed by a volume STT in which the electrons (black arrows) transfer their angular momentum to the localized magnetic moments. The DW motion is generally in the electron flow direction.*

3d-5d transition metal interfaces

DMI+SHE +STT induced motion

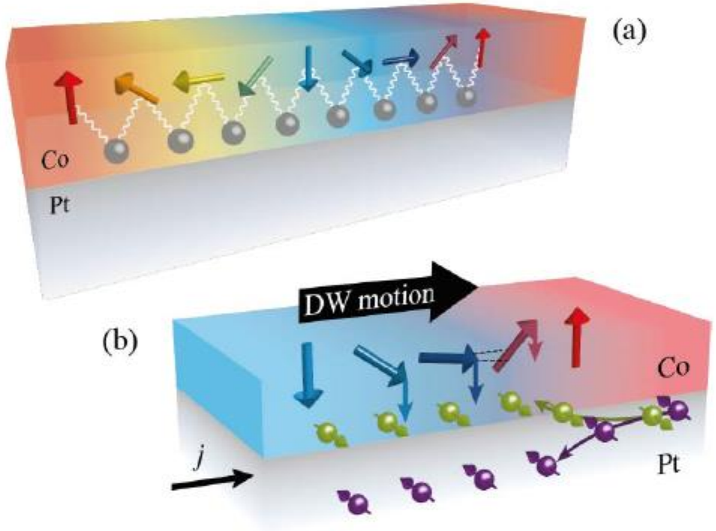

Fig. 7. *Magnetic DWs in a ferromagnetic material (e.g., Co). (a) DW chirality in subsequent DWs is conserved due to the DMI at the interface to a heavy metal layer (such as Pt). (b) The electrical current in the heavy metal layer creates a spin current due to the spin Hall effect which diffuses into the ferromagnetic layer. The spins are polarized such that they exert a torque on the magnetization, rotating them out of the DMI-favored orientation. Hence, an effective DMI field is created which exerts a CST on the magnetic moments which finally moves the DW along the current flow direction [51], [53].*

Chiral spin torque (CST)

DOI: 10.1109/JPROC.2020.2975719

(Some of the) Hall effects

Hall effect (HE): The longitudinal current I_x under vertical external magnetic filed H_z contributes to the transversal voltage V_y due to the Lorentz force experienced by carriers.

Anomalous Hall effect (AHE). The electrons with majority and minority spin (due to spontaneous magnetization M_z) have opposite "anomalous velocity" due to spin-orbit coupling. The spin polarization of the current causes unbalanced electron concentration at two transversal sides and leads to finite voltage V_y.

Spin Hall effect (SHE). In nonmagnetic conductor, equivalent currents in both spin channels with opposite "anomalous velocity" leads to balanced electron concentration at both sides while net spin current in transversal direction. Consequence of SOC

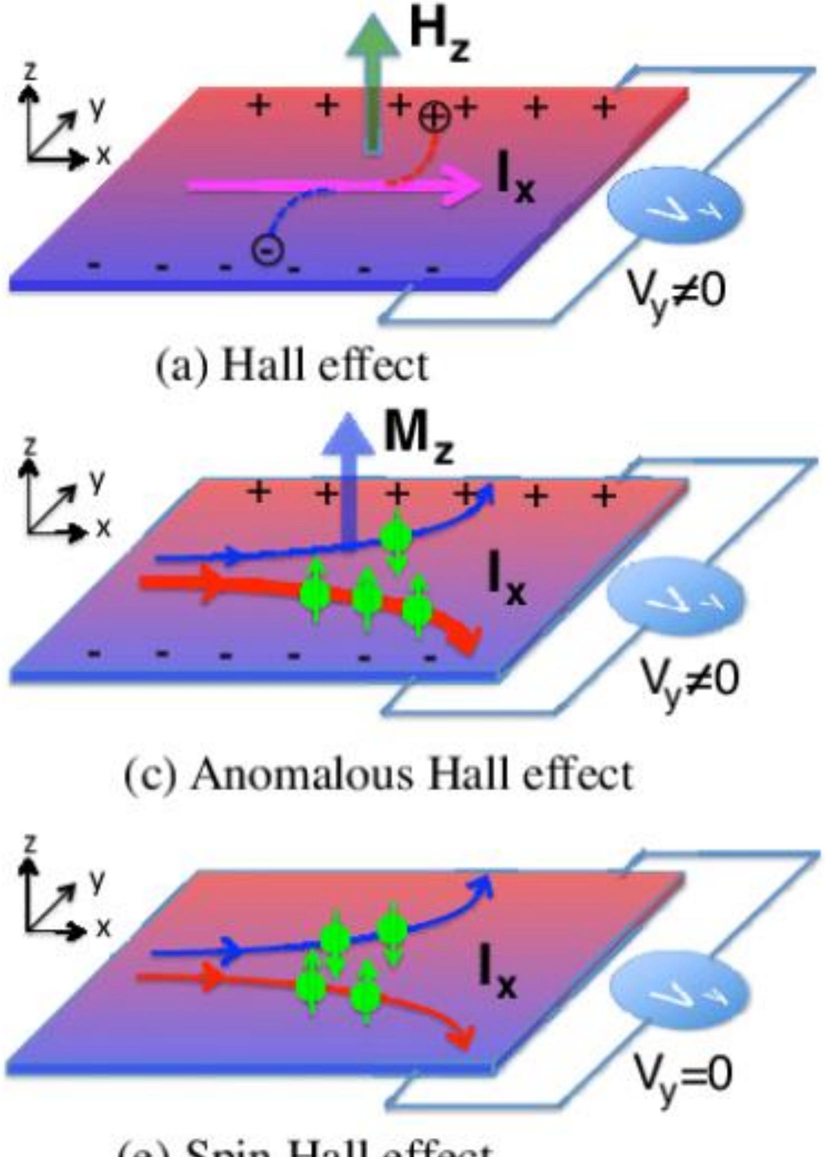

(a) Hall effect

(c) Anomalous Hall effect

(e) Spin Hall effect

Current-driven chiral ferromagnetic domain walls

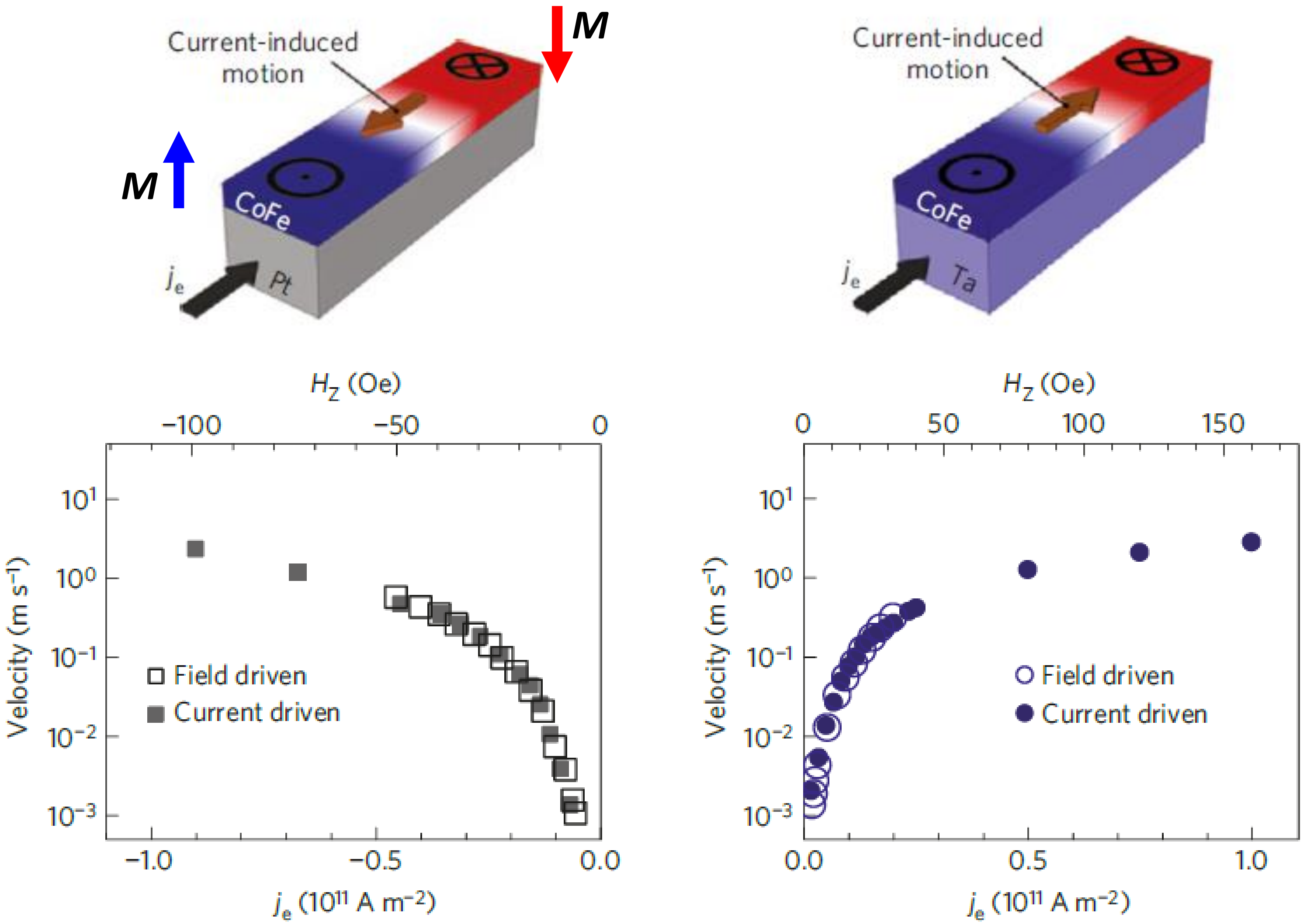

STT from Spin Hall Effect (SHE) drives DWs in opposite directions in Pt/CoFe/MgO and Ta/CoFe/MgO

DOI: 10.1038/NMAT3675

Spin Hall effect: reversed spin polarized currents for Pt *vs* Ta

SOC has opposite effect in Pt *vs* Ta

Pt: more than half filled

Ta: less than half filled

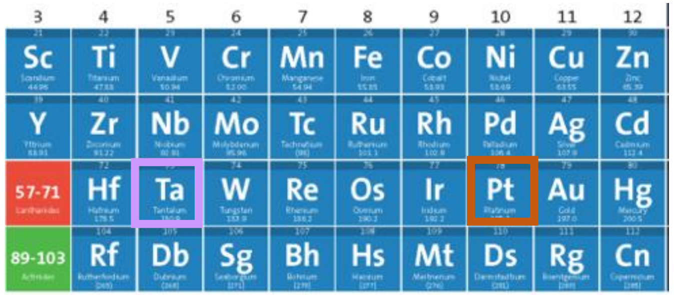

AHE detection

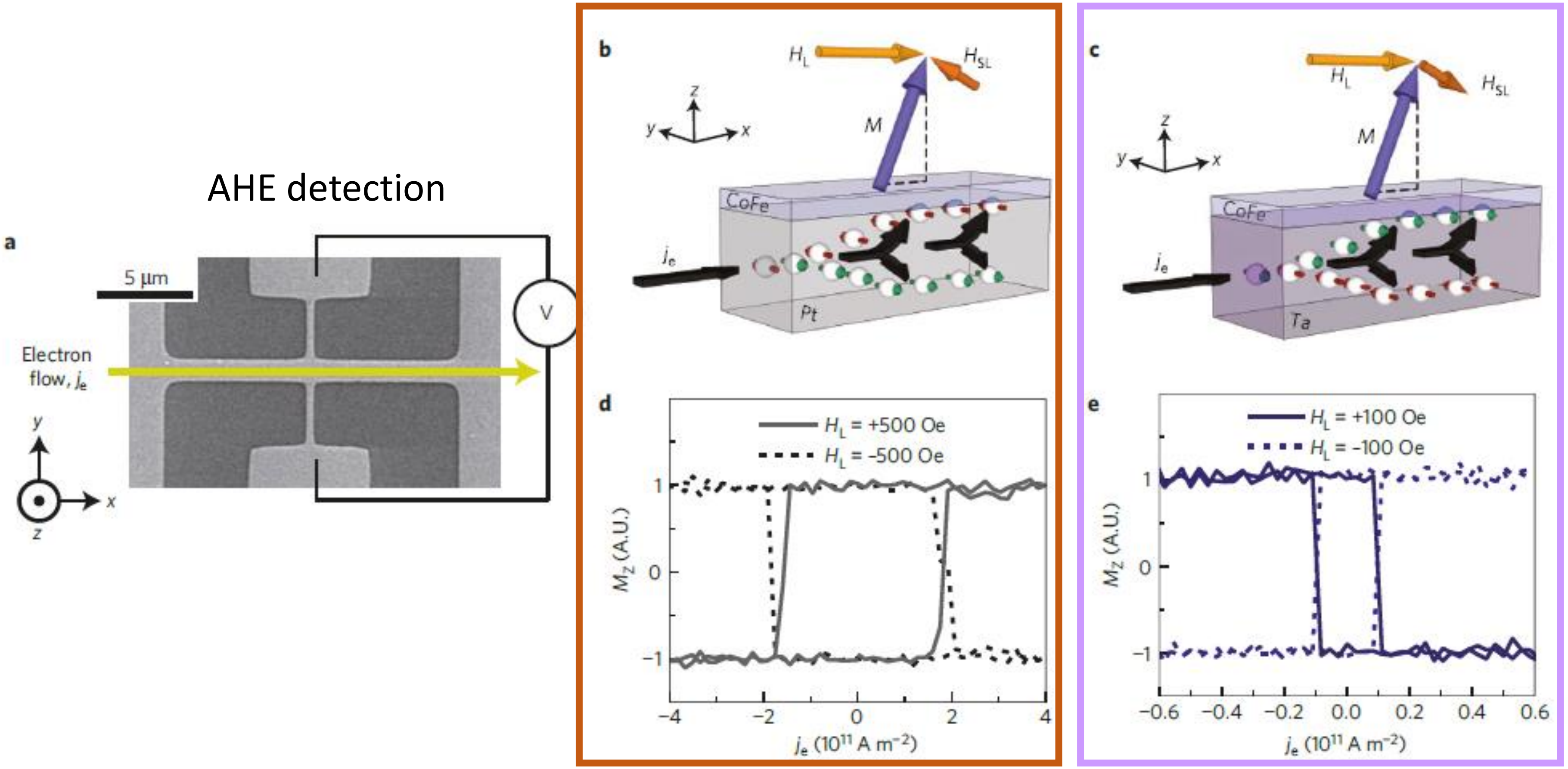

Figure 2 | Current-induced switching under a constant in-plane longitudinal field. a, Scanning electron micrograph of a Hall cross. **b**,**c**, Illustrations of Pt/CoFe/MgO (**b**) and Ta/CoFe/MgO (**c**) in the up magnetization state with the injected electron current and applied longitudinal field H_L in the +*x* direction. Owing to the combination of the current-induced Slonczewski-like torque (producing an effective field H_{SL}) and the applied longitudinal field, up magnetization is stable in Pt/CoFe/MgO whereas it is unstable in Ta/CoFe/MgO. **d**,**e**, Out-of-plane magnetization M_z (normalized anomalous Hall signal) as a function of electron current density j_e under a constant H_L in Pt/CoFe/MgO (**d**) and Ta/CoFe/MgO (**e**). The magnitude of H_L is 500 Oe for Pt/CoFe/MgO (**d**) and 100 Oe for Ta/CoFe/MgO (**e**). When H_L is reversed from +*x* (solid line) to −*x* (dotted line), the stable magnetization direction under a given current polarity reverses.

DOI: 10.1038/NMAT3675

Current-driven chiral ferromagnetic domain walls

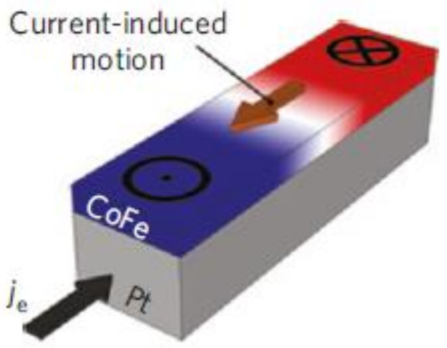

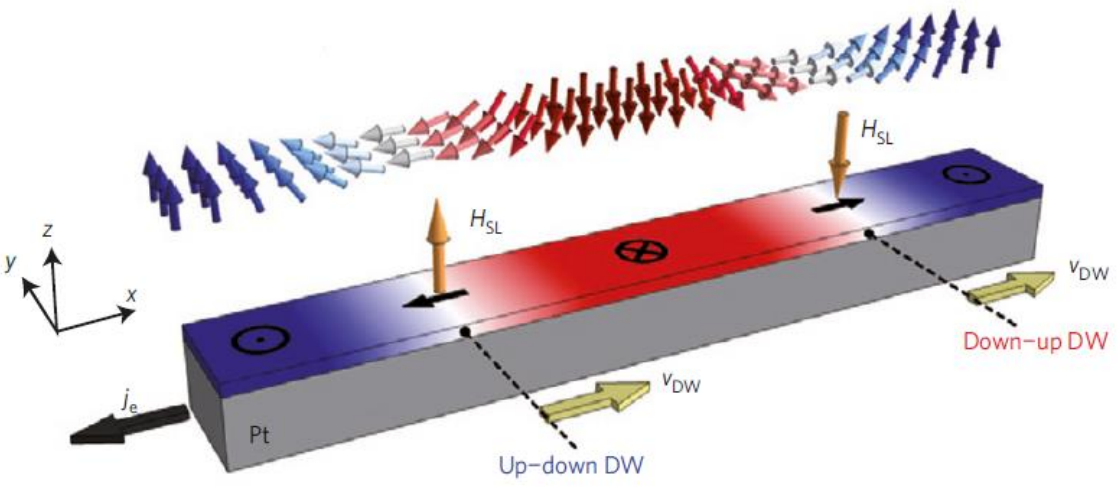

Néel DWs

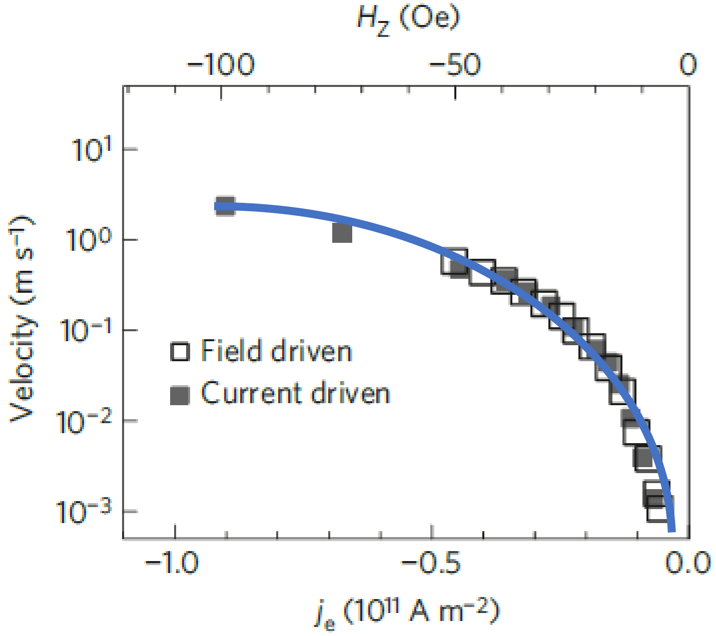

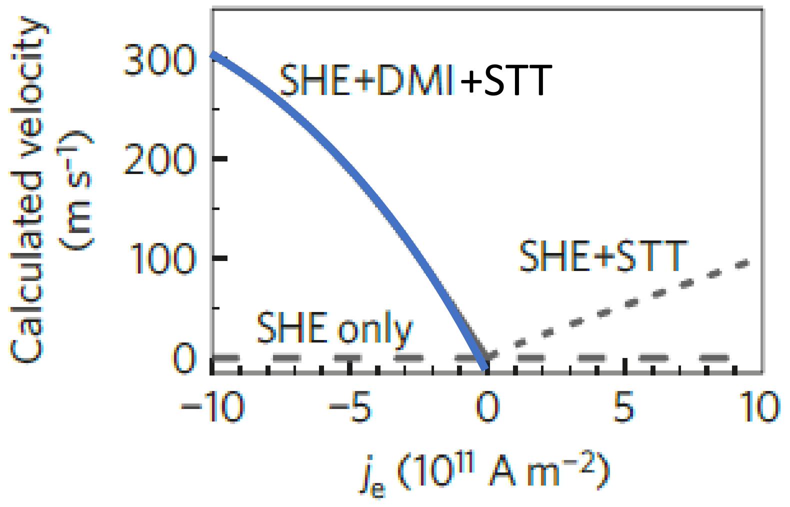

DMI is necessary to stabilize Néel DWs. A perpendicular H_{sl} field would have no effect on Bloch DWs

$$H_{SL}^0 = \frac{\hbar j_e \theta_{SH}}{2eM_{sat}t_{CoFe}}$$

j_e generates an effective field H_{SL} resulting in a damping like torque $\tau_{DL} \propto \frac{\gamma}{1+\alpha^2}\frac{\alpha}{m}\left(\boldsymbol{m} \wedge [\boldsymbol{m} \wedge H_{SL}^0]\right)$

DOI: 10.1038/NMAT3675

Spin torque in non-uniform magnetization textures

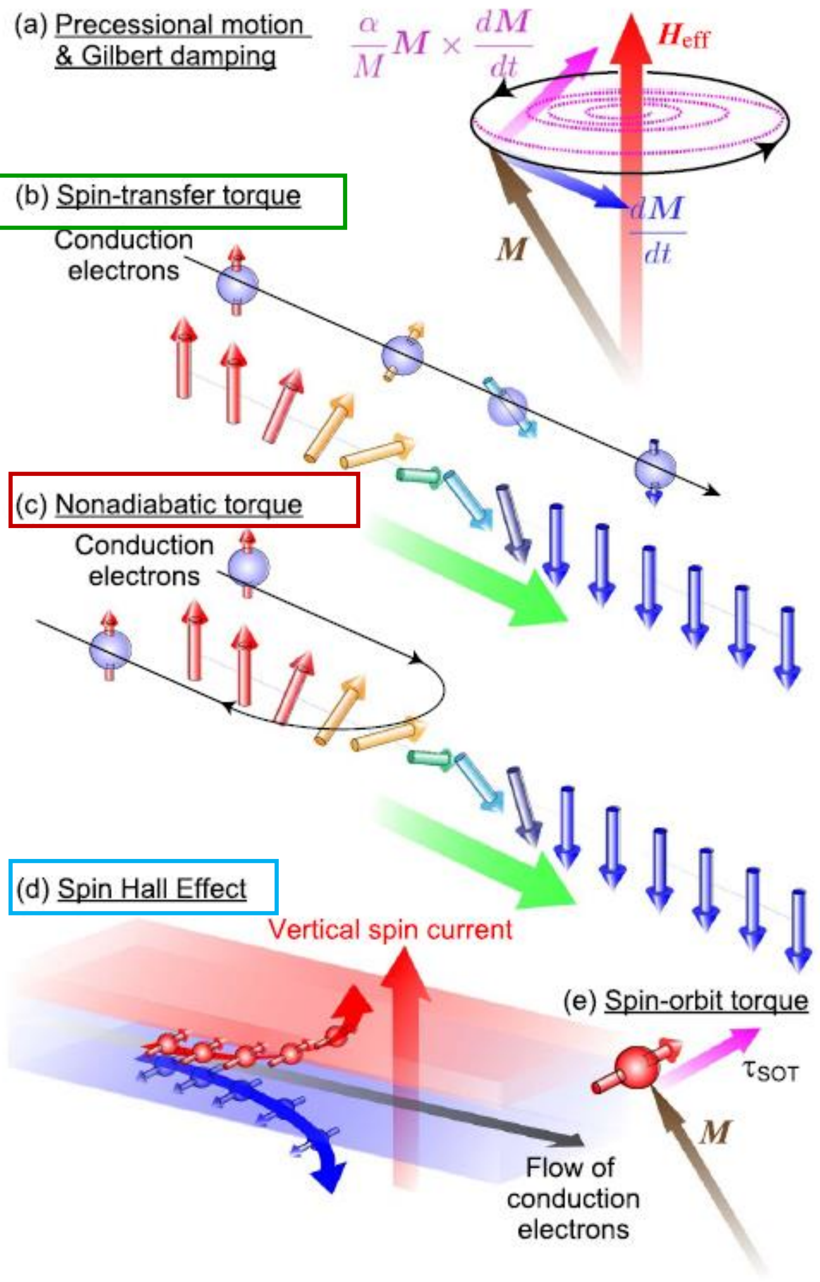

$$\frac{\mathrm{d}\boldsymbol{m}}{\mathrm{d}t} = -\gamma \boldsymbol{m} \times \boldsymbol{B}^{\mathrm{eff}} + \alpha \boldsymbol{m} \times \frac{\mathrm{d}\boldsymbol{m}}{\mathrm{d}t}$$

$$+ \frac{\gamma \hbar p}{2eM_s} (\boldsymbol{j}_e \cdot \nabla) \boldsymbol{m} - \beta \frac{\gamma \hbar p}{2eM_s} [\boldsymbol{m} \times (\boldsymbol{j}_e \cdot \nabla) \boldsymbol{m}]$$

$$+ \frac{\gamma \hbar |\theta_{SH}| j_e}{2eM_s} \cdot \frac{1}{t} \boldsymbol{m} \times [\boldsymbol{m} \times (\hat{\boldsymbol{j}}_e \cdot \boldsymbol{\nabla}) \boldsymbol{m}]$$

Adiabatic torque:
- transport processes in which the spin of an electron passing through a magnetic domain wall adiabatically follows the local magnetization direction resulting in a spin flip.
- the loss of spin angular moment is transferred as a spin-transfer torque to the magnetization

Non-adiabatic torque:
- it is characterized by a dimensionless parameter β (efficiency).
- Various mechanisms have been proposed, such as momentum transfer, DW distortion or spin-flip scattering

Spin Orbit Torque (SOT) via Spin Hall Effect (SHE):
- Consequence of SOC when combining a FM and an heavy metal NM layers
- $\theta_{SH} = \frac{j_S}{j_e}$ spin to charge conversion factor

DOI: 10.1103/PhysRevLett.93.127204; 10.1103/PhysRevB.70.024417 https://doi.org/10.1088/1361-648X/ad861b

Skyrmion based memory

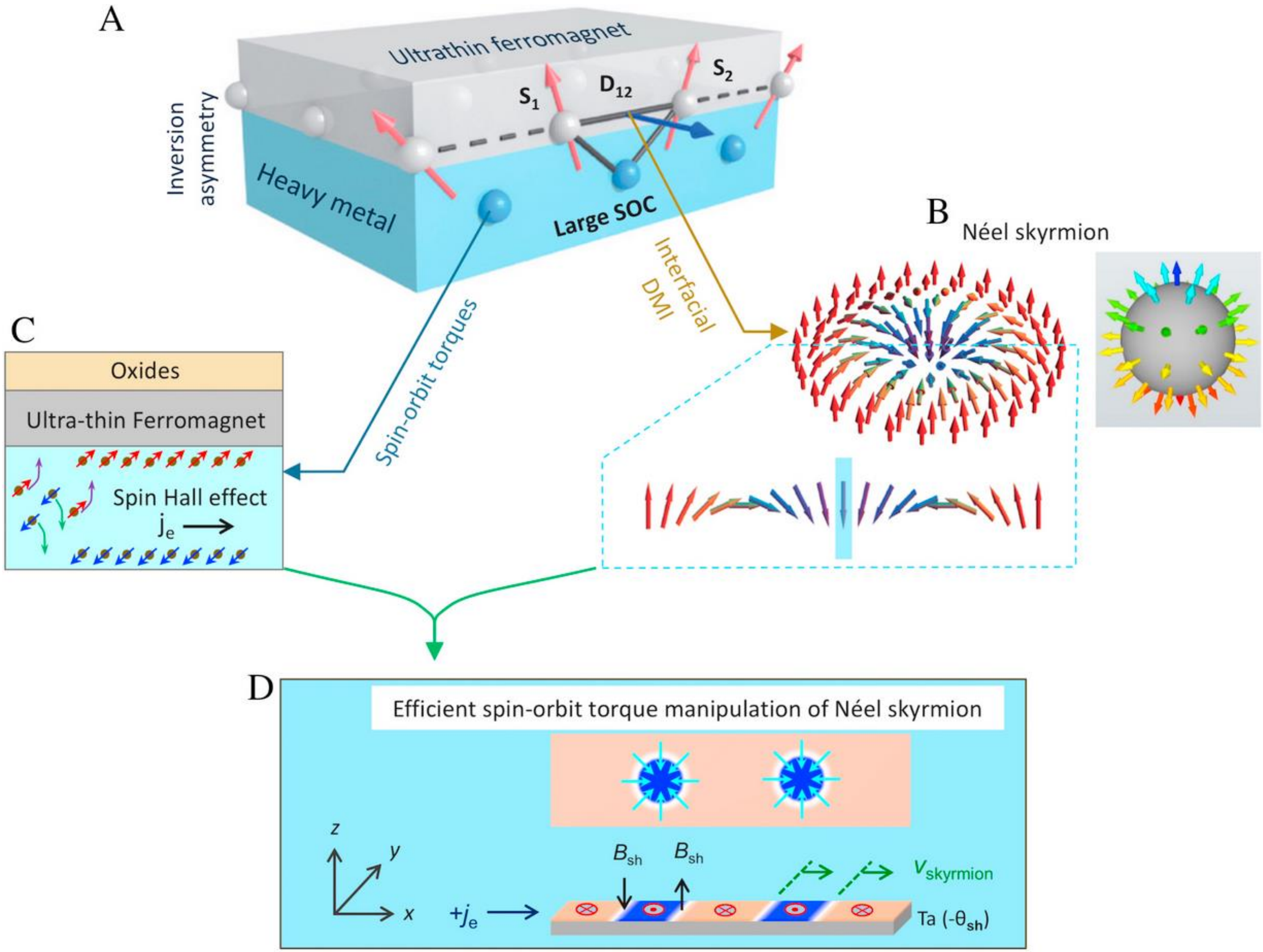

https://doi.org/10.1016/j.physrep.2017.08.001

Skyrmion based racetrack memory

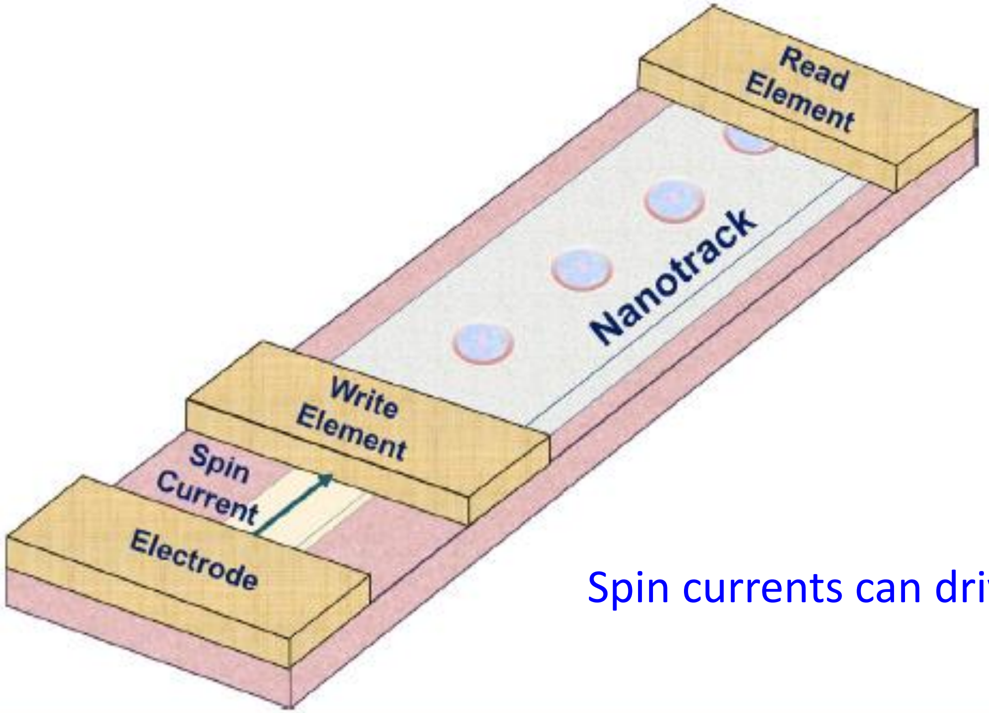

FIGURE 14

Schematic illustration of a Skyrmion based racetrack memory. The dots represent Skyrmions.

in a Skyrmion based memory, the Skyrmions are displaced.
In the Skyrmion based memory, the presence or absence of a Skyrmion represents 1 and 0 states.

Spin currents can drive skyrmions.

Similarly to DWs, skyrmions are non-uniform magnetization textures.
Then, adiabatic, non-adiabatic and SHE torques also apply

https://doi.org/10.1016/j.mattod.2017.07.007

Skyrmion motion induced by a current

Skyrmion speeds in tracks tend to be limited by phenomena such as the skyrmion Hall effect (similar to the Magnus effect experienced by a spinning object in a fluid) , which deflects and damps the skyrmion motion.

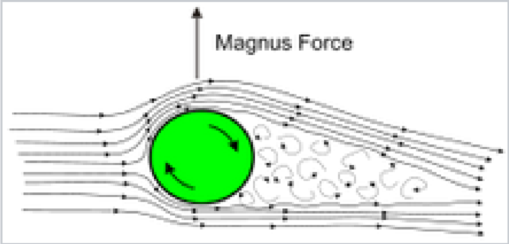

The Magnus effect, depicted with a backspinning cylinder or ball in an airstream. The arrow represents the resulting lifting force. The curly flow lines represent a turbulent wake. The airflow has been deflected in the direction of spin.
Air is carried around the object; this adds to the velocity of the airstream above the object and subtracts below resulting in increased airspeed above and lowered airspeed below.

https://en.wikipedia.org/wiki/Magnus_effect

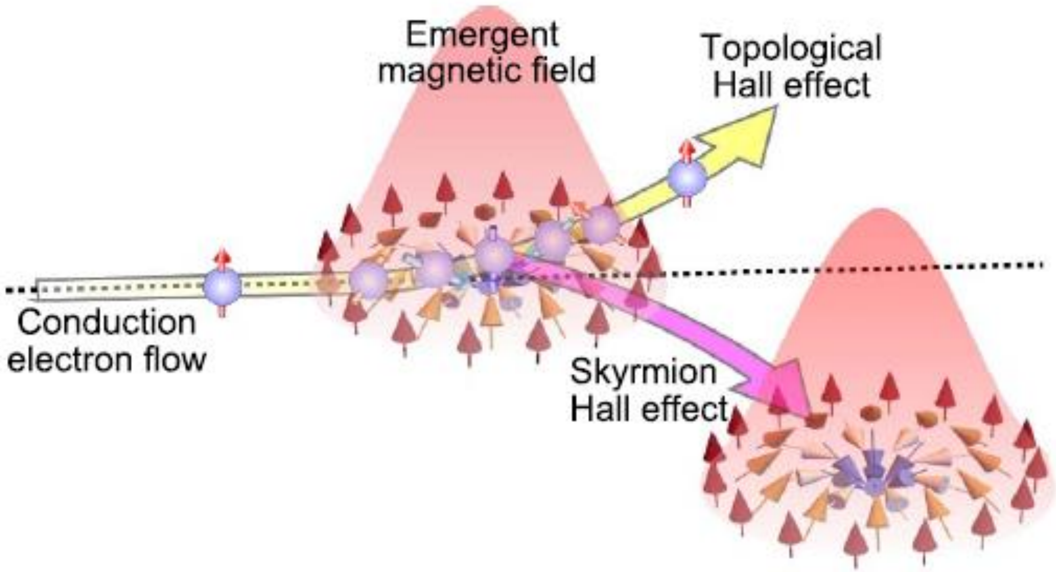

- Conduction electrons of the electric current injected into the ferromagnet (FM) becomes spin-polarized parallel to the FM magnetization through exchange coupling.
- Spin angular momenta of the conduction electrons are transferred to the noncollinear skyrmion magnetizations which drives the skyrmion dominantly towards the current direction.
- The flow of the conduction electrons is deflected by the emergent magnetic field generated by the noncollinear skyrmion magnetizations, which results in the Hall motion of the conduction electrons (topological Hall effect).
- The reaction force of this topological Hall effect acts on the skyrmion, which causes subsequent transverse motion of skyrmion perpendicular to the injected electric current (skyrmion Hall effect).

Skyrmions in synthetic antiferromagnets (SAF)

Fig. 2. Skyrmions in compensated SAF. (**A**) Composition of the SAF stack (see text for thicknesses). (**B**) Normalized magnetic moment as a function of the out-of-plane external magnetic field measured by vibrating sample magnetometry. Black and red lines correspond to decreasing and increasing magnetic field, respectively. (**C**) MFM images measured at zero applied magnetic field after applying sequentially an in-plane field of ~400 mT followed by a perpendicular field of 170 mT.

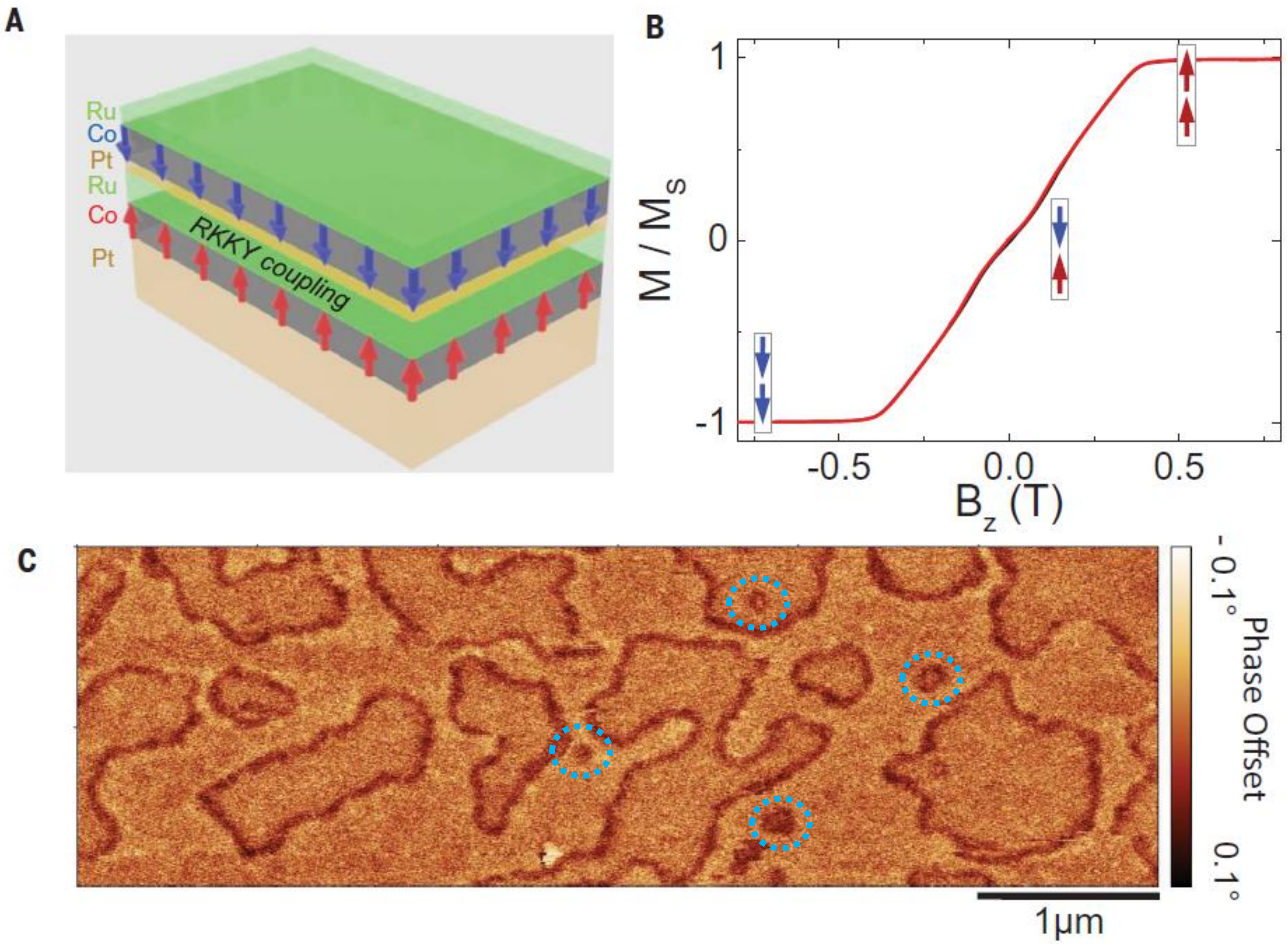

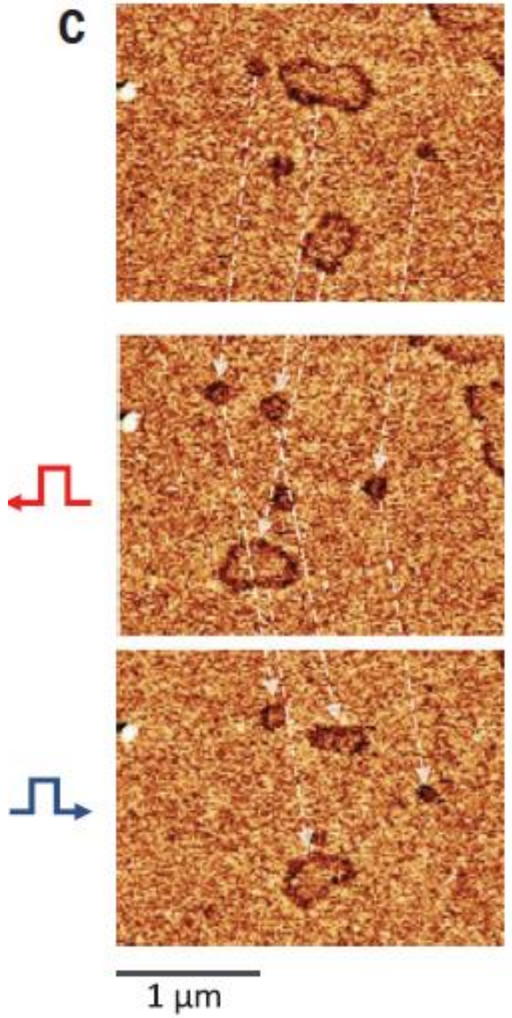

MFM images before injection (top), after injection of a negative current pulse (middle), and after injection of a positive current pulse (bottom) with width 0.55 ns and density –8.2 × 10^{11} and 7.9 × 10^{11} A/m^2, respectively. All measurements performed at zero applied magnetic field and roomT. The white lines in (A) and (C) connect the positions of the skyrmions before and after the current pulses.

Science (2024) DOI: 10.1126/science.add5751

Skyrmions in compensated synthetic antiferromagnets

EPFL

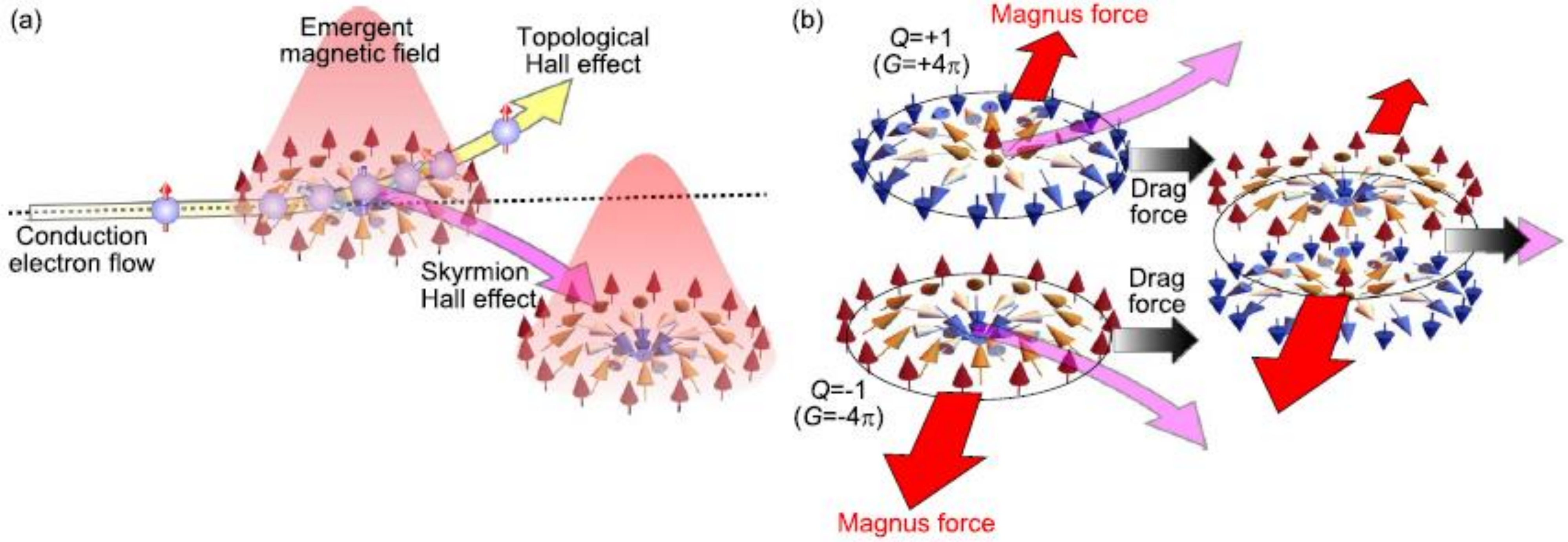

Compensation of Skyrmion Hall effect and enhanced velocity in SAF Skyrmions.

(a) Conduction electrons of the electric current injected into the ferromagnet becomes spin-polarized parallel to the background ferromagnetic magnetization through exchange coupling. Spin angular momenta of the conduction electrons are transferred to the noncollinear skyrmion magnetizations which drives the skyrmion dominantly towards the current direction.
The flow of the conduction electrons is deflected by the emergent magnetic field generated by the noncollinear skyrmion magnetizations characterized by a quantized topological charge, which results in the Hall motion of the conduction electrons (topological Hall effect). The reaction force of this topological Hall effect acts on the skyrmion, which causes subsequent transverse motion of skyrmion perpendicular to the injected electric current (skyrmion Hall effect).
(b) Vanishing of the skyrmion Hall effect for antiferromagnetic skyrmions. An antiferromagnetic skyrmion can be regarded as a pair of ferromagnetic skyrmions with opposite topological charges. Consequently, opposite contributions of driving forces to the transverse motion from these two skyrmions cancel each other, resulting in the absence of skyrmion Hall effect.

Science (2024) DOI: 10.1126/science.add5751 https://doi.org/10.1088/1361-648X/ad861b

Enhanced velocity in SAF Skyrmions

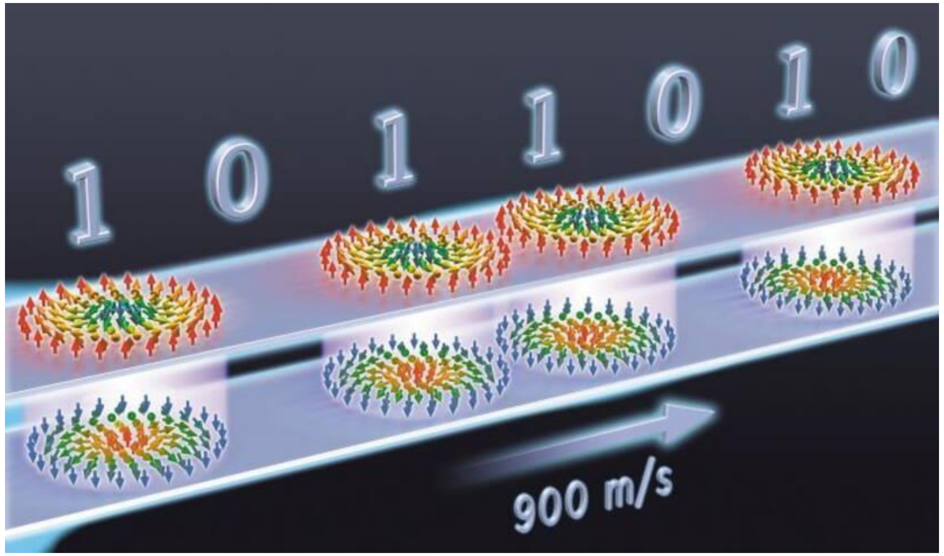

https://www.geo.fr/sciences/c-est-quoi-les-skyrmions-ces-nanobulles-magnetiques-qui-vont-rendre-vos-ordinateurs-10-fois-plus-rapides-spintronique-nanoaimants-cnrs-219854

SF: FM skyrmion
SAF: AFM skyrmion

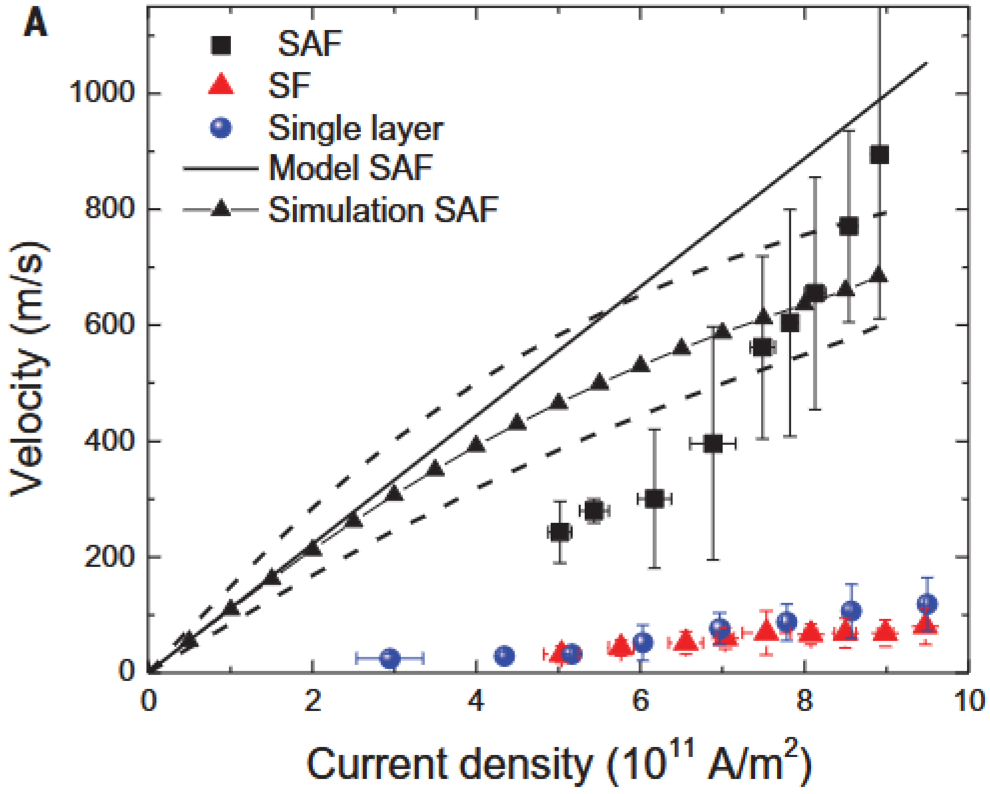

Science (2024) DOI: 10.1126/science.add5751

Skyrmion size

SAF Skyrmion size: balance between (i) the DMI energy which favours larger skyrmions, (ii) the cost in anisotropy and exchange energy at larger radius, which favours smaller skyrmions, and (iii) the curvature energy cost at low radius due to the exchange energy

FM Skyrmions: as before with in addition the stray field (dipolar energy) which tends to increase the Skyrmion

Table 1. Selection of thin film multilayered materials illustrating Néel skyrmion stabilization. We indicate the material (multilayer system), the measured diameter of the skyrmion core, the magnitude of the DMI $|D| \left(\frac{mJ}{m^2}\right)$, the temperature of the skyrmion stability and the reference of the paper containing the study.

Multilayer System	Diameter of Skyrmion Core (nm)	$\|D\| \left(\frac{mJ}{m^2}\right)$	Temperature of Skyrmion Stability (K)	Reference
Pt/Co/Ta	75–200	1.3	$\lesssim 300$	[5]
Pt/Co/MgO	70–130	2.0	$\lesssim 300$	[6]
Ir/Co/Pt	25–100	N.A.	$\lesssim 300$	[7]
$[Ir/Co/Pt]_{10}$	100	2	> 300	[8]
Pt/CoFeB/MgO	<250	1.35	$\lesssim 300$	[9,10,11]
Pd/CoFeB/MgO	<200	0.78	$\lesssim 300$	[12]
W/CoFeB/MgO	250	0.3–0.7	$\lesssim 300$	[13]
Ta/CoFeB/MgO	300	0.33	$\lesssim 300$	[14]
Ta/CoFeB/Ta/MgO	1000–2000	0.33	>300	[14]

SAF Skyrmions:

skyrmion diameter $d \approx 2.7\Delta \frac{\left(\frac{D}{D_c}\right)^2}{\sqrt{1-\left(\frac{D}{D_c}\right)^2}}$,

where $\Delta = \sqrt{\frac{A}{K_{eff}}}$ is the domain wall width,

D is the DMI constant,

$D_c = \frac{4\sqrt{A\,K_{eff}}}{\pi}$,

A is the exchange constant,

K_{eff} is the effective PMA

Skyrmion size bigger than DW

https://doi.org/10.3390/nano12244411